Hybrid automatic repeat request protocols for user cooperation and relaying scheme for correlated sources

Haifa Fares Jridi

N° d'ordre : 2011telb0224

Thèse

présentée à

TELECOM Bretagne

en habilitation conjointe avec l'Université de Bretagne-Sud

pour obtenir le grade de

Docteur de TELECOM Bretagne

Mention : *Sciences et Technologies de l'Information et de la Communication (STIC)*

par

Haïfa Farès

Hybrid Automatic Repeat Request Protocols for User Cooperation & Relaying Scheme for Correlated Sources

---

soutenue le 07 Décembre 2011 devant la commission d'examen :

Composition du Jury :

Président :	Maryline Hélard, professeur, INSA Rennes
Rapporteurs :	Guido Montorsi, professeur, Politechnico di Torino Raymond Knopp, professeur, Eurecom Sophia Antipolis
Examinateurs :	Walaa Hamouda, maître de conférences, Concordia University Laura Condé, maître de conférences, Université de Bretagne-Sud Alexandre Graell i Amat, maître de conférences, Chalmers University Charlotte Langlais, maître de conférences, Télécom Bretagne Marion berbineau, directrice de recherche, Université de Lille Nord
Invité :	Iyad Dayoub, maître de conférences, Université de Valenciennes

"If you want to be incrementally better: Be competitive. If you want to be exponentially better: Be cooperative."

Mitch Anthony

Abstract

Cooperative communication has recently been introduced as a new method to push forward reliability and capacity of future wireless networks. The basic idea of cooperative communications is that all nodes in a network may help each other to transmit information to a destination, under constraints on power, complexity or delay. While a single antenna is employed at each node, cooperative communications allow to share several antennas distributed over different nodes in order to benefit from spatial diversity.

Nevertheless, it was shown that cooperative communications suffer from throughput degradation due to the fixed cooperative phase. Therefore, to overcome this drawback, we can use Hybrid automatic repeat request (HARQ), a common technique used to make a wireless link reliable and transmissions more efficient. However, most of these works explore exclusively the case of one source node assisted by one or multiple relay nodes. Only few works extended the idea of cooperative HARQ to the case of user cooperation.

In this thesis, we explore cooperative HARQ protocols over the user cooperation system, a configuration that has not been fully explored yet. The considered system consists of two sources which cooperate to communicate statistically independent data to a single destination. Each source can operate in two different modes: transmission mode, by transmitting its own local information, or relaying mode, by helping the partner node to transmit its information.

The first part of the thesis is devoted to investigate the impact of employing hybrid automatic repeat request (HARQ) protocols, which send back ACK or NACK to the transmitting nodes, over a turbo coded cooperation scheme. This cooperative scheme is adopted as a starting point since it integrates user cooperation with capacity approaching channel coding, particularly turbo code. Instead of repeating the received information, the source decodes the partner's information and transmits additional parity bits according to an overall distributed turbo code scheme. We exploit the limited feedback to define three different cooperative HARQ protocols: destination-level HARQ, relay-level HARQ and two-level HARQ. These protocols aim mainly to preserve the overall system throughput by controlling the cooperation phase at the destination node, and to increase diversity by allowing retransmission to the partner node which strengthens the inter-source link.

We further analyze the probability of outage of the proposed protocols, characterize their diversity-multiplexing tradeoff and evaluate them according to different parameters: channel conditions, transmission rate, and resource allocation.

Furthermore, we analyze the improvement of the proposed cooperative HARQ protocols over the original turbo coded cooperation system, as well as over a conventional point-to-point incremental-redundancy HARQ system, in terms of frame error probability and throughput efficiency. Thanks to this analytical study, we define the system retransmission gain and the system cooperation gain, which serve as decision parameters to determine the geometric conditions under which cooperative HARQ protocols are useful. These proposed protocols fit well for applications such as wireless vehicular networks.

In the second part of the thesis, we consider wireless sensor networks, where neighboring sensors measure data that is statistically dependent. Source correlation can be exploited at the receiver side. As a third main contribution of the thesis, we derive bounds on the error probability in an uncoded decode-and-forward cooperative system with two correlated information sources and one relay. Furthermore, we demonstrate the performance gain that can be obtained by exploiting the correlation between the sources and we compare these results to a correlation-aware system without relay.

Résumé

La demande croissante des applications gourmandes en débits et des services de haute fiabilité (streaming vidéo et transfert de données) a considérablement augmenté les défis pour les opérateurs de réseaux de télécommunications. Ces exigences ont été en partie satisfaites par la technologie mûre de communication filaire par fibre optique. Néanmoins, cette solution ne répond pas à une exigence primaire de la clientèle: l'accès continu à l'information. Par conséquent, les communications sans fil restent toujours l'un des sujets les plus étudiés dans le domaine des communications modernes. Néanmoins, le canal sans fil souffre de divers problèmes tels que l'atténuation du signal, les évanouissements et les problèmes d'interférence, qui imposent de grands défis pour assurer une transmission fiable et la gestion d'accès partagé. Bien que la recherche dans ce domaine ait connu des résultats remarquables, des efforts supplémentaires sont encore nécessaires afin de fournir des débits comparables à la moyenne dans le domaine filaire. Par conséquent, le défi pour la communauté de recherche pour les réseaux sans fil est de concevoir des systèmes de communication qui assurent une transmission fiable et une efficacité spectrale élevée tout en atténuant les effets d'évanouissements et d'interférence. Les évanouissements peuvent être combattus en utilisant la diversité en temps, fréquence ou espace, en transmettant le signal sur plusieurs canaux qui subissent des évanouissements indépendants.

La forme originelle de la communication coopérative est propre aux réseaux de capteurs sans fil et réseaux ad hoc, où les données sont acheminées grâce à un routage multi-saut. Cependant, dans les réseaux cellulaires, les techniques de coopération constituent une alternative intéressante à la technique multi-antenne qui offre essentiellement de la diversité spatiale. La coopération entre noeuds d'un système de communication sans fil permet de combattre les évanouissements des canaux et d'améliorer ainsi la diversité globale du système. Entre autres, les techniques de coopération sont apparues afin de répondre à deux objectifs : l'extension de couverture de la cellule ou l'augmentation de la capacité à l'intérieur de la cellule pour les utilisateurs dont le lien radio direct avec la station de base est détérioré. Ces techniques consistent à utiliser des terminaux relais entre un terminal source et un terminal destination. Les relais sont chargés de coopérer

avec la source pour transmettre les informations de la source et/ou leurs propres informations jusqu'à la destination. Un terminal peut donc coopérer avec un ou plusieurs terminaux intermédiaires afin de transmettre ses données à la destination. Ainsi, même si le terminal source possède une seule antenne, la destination reçoit plusieurs versions du signal émis. De surcroît, les protocoles de retransmission (HARQ- Hybrid Automatic Repeat reQuest) sont des techniques couramment utilisées pour accroître la fiabilité du lien radio. Ainsi, les protocoles de coopération peuvent adopter ces techniques HARQ, exploitant les messages de retour en provenance des relais et/ou de la destination. Dans ce contexte, les protocoles de retransmission coopératifs sont considérés comme des technologies particulièrement prometteuses en raison de leur exploitation opportuniste à la fois de la diversité spatiale et des ressources temporelles. Ceci répond à deux objectifs spécifiques : pallier le problème de dégradation de l'efficacité spectrale de tels systèmes où une phase supplémentaire de coopération est toujours présente, et renforcer les liens source-relais et source-destination qui influent considérablement sur les performances.

Dans une première partie de la thèse, nous commençons par présenter le concept des communications coopératives de façon générale, ensuite nous décrivons le schéma de coopération de base étudié : la coopération codée, et nous étudions les protocoles de retransmission HARQ coopératifs appliqués à un couple de sources coopérant pour communiquer avec une même destination. Ces protocoles HARQ coopératifs associent le protocole de retransmission hybride Turbo au niveau de la couche liaison de données et la coopération turbo codée au niveau de la couche physique. Ainsi, nous proposons trois protocoles HARQ. Un premier, appelé Destination-Level HARQ (DL-HARQ), est proposé afin d'éviter la dégradation de l'efficacité spectrale du système due à une utilisation canal inutile lors de la phase de coopération lorsque l'information est correctement reçue à la destination dès la première phase. Un deuxième protocole HARQ coopératif, appelé Relay-level HARQ (RL-HARQ), est défini dans le but de favoriser la coopération entre les deux sources en améliorant la qualité du lien entre les deux. Enfin, un troisième protocole combinant les deux précédents, nommé Two-Level HARQ (TL-HARQ), est proposé. Cette appellation trouve son origine dans les deux niveaux de décision de la retransmission conditionnés par les messages de retour provenant de la destination et ensuite ceux du partenaire.

Deuxièmement, nous explorons un autre domaine d'application de la communication coopérative. Nous considérons des réseaux de capteurs où les données provenant de capteurs voisins géographiquement sont statistiquement dépendantes. Cette corrélation entre sources peut être exploitée à l'émetteur et du côté du récepteur, à travers des techniques de codage conjoint source-canal, pour améliorer les performances. L'objectif est donc double: premièrement, exploiter la corrélation entre sources pour permettre des communications fiables, deuxièmement, permettre des économies d'énergie importantes

pour la transmission de données par l'utilisation de la compression des données. Dans cette thèse, nous analysons les performances d'un système de communication coopératif en exploitant la corrélation entre sources du côté du récepteur. Nous montrons que la prise en compte de la corrélation à la fois au niveau du relais et de la destination entraîne des gains de performance significatifs.

Cette thèse est organisée dans l'ordre classique, où les concepts de bases sont présentés dans le deuxième chapitre et les nouvelles contributions dans les chapitres suivants. En guise d'introduction aux thèmes étudiés dans cette thèse, nous présentons dans le chapitre 2, le modèle général du canal radio, quelques notions de base sur la théorie de l'information ainsi que les systèmes de contrôle d'erreur, qui sont nécessaires pour les prochains chapitres. Tout d'abord, nous présentons les propriétés du canal sans fil qui guideront les décisions de conception des systèmes de communication proposés. Ensuite, nous présentons un aperçu sur les codes correcteurs d'erreurs et les protocoles de retransmission ainsi que les outils utilisés pour analyser leur comportement. Le chapitre est terminé par une discussion brève des techniques de transmission multi-sources. Le problème de corrélation entre sources est également abordé afin de suggérer une extension dans un contexte coopératif.

Dans le chapitre 3, nous résumons les concepts de base des communications coopératives. En particulier, nous commençons par réviser les principaux résultats du canal à relais et nous adressons le schéma de codage turbo distribué pour un canal à relais. De plus, nous donnons une brève description des protocoles HARQ coopératifs proposées dans la littérature. Par la suite, le schéma de coopération codée et en particulier le schéma de coopération turbo codée, utilisé comme point de départ pour concevoir les protocoles HARQ proposés, sont détaillés. Suite à cet aperçu de l'état de l'art, la première contribution de cette thèse est donnée à la fin de ce chapitre. Trois protocoles HARQ différents appliqués pour un réseau sans fil à deux sources avec de la coopération turbo codée, sont formellement introduits et évalués. L'objectif des protocoles de retransmission ARQ appliqués à un réseau sans fils coopératif à trois noeuds, doit être double : d'abord, augmenter l'efficacité spectrale du système en évitant les transmissions inutiles; ensuite, améliorer les performances en termes de taux d'erreurs en renforçant les liens radios critiques. Par rapport au cas non coopératif, la coopération codée peut souffrir d'une dégradation de l'efficacité spectrale, puisque les deux phases sont toujours occupées pour la transmission d'un paquet unique relatif à une des deux sources. Cette dégradation est d'autant plus visible quand l'information des deux sources est correctement décodée dès la première phase. Dans ce cas précis, la phase de coopération n'est plus nécessaire.

Pour éviter cet inconvénient, le protocole DL-HARQ peut être implanté à la destination afin de contrôler la phase de coopération. D'autre part, il a été prouvé que le gain de diversité apporté par les systèmes avec coopération codée est conditionné par la qualité du canal inter-source. En effet ce gain de diversité ne peut être obtenu que si le décodage de l'information réalisé au niveau du noeud partenaire est correct. Il convient donc de concevoir des protocoles HARQ qui permettent de renforcer le lien entre les sources. Un autre problème de la coopération turbo codée, est que, selon les caractéristiques du canal, le schéma du codage canal distribué résultant peut être asymétrique, c'est à dire, il favorise une source par rapport à l'autre. Le protocole RL-HARQ est donc introduit dans le but de pallier à ces deux problèmes majeurs de la coopération turbo codée. Une phase supplémentaire de transmission au partenaire est désormais possible, en se basant sur le message de retour en provenance du partenaire, afin de renforcer le lien inter-source tout en permettant une plus grande symétrie entre les sources.

Les deux protocoles DL-HARQ et RL-HARQ peuvent être combinés afin d'améliorer à la fois l'efficacité spectrale du système et les performances en termes de taux d'erreurs. Nous rappelons que la désignation TL-HARQ provient du fait que le protocole de retransmission fonctionne à deux niveaux. Dans un premier temps, les messages de retour en provenance de la destination doivent être analysés afin de juger de l'utilité de la phase de coopération. Ce premier niveau de décision évite des utilisations du canal non justifiées lorsque les paquets peuvent être correctement reçus lors de la première phase de diffusion. Dans un deuxième temps, si des messages de retour négatifs ont été envoyés à la fois par la destination et par les deux sources, une phase de retransmission vers les noeuds partenaires (perçue aussi par la destination) s'avère aussi nécessaire avant d'accomplir la phase de coopération. L'objectif de ce deuxième niveau de décision est d'améliorer la qualité du canal inter-source, qui a une grande influence sur les performances des systèmes adoptant le schéma de la coopération turbo codée.

Afin d'évaluer les performances de ces protocoles de retransmission appliqués au schéma de la coopération codée, deux analyses peuvent être faites. Nous donnons d'abord les résultats de simulation en termes de taux d'erreurs binaires (TEB) et d'efficacité spectrale (η) pour les divers protocoles de retransmission coopératifs et nous les comparons ensuite aux performances du cas de la coopération turbo codée sans HARQ. Le protocole DL-HARQ permet à lui seul un certain gain de codage, grâce à un meilleur rendement du système (moins d'occupation du canal de transmission). Cependant, la pente de la courbe de ce protocole demeure la même que celle du schéma de la coopération turbo codée car le niveau de coopération reste le même. Par ailleurs, l'ordre de diversité du protocole RL-HARQ est significativement amélioré grâce à l'amélioration de la qualité du canal inter-source. Ainsi, les performances en termes de TEB sont meilleures pour un niveau élevé de SNR. L'efficacité spectrale d'un système adoptant le schéma de

la coopération turbo codée sans protocole de retransmission est limitée au rendement du code lorsqu'une modulation BPSK est utilisée, puisque les deux phases du processus de transmission sont tout le temps allouées pour la transmission d'une trame. Une dégradation de l'efficacité spectrale du système est observée pour le protocole RL-HARQ par rapport au schéma de coopération turbo codée de base. Ceci est dû au fait que des phases de retransmission vers les noeuds partenaires sont possibles même si le paquet a été correctement décodé lors de la première phase de transmission. Notez que dans ce cas, la fiabilité est améliorée (en termes de TEB) mais pas suffisamment pour compenser la perte de débit. Ce phénomène est plus visible lorsque le canal entre les deux sources est de mauvaise qualité. D'autre part, le protocole DL-HARQ évite cette dégradation du débit en contrôlant la phase de coopération, qui ne s'effectuera que si elle s'avère nécessaire. Les meilleurs résultats sont donc obtenus par le protocole TL-HARQ, car il combine l'information de retour en provenance de la destination (augmentant le débit du système) et du partenaire (plus grande fiabilité).

La mise en oeuvre de n'importe quelle nouvelle technologie est généralement entravée par les défis qui émergent avec elle. Les protocoles de retransmission coopératifs ne font en aucun cas une exception à cette règle. Il est à noter que tous les problèmes identifiés ne sont pas spécifiques aux protocoles de retransmission coopératifs, mais sont hérités des paradigmes de la coopération et de la retransmission. Par conséquent, dans le chapitre 4, nous analysons le comportement des protocoles HARQ proposés en termes de probabilité de coupure afin de les évaluer en fonction de différents paramètres: les conditions du canal, le rendement et l'allocation du temps. En effet, en dérivant les probabilités de coupure de ces trois protocoles coopératifs, en nous appuyant sur l'étude faite pour la technique de la coopération codée, nous avons pu valider les résultats de simulations puisque la probabilité de coupure n'est autre qu'une limite inférieure des performances, abstraction faite du design du code utilisé.

D'autre part, nous avons aussi pu examiner l'effet de plusieurs paramètres qui influencent fortement les performances, tels que le débit et le niveau de coopération. En effet, quand nous examinons les courbes de la probabilité de coupure des différents protocoles de coopération en fonction du débit adopté pour la transmission, nous réalisons qu'il y a deux régimes de fonctionnement : pour un régime à bas débit, tous les protocoles ARQ coopératifs offrent une amélioration significative par rapport au schéma de base de la coopération codé sans retransmission. Le protocole TL-HARQ possède toujours de meilleures performances. Toutefois, pour un régime à haut débit, le schéma de la coopération codée ainsi que le protocole RL-HARQ génèrent des performances pires que celles offertes par la transmission directe sans coopération. Ceci est dû au fait que la perte en efficacité spectrale en allouant plus de ressources pour renforcer la transmission va à l'encontre de l'exigence de débit. Cependant, pour les protocoles où un niveau

de contrôle de la retransmission est ajouté au niveau de la destination (DL-HARQ et TL-HARQ), les performances sont, au pire, égales à celles offertes par une transmission classique point-à-point.

De surcroît, nous démontrons que les protocoles ont tous le même ordre de la diversité. Afin de mieux les distinguer, nous effectuons une analyse du compromis diversité-multiplexage (DMT). La première remarque importante que nous pouvons tirer de cette analyse de la DMT est que les performances relatives au système à base de la coopération codée pour $\alpha > 2/3$ sont pires que celles d'un système de référence de transmission directe. Par conséquent, lors du partitionnement du code entre les deux sources, cette limite doit être prise en compte. Même remarque est valable pour le protocole RL-HARQ. L'explication la plus intuitive d'une telle perte est le fait que même en augmentant le gain de multiplexage, la destination est contrainte, pour ces protocoles (CCoop et RL-HARQ), d'attendre un ou plusieurs intervalles de temps supplémentaires pour transmettre le paquet suivant. Cette perte dans le cas du RL-HARQ est présente même pour $\alpha \leq 1/3$. Cependant, nous notons que même si le protocole TL-HARQ offre les meilleures performances en termes de TEB et d'efficacité spectrale, ce protocole ne garantit le meilleur compromis diversité-multiplexage que si $\alpha \leq 1/3$. Cette étude de la probabilité de coupure associée la DMT constitue la deuxième contribution de la thèse.

Par ailleurs, nous définissons deux paramètres (gain de coopération et gain de retransmission) pour évaluer les avantages des protocoles proposés par rapport aux deux systèmes de référence : un système HARQ point-à-point basé sur la redondance incrémentale et un système conventionnel de coopération turbo codée lorsque aucune retransmission n'est autorisée. Ce cadre analytique est adopté pour déterminer les conditions géométriques dans lesquelles l'implantation des protocoles HARQ coopératifs est utile, tout en prenant en compte cette fois le codage canal utilisé. Cette étude analytique constitue la troisième contribution majeure de la thèse.

Le chapitre 5 est consacré à une discussion de deux types de détecteurs à la destination dans un système coopératif avec deux sources d'information corrélées et un relais. En tant que quatrième contribution principale de la thèse, nous dérivons des bornes de la probabilité d'erreur de ce système. Nous démontrons qu'un gain significatif de performance peut être obtenu en exploitant la corrélation entre les sources. En outre, nous comparons ces résultats à un système corrélé sans relais. L'ajout d'un relais à un tel système est particulièrement profitable pour une corrélation entre les sources. Finalement, le contenu de cette thèse est résumé, les principaux résultats sont rappelés et des conclusions sont tirées au chapitre 6. Quelques perspectives pour des travaux futurs sont aussi adressées.

Remerciements

Le travail présenté dans ce rapport vient couronner trois années de travail en vue d'obtenir le titre de Docteur de Télécom Bretagne.

Quoique cet ouvrage représente une très grande satisfaction personnelle, il demeure important d'exprimer mes remerciements à tous ceux qui de façon directe ou indirecte m'ont aidé à réaliser ce travail. Il est donc grand temps, de me lancer dans l'exercice délicat des "remerciements".

J'adresse tout d'abord mes remerciements à mon premier encadrant Alexandre Graell i Amat qui a su m'orienter dans mon travail. J'ai été impressionnée par la richesse de son savoir et ses hautes qualités scientifiques. Je tiens également à exprimer ma gratitude à ma deuxième encadrante Charlotte Langlais qui a eu confiance dès le début en mes capacités. Ses conseils avisés et son sens du détail, alliés à son ouverture et sa bonne humeur, m'ont été extrêmement utiles.

Je souhaite remercier Marion Berbineau pour son rôle en tant que directrice de thèse ainsi que Michel Jézéquel, responsable du département électronique, pour m'avoir accueillie dans son équipe de recherche et pour toute aide logistique qu'il a pu me fournir pour mener à bien mon travail.

Je remercie Guido Montorsi et Raymond Knopp, rapporteurs de thèse, pour avoir accepté de lire et évaluer ce manuscrit, et pour le temps consacré à ce travail.

Merci aussi à Maryline Hélard pour avoir présider le jury de thèse, ainsi qu'à Walaa Hamouda, Laua Conde et Iyad Dayoub pour avoir accepté de faire partie du jury et de lire avec sérieux ce rapport.

Je ne peux m'empêcher d'avoir une pensée émue pour tous mes amis et camarades de bureau qui se sont succédés tout au long de ces trois années : Daoud Karakolah, Roua Youssef et Ammar El Falou, ainsi que tous les autres thésards du département. Avec vous, la bonne humeur est indissociable du bon café, des gâteaux et autres douceurs.

Je ne passerai pas sans avoir exprimer mes vifs remerciements à tout le personnel du département électronique de Télécom Bretagne et celui du service ressources humaines de l'école.

La réalisation de ce travail n'aurait pas été possible sans le soutien moral et affectif d'êtres chers. Je remercie donc les membres de ma famille et mes amis qui ont su, me

comprendre dans tous les moments. Un grand merci à Maher pour m'avoir supportée dans tous les sens du terme. Je remercie également mes parents pour leur appui et leur dévotion. A mon père, tu aurais aimé que je sois Docteur en médecine, je te dédie donc ce titre de Docteur en sciences. Finalement, un dernier merci à mes soeurs et mon frère, vos sourires me faisaient énormément du bien.

Contents

List of Figures

List of Tables

Abbreviations

APP	**A** **P**osteriori **P**robability
AF	**A**mplify-and-**F**orward
ARQ	**A**utomatic **R**epeat Re**Q**uest
AWGN	**A**dditive **W**hite **G**aussian **N**oise
BER	**B**it **E**rror **R**ate
BPSK	**B**inary **P**hase **S**hift **K**eying
CCoop	**C**oded **Coop**eration
CDMA	**C**oded **D**ivision **M**ultiple **A**ccess
CF	**C**ompress-and-**F**orward
CRC	**C**yclic **R**edundancy **C**ode
DF	**D**ecode-and-**F**orward
DL-HARQ	**D**estination **L**evel-**H**ybrid **A**utomatic **R**epeat Re**Q**uest
DMT	**D**iversity-**M**ultiplexing **T**radeoff
DTC	**D**istributed **T**urbo **C**ode
ESE	**E**lementary **S**ignal **E**stimator
FDMA	**F**requency **D**ivision **M**ultiple **A**ccess
FEC	**F**orward **E**rror **C**orrecting
FER	**F**rame **E**rror **R**ate
GPS	**G**lobal **P**ositioning **S**ystem
GSM	**G**lobal **S**ystem for **M**obile
HARQ	**H**ybrid **A**utomatic **R**epeat Re**Q**uest
HSPA	**H**igh **S**peed **P**acket **A**ccess
IDMA	**I**nterleaved **D**ivision **M**ultiple **A**ccess
IR-HARQ	**I**ncremental **R**edundancy-**H**ybrid **A**utomatic **R**epeat Re**Q**uest
ITS	**I**ntelligent **T**ransportation **S**ystem
LOS	**L**ine **O**f **S**ight

LLR	**L**og-**L**ikelihood **R**atio
LTE	**L**ong **T**erm **E**volution
MAP	**M**aximum **A** **P**osteriori
MIMO	**M**ultiple-**I**nput **M**ultiple-**O**utput
MLD	**M**aximum **L**ikelihood **D**ecoding
MMSE	**M**inimum **M**ean **S**quare **E**rror
MRC	**M**aximum **R**atio **C**ombining
M2M	**M**obile-to-**M**obile
NLOS	**N**o **L**ine **O**f **S**ight
PCCC	**P**arallel **C**oncatenated **C**onvolutional **C**ode
RL-HARQ	**R**elay **L**evel-**H**ybrid **A**utomatic **R**epeat Re**Q**uest
RSC	**R**ecursive **S**ystematic **C**onvolutional
SISO	**S**oft-**I**nput **S**oft-**O**utput
SOVA	**S**oft **O**utput **V**iterbi **A**lgorithm
SNR	**S**ignal-to-**N**oise **R**atio
TL-HARQ	**T**wo **L**evel-**H**ybrid **A**utomatic **R**epeat Re**Q**uest
TCCoop	**T**urbo **C**oded **Coop**eration
TDMA	**T**ime **D**ivision **M**ultiple **A**ccess
WiMAX	**W**orldwide **i**nteroperability **M**icrowave for **A**ccess
WLAN	**W**ireless **L**ocal **A**rea **N**etwork

Notations

N_0	Total noise power
σ^2	Variance of the Gaussain noise
β	Path-loss exponent
P	Transmitting power
h	Channel coefficient
w	Additive white Gaussian noise
γ	Instantaneous SNR
W	Channel bandwidth
ρ	Received SNR
$\mathcal{E}$	Expectation operation (mean)
R	System rate
H	Entropy
I	Mutual information
C	Channel capacity
P_{out}	Outage probability
Γ	Mean value of SNR
$\mathcal{C}$	Encoder
η	Throughput efficiency
P_e	Maximum likelihood error probability
r	Multiplexing gain
r_{e}	Effective multiplexing gain
d	Diversity gain
$d(r)$	Diversity-multiplexing tradeoff
R_c	Channel code rate
π	Interleaver
L_a	A priori LLR

L	A posteriori LLR
L_{ch}	Channel LLR
$\mathcal{C}^{-1}$	Decoder
ν	Battacharyya noise parameter
c_0	Turbo code threshold
c_0^P	Punctured turbo code threshold
α	Permeability rate of a punctured code
ϱ	Reliability
T	System throughput
$E[\mathcal{R}]$	Average reward
$E[D]$	Expected inter-renewal time
q	Number of sources in a multiple access scenario
$\mathcal{S}$	Spreading factor
$L_{e,\mathrm{ESE}}$	Extrinsic a posteriori LLR generated by the ESE
$L_{e,\mathcal{C}^{-1}}$	Extrinsic a posteriori LLR generated by the decoder $\mathcal{C}^{-1}$
ζ_{s_i}	Distortion in a multiple access scenario with respect to source s_i
$\mathcal{I}(x)$	Indicator function of the outage status with reference to the received rate x
$\mathcal{O}$	Outage event
C^+	Capacity expression for high-SNR regime
$\mathcal{O}^+$	Outage event for high-SNR regime
μ	Exponential order of the channel coefficient
τ	Asymmetry degree between uplink SNRs
ε	Frame error probability bound
$\bar{\eta}$	Approximated throughput efficiency bound
G_f^{Coop}	Frame error probability cooperation gain
G_t^{Coop}	Throughput efficiency cooperation gain
G_f^{Rtx}	Frame error probability retransmission gain
G_t^{Rtx}	Throughput efficiency retransmission gain
a	Correlation amount between information sources
γ_{opt}	Virtual source-relay-destination channel SNR

To my family...

Chapter 1

Introduction

1.1 Overview and Motivations

The combination of a growing demand for bandwidth-intensive applications and high-reliability services such as video streaming, gaming and data transfer, has increased dramatically the challenges for telecommunications network operators. This demand has been supported by the highly mature wired (optical) communication technology. Nevertheless, this solution is not responding to a primary customer requirement: the continual access to information. Therefore, wireless communication is still one of the most researched areas in the field of modern communication in the aim of making mobile communication an "anywhere, anytime, anyway, anything" technology.

Nevertheless, the wireless channel suffers from signal attenuation and interference problems, which impose major communication challenges such as avoiding fading and shared access. Although the research in this field has achieved remarkable results, further efforts are still needed in order to provide throughput comparable to the wired medium. Consequently, the challenge for the wireless research community has always been to design communication systems which continue to achieve reliable transmission, high spectral and power efficiency and are able to mitigate the fading and interference effects. The effects of fading can be combated by using diversity in time, frequency or space, by transmitting the signal over multiple channels that experience independent fading. Among all these diversity techniques, a crucial tool for mitigating fading while preserving the spectral resources (time and frequency) is spatial diversity, carried out through multiple-antenna implementation at the source and/or the destination terminals.

On the other hand, to benefit from spatial diversity gain offered by the multiple-input-multiple-output (MIMO) technology [Win87], antennas need to be sufficiently spaced, typically one half of the wavelength, to enable transmission via spatially uncorrelated channels. Many wireless devices have limited size or hardware complexity, therefore it

is not always possible to employ multiple antennas at the device. Due to these practical constraints, the MIMO implementation is often limited to base stations and access points. Cooperation between wireless terminals has been recently proposed as an efficient alternative to provide spatial diversity, while avoiding the terminal size constraint. The key idea of cooperative communications is that several nodes in a wireless network can achieve spatial diversity by relaying messages from each other. The idea is then to exploit the inherent broadcast nature of the wireless channel. On this line, cooperative retransmission protocols are considered as particularly promising technology due to their opportunistic and flexible exploitation of both spatial diversity and time resources. These protocols are in the border line between two important communication paradigms, cooperation from neighboring terminals and opportunistic reallocation of available resources to terminals with a satisfactory channel state (retransmission process). Indeed, conventional cooperative schemes commonly assign a dedicated (continuously fixed) resource to neighboring terminals to relay the information from the source. It was recognized that this approach can lead to a possible waste of resources due to unnecessary transmissions [ABS08]. For example, if the source can deliver its message to the destination without any assistance, the resource assigned to relaying is needlessly wasted. The cooperative retransmission protocols are proposed to enable significant resources savings by avoiding unnecessary transmissions, as the relays are involved only if their assistance is needed [SSBNC06].

Many cooperative retransmission protocols have been proposed in the context of wireless cellular networks. The key idea of this concept was originally proposed in [ZV05]. Furthermore, conventional retransmission protocols have been extended to cooperative relaying systems in order to make the wireless link more reliable and cooperative communication more efficient [ZHF04, NAGS05, YZQ06, YZQ07, SSBNC06, Nar08, LL08, AFH08, LSBM10].

The reliability of cooperative Hybrid Automatic Repeat Request (HARQ) protocols with respect to conventional ones (without cooperation) is verified in [ZHF04, YZQ06, YZQ07], since it offers spatial diversity and path loss reduction by relaying. On the other hand, in [NAGS05], authors showed the efficiency of cooperative HARQ compared to the non-ARQ cooperation by avoiding unnecessary transmissions. Further works on cooperative HARQ protocols evaluated their performance by adopting an information theoretic approach. The assets of cooperative HARQ protocols have been investigated from the standpoint of outage behavior [LTW04, LSBM10], throughput [ZV05, SSBNC06, SSBN06] and diversity-multiplexing tradeoff (DMT) [NAGS05, AGS05, TDK07, AGS08]. Furthermore, other works studied these protocols from an optimization point of view by maximizing the throughput as a function of the transmission rate or the relay location [Nar08, LL08]. All these works explore exclusively the case of

one source node assisted by one or multiple relay nodes. Only few works extended the idea of cooperative HARQ to the case of user cooperation [AFH08, ZWW09].

The user cooperation can be used instead of relaying, enabling the relay mobile to simultaneously transmit its own independent information over the wireless network. This, as we will show, is preferred to the relaying scheme, since it provides higher throughput and robustness to channel variations for *both* the transmitting and relaying mobiles. Moreover, in the traditional relaying scheme, where there is a limited number of relay nodes, the sources have to compete with each other by queuing to enjoy the possible diversity gain offered by the relay, since it can assist only one source at a time. However, in multiple-source systems, we can overcome the shortage of relays and consequently we avoid user competition by favorizing rather user cooperation.

In [AFH08], it was proposed an adaptive HARQ protocol based on an incremental redundancy scheme with rate-compatible punctured convolutional codes (RCPCs). By employing a feedback channel from the partner node, each user incrementally decreases its coding rate in the first cooperation phase in order to increase its chances of being correctly decoded by the partner node. Thus, it benefits from spatial diversity, while preserving as much resources as possible to provide relaying diversity for the other user. In [ZWW09], cooperation and HARQ were implemented by a distributed space-time code. In particular, two HARQ protocols for the two-source cooperating system employing Alamouti space-time codes were investigated. According to different feedback schedules at the destination, two basic retransmission protocols,namely post-cooperating and pre-cooperating, were proposed and analyzed.

The contributions of this dissertation consist of two point. First, we propose to combine the user cooperation strategy with HARQ protocols based on capacity-approaching channel codes; in particular, we consider turbo codes. The goal of these cooperative HARQ protocols in the two-source network, based on the turbo coded cooperation scheme, is twofold: first to increase throughput, by avoiding transmissions when unnecessary; second to improve error rate performance by increasing distributed spatial diversity gain. In addition, combining HARQ protocols with the turbo coded cooperation scheme, we benefit not only from cooperative/retransmission diversity, but also from coding and turbo processing gain.

Second, we explore another application domain of cooperative communications. We consider wireless sensor networks, where neighboring sensors measure data that is statistically dependent. Source correlation can be exploited at the transmitter and at the receiver side, through joint source-channel coding techniques, to improve performance. Several works on joint source-channel coding can be found in the literature [LZG02]. The aim of these works is twofold: first, to exploit the source correlation to allow reliable communication [LZG02]; second, to enable significant power savings for data transmission through the use of data compression for the sake of a longer sensor lifetime. Most

of these previous works explore exclusively the case of non-cooperative communications. Recently, few works extended the idea to cooperative networks, e.g. [BSTS10], where sensors can transmit data through common processing nodes before reaching the destination. However, these works are very limited and consider very specific cases. In this thesis, source correlation can be exploited at the receiver side. We show that taking into account the source correlation at the relay and at the destination leads to significant performance gains.

1.2 Contributions and Outlines of the Dissertation

This thesis is organized in the typical-order way, where the basic concepts are presented in the beginning and the new contributions in the following chapters.

As an introduction to the topics studied in this thesis, we provide in Chapter 2, a fairly general system model of wireless channel, some basic concepts about information theory and the basic ideas behind error control systems, which are required for the next chapters. First, we present wireless channel impairments that will guide the design decisions of the proposed communication systems. We provide an overview of forward error correcting codes and retransmission protocols and the tools to analyze their behavior. The chapter is completed by addressing multi-source transmission techniques and presenting the source correlation problem, suggested to be extended to cooperative networks.

In Chapter 3, we summarize the basic concepts of cooperative communications. In particular, we start by reviewing the key results of the relay channel and we address the existing distributed turbo coding scheme for this model. In addition, we give a brief review of cooperative HARQ protocols proposed in the literature. We further detail the coded cooperation scheme as well as the turbo coded cooperation scheme, used as a starting point to design proposed cooperative HARQ protocols. Beside giving an overview of the state-of-the-art, the first contribution of the thesis is provided in the end of this chapter. So, we formally introduce and evaluate three different HARQ protocols for a two-source wireless network with turbo coded cooperation. They consider both link reliability and system efficiency.

The implementation of almost any novel technology is typically hindered by the new challenges that emerge with it. Cooperative retransmission protocols are by no means exception to this rule. It is noted that all identified issues are not specific to cooperative retransmissions, but are inherited from cooperative and retransmission paradigms. Therefore, in Chapter 4, we analyze the outage behavior of the proposed HARQ protocols in order to evaluate them according to different parameters: channel conditions, rate and time allocation. As it is shown that the protocols have the same diversity order, to better distinguish between them, we perform a diversity-multiplexing tradeoff

analysis. Furthermore, we define two parameters to assess the benefits of the proposed protocols over the non-cooperative point-to-point incremental redundancy scheme as well as over the conventional turbo coded cooperative system when no retransmission is allowed. The basis of this performance analysis is the so-called code threshold of a turbo code ensemble, given in [SLS03]. Combined with the outage concept, a frame error probability bound can be derived, that predicts well the simulation results. This analytical framework is adopted to determine the geometric conditions under which using cooperative HARQ protocols is useful.

Chapter 5 is devoted to a discussion of two types of detectors at the destination in an uncoded decode-and-forward cooperative system with two correlated information sources and one relay. As a third main contribution of the thesis, we derive bounds on the error probability of this considered system. Furthermore, we demonstrate the performance gain that can be obtained by exploiting the correlation between the sources and we compare these results to a correlation-aware system without relay.

The contents of this thesis are summarized, the main results are pointed out and conclusions are drawn, in Chapter 6. Proposals for future work are outlined as well.

Chapter 2

Point-to-Point Communications

Before addressing cooperative techniques over wireless networks, we start by a brief review of point-to-point communication systems. In this chapter, we provide an overview of the wireless channel and the basic ideas behind error control systems. First, in Section 2.1 we describe the significant channel distortions affecting wireless transmissions. The considered channel conditions guide the design decisions of the communication system. Thereafter, in Section 2.2 common information theoretic tools that are relevant to study the wireless channel, are reviewed. In Sections 2.4 and 2.5, two common techniques of error control are presented: *forward error correcting* (FEC) codes and retransmission protocols. These concepts are presented in order to facilitate the understanding of their contribution when extended in the context of a cooperative system. Furthermore, in Section 2.6, we address multi-source transmission techniques used to separate each source data and we describe in more details the technique adopted in our work for non-orthogonal scenarios, i.e., scenarios with superposed transmitted signals. This signal superposition is noted when different sources are allocated the same transmission slot and frequency band. Finally, in Section 2.7, we present the problem of transmission of correlated sources over a multiple access channel.

2.1 Wireless Channel Impairments

In this section, we discuss the properties of the wireless channel, which motivates the design decisions made in this thesis. In a wireless network, the data which is transferred from a transmitter to a receiver has to propagate through a physical medium, or wireless channel. During propagation several phenomena will distort the signal. In the following we briefly describe the channel impairments (noise, path loss propagation and fading) which can be modeled stochastically, as presented in the last sub-section.

2.1.1 Noise

For a typical communication system, the noise is generally modeled as an additive distortion. The main sources of noise in a wireless network are the combination of a wide variety of sources, ambient heat in the transmitter/receiver, co-channel and adjacent channel interference from other communications systems, climatic phenomena and even cosmic background radiation [Wic95]. This noise is stochastically modeled using a zero-mean Gaussian probability density with variance σ^2. The total noise power will be $N_0 = 2\sigma^2$. This noise model is known as *additive white Gaussian noise* (AWGN). The *signal-to-noise ratio* (SNR) is a widely used value to indicate the signal quality at the receiver. It is an important parameter used to quantify the noise with respect to the signal.

2.1.2 Path Loss and Fading

The signal is attenuated mainly by the effects of path loss and fading, both representing multiplicative distortions. The path loss effect is defined as the signal power attenuation resulting from propagation over long distances. As long as the distance between the transmitter and the receiver does not change too much, it can be assumed to be constant for the whole transmission.

When the receiver and the transmitter are separated by a distance d, it is generally considered that the power of the received signal is attenuated proportionally to $d^{-\beta}$, where β denotes the path-loss exponent and it is often assumed to be $2 \leq \beta \leq 6$ [Ber00]. For instance, the path loss exponent β is assumed to be 2 in the case of propagation in free space. For lossy environments, β can be in the range of 4.

Furthermore, in wireless channels, the presence of obstacles cause different effects such as reflections, diffractions or shadowing effects, resulting in multi-path propagation which induces fadings. The so-called multi-path propagation causes that different parts of the transmitted signal spectrum to be attenuated differently, which is known as frequency-selective fading. In addition to this, due to the mobility of transmitter and/or receiver or some other time-varying characteristics of the transmission environment, the principal characteristics of the wireless channel change in time which results in time-varying fading of the received signal.

A lot of statistical models exist to describe the time-varying nature of the received signals. The most known are the Rayleigh distribution in the *no line of sight* (NLOS) case and the Rice distribution in the *line of sight* (LOS) case. In the course of the thesis, we will consider the Rayleigh distribution to model fading channels.

The coherence bandwidth measures the separation in frequency after which two signals will experience uncorrelated fading.

- In flat fading, the coherence bandwidth of the channel is larger than the bandwidth of the signal. Therefore, all frequency components of the signal will experience the same magnitude of fading.
- In frequency-selective fading, the coherence bandwidth of the channel is smaller than the bandwidth of the signal. Different frequency components of the signal therefore experience decorrelated fading.

2.1.3 Channel Model

We consider a Rayleigh flat fading channel with AWGN. The receiver is at distance d of the transmitter, which is transmitting with power P. At the destination, the received symbol y from the transmitter is given by:

$$y = hx + w \tag{2.1}$$

where x denotes the modulated symbol. Throughout this thesis, we consider *binary phase shift keying* (BPSK) modulation, i.e., $x \in \{\pm 1\}$. w is the AWGN and h is a zero-mean, circularly symmetric complex Gaussian random variable and is assumed to be constant over the transmission of a frame. This block fading channel model is considered in order to investigate the ability of the distributed spatial diversity to enhance link level performance in scenarios where temporal diversity is limited or unavailable. We denote by γ the instantaneous SNR and it is given by

$$\gamma = \frac{|h|^2 P}{N_0 W} = |h|^2 \rho \tag{2.2}$$

where W is the channel bandwidth and ρ is the received SNR.

The energy per bit to noise ratio is denoted by γ^b, and is given by

$$\gamma^b = \gamma / R \tag{2.3}$$

where R is the rate of the system, including the effective channel utilizations.

2.2 Channel Capacity

This section introduces most of the basic definitions required for the subsequent development of the theory. The concept of information is too broad to be captured completely by a single definition. However, for any probability distribution, we define the *entropy* as an intuitive notion of what a measure of information is. This notion is extended to define the *mutual information*. The notions of *capacity* and *outage* are

given to introduce the limits for channel coding. Finally, the trade-off between diversity and multiplexing, known as *diversity-multiplexing tradeoff* (DMT) is formally defined.

2.2.1 Entropy and Mutual Information

We will first introduce the concept of entropy, which is a measure of uncertainty of a random variable. Let X be a discrete random variable with alphabet $\mathcal{X}$ and a probability mass function $p(x) = \Pr(X = x),\ x \in \mathcal{X}$. The entropy $H(X)$ of a discrete random variable X is defined by

$$H(X) = -\sum_{x \in \mathcal{X}} p(x) \log_2 p(x) \tag{2.4}$$

We now extend the definition to a pair of random variables. The joint entropy $H(X,Y)$ of a pair of discrete random variables (X,Y) with joint distribution $p(x,y)$, where y takes values in an alphabet $\mathcal{Y}$, is defined as

$$H(X,Y) = -\sum_{x \in \mathcal{X}} \sum_{y \in \mathcal{Y}} p(x,y) \log_2 p(x,y) \tag{2.5}$$

We also define the conditional entropy of Y given the knowledge of X as

$$H(Y|X) = -\sum_{x \in \mathcal{X}} \sum_{y \in \mathcal{Y}} p(x,y) \log_2 p(x|y) \tag{2.6}$$

The naturalness of the definition of joint entropy and conditional entropy is exhibited by the following *chain rule*

$$\begin{aligned} H(X,Y) &= H(X) + H(Y|X) \\ &= H(Y) + H(X|Y) \end{aligned} \tag{2.7}$$

For a continuous random variable X with a probability density function $p(x)$, the entropy is replaced by the differential entropy which is defined as

$$H(X) = -\int_{x \in \mathcal{A}} p(x) \log_2 p(x) dx \tag{2.8}$$

where $\mathcal{A}$ is the support set of the random variable X. We now define the mutual information, a measure of the amount of information that one random variable contains about another random variable. The mutual information $I(X,Y)$ is defined as the relative entropy between the joint distribution and the product distribution $p(x)p(y)$, i.e.,

$$I(X;Y) = -\sum_{x \in \mathcal{X}} \sum_{y \in \mathcal{Y}} p(x,y) \log_2 \frac{p(x,y)}{p(x)p(y)} \tag{2.9}$$

From the definitions of entropy and mutual information, we can show that

$$\begin{aligned} I(X;Y) &= H(X) - H(X|Y) \\ &= H(Y) - H(Y|X) \end{aligned} \tag{2.10}$$

In the continuous domain, the mutual information is given by

$$I(X;Y) = -\int p(x,y) \log_2 \frac{p(x,y)}{p(x)p(y)} \tag{2.11}$$

2.2.2 Capacity and Outage Probability

A key information theoretic result, established by Shannon [Sha48], defines the channel capacity as the maximum of the mutual information between the input and output of the channel, with respect to the input distribution.

$$C = \max_{p(x)} I(X;Y) \tag{2.12}$$

Given a transmitted power constraint P, a bandwidth W, and an AWGN channel with N_0 total power, then the channel capacity for Gaussian distributed input variables is given by

$$\begin{aligned} C &= W \log_2 \left(1 + \frac{P}{W N_0}\right) \\ &= W \log_2 (1+\rho) \quad \text{bits per channel use} \end{aligned} \tag{2.13}$$

Consequently, this formula highlights the interplay between 3 key system parameters: channel bandwidth, average transmitted or received signal power and noise power at the channel output.

The outage probability is an important measure for the performance evaluation of communication systems over block fading channels. It can be defined as the probability that the capacity of the channel falls below R, the required data rate. It can then be written as

$$P_{\text{out}} = \Pr(C < R) \tag{2.14}$$

In this case, we say that the channel is in outage. Figure 2.2.2 shows the unconstrained outage probability for a rate R = 1/2 with Gaussian input variables, given by

$$\begin{aligned} P_{\text{out}} &= \Pr\left(\log_2\left(1 + |h|^2\rho\right) < R\right) \\ &= \Pr\left(\log_2(1+\gamma) < R\right) \\ &= 1 - \exp\left(-\frac{2^R - 1}{\Gamma}\right) \end{aligned} \tag{2.15}$$

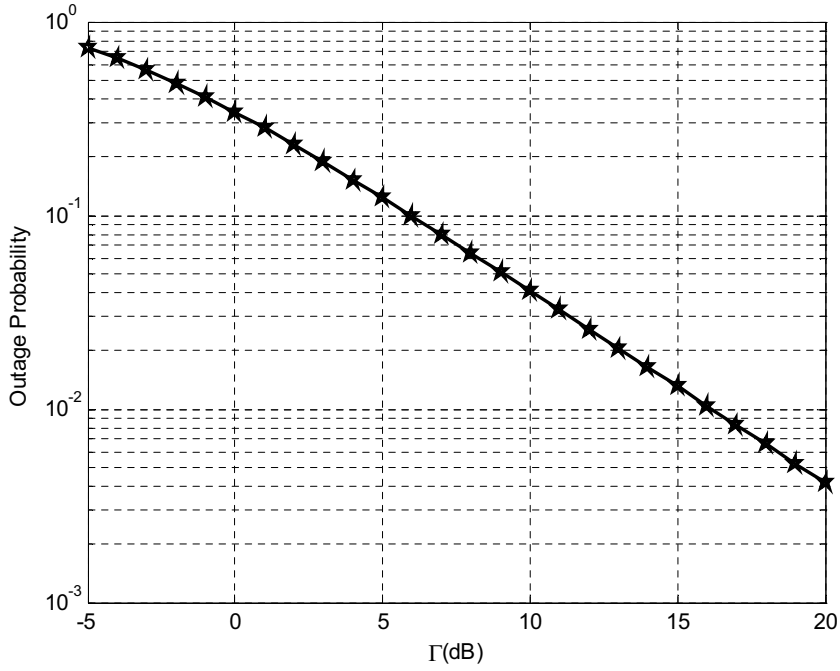

FIGURE 2.1: Outage probability for Gaussian distributed input variables for a rate R = 1/2 over Rayleigh block fading channel.

where $\Gamma = \rho\mathcal{E}[|h|^2]$ denotes the mean value of the SNR of the channel.

2.3 Diversity Techniques

Diversity techniques are used to mitigate the effects of fadings due to the multi-path phenomenon. The basic concept of diversity is to transmit the signal over several independent diversity branches to get independent signal replicas via:

- time diversity,
- frequency diversity,
- space diversity.

In frequency diversity, the message is transmitted on multiple carrier frequencies spaced sufficiently far apart so as to provide independent fading versions of the channel. In time diversity, the message is transmitted in different time slots, providing signal repetition [Pro00]. Both of these methods are wasteful in that they are using excessively the channel bandwidth. Another method to mitigate the effects of fading is spatial diversity. With spatial diversity, multiple receiving antennas are spaced at least half a wavelength of the carrier frequency apart to ensure that the signals reaching them are statistically independent [WSG94]. The cooperative diversity achieves antenna diversity gain by using the cooperation of distributed antennas belonging to each node. It is known

as macroscopic spatial diversity and it is performed by exploiting the inherent broadcast nature of the wireless channel.

2.3.1 Diversity-Multiplexing Tradeoff

The DMT was formally defined and studied in the context of point-to-point coherent multiple antenna communications in [ZT03]. It is defined in order to understand the interplay between rate and reliability in the high SNR regime. In [ZT03], it was found that the design of channel codes aim to achieve either the full diversity or the full multiplexing gain offered from the channel. Furthermore, the DMT framework is usually adopted as a helpful performance metric to stress the difference between several systems achieving the same diversity order.

Next, we summarize several important definitions that will be used for the DMT analysis:

1. A function $f(\rho)$ is said to be *exponentially equal to* ρ^b when

$$\lim_{\rho\to\infty} \frac{\log\left(f(\rho)\right)}{\log\left(\rho\right)} = b. \tag{2.16}$$

   Exponential equality is denoted by $\doteq$, i.e., $f(\rho) \doteq \rho^b$. b is called the *exponential order* of $f(\rho)$.

2. We consider a family of codes $\{\mathcal{C}(\rho)\}$ such that the code $\mathcal{C}(\rho)$ has a rate $R(\rho)$, a throughput efficiency $\eta(\rho)$ and a maximum likelihood error probability $P_e(\rho)$. For this family, the multiplexing gain, the effective multiplexing gain (also known as the effective rate), and the diversity gain are defined, respectively, as:

$$r = \lim_{\rho\to\infty} \frac{R(\rho)}{\log\left(\rho\right)} \tag{2.17}$$

$$r_{\mathrm{e}} = \lim_{\rho\to\infty} \frac{\eta(\rho)}{\log\left(\rho\right)} \tag{2.18}$$

$$d = -\lim_{\rho\to\infty} \frac{\log\left(P_e(\rho)\right)}{\log\left(\rho\right)} \tag{2.19}$$

Depending on the choice of the system multiplexing gain r, a different level of diversity performance, $d(r)$, can be achieved. For a coherent MIMO channel with M transmit antennas and N receive antennas, and for any multiplexing gain $r \leq \min(M, N)$, the optimal diversity gain $d(r)$ is given by the piecewise linear function joining the points $(i, (M, i)(N, i))$ for $i = 0, ..., \min(M, N)$. $d(r)$ is achieved by the random Gaussian independent and identically distributed (i.i.d.) code ensemble for all frame durations $t \geq M + N - 1$. This is depicted in Figure 2.2.

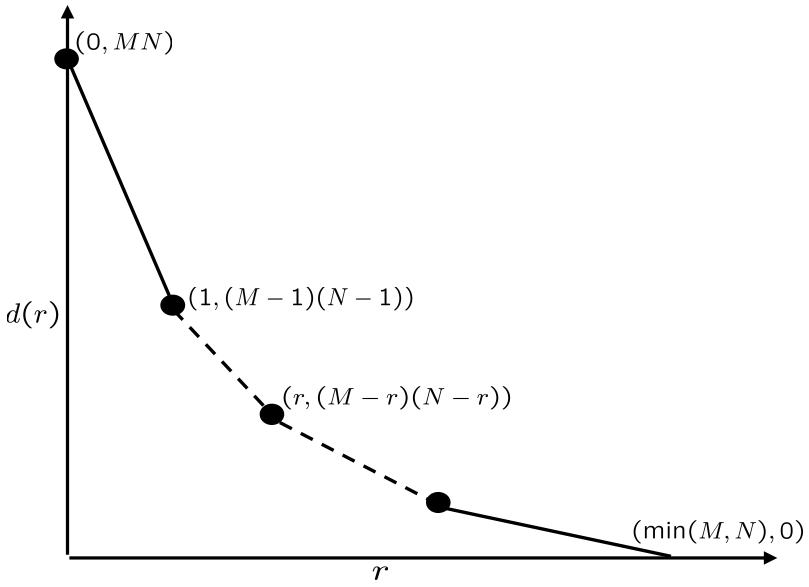

FIGURE 2.2: The optimal diversity-multiplexing tradeoff of a MIMO system.

2.4 Background on Forward Error Correcting

The diversity techniques were introduced to combat wireless channel impairments. However, these techniques remain mostly insufficient to guarantee a reliable transmission. Therefore, we have to further use the FEC scheme, a system of error control for data transmission. *Forward* refers to the non feedback aspect of error control where a code automatically corrects errors detected at the receiver. The main idea behind channel coding is to introduce a carefully designed redundancy to the information data in order to make the transmission more reliable. However, this operation causes a reduction in data rate or an expansion in bandwidth. In this section, we describe some well-known channel codes considered in the course of the thesis.

2.4.1 Rate Compatible Punctured Convolutional Codes

Convolutional codes are extensively used in various applications in order to achieve reliable transmission. Figure 2.4.1 shows the block diagram of a convolutional encoder with memory $m = 3$. D represents the memory register, responsible of forwarding the bits with a delay of one time unit. Such a code is referred to as systematic, since the input being encoded is included in the output sequence. The code is recursive because the current memory bits are fed back to compute the new memory bits. The code rate is $R_c = 1/2$. It is defined as the ratio between the information bits and the total coded bits, which corresponds for this example to two coded bits for each information bit. The generator polynomials in octal form of this *recursive systematic convolutional* (RSC) code are $(13, 15)_8$.

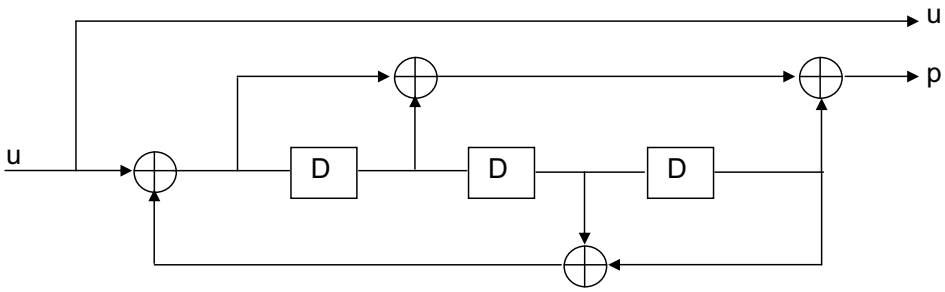

FIGURE 2.3: Encoder structure of rate 1/2 recursive systematic convolutional code with memory $m = 3$.

These codes are characterized by a fixed code rate. However, in some cases, one would like to be more flexible. Variable-rate codes are then required, adapted to the source and channel needs. Punctured convolutional codes, first introduced by Cain, Clark, and Geist [CCG79], are mainly used to meet flexibility needs. This can be achieved by not transmitting certain coded bits, namely, by puncturing the code, without changing the encoder/decoder basic structure. Punctured codes are typically used to obtain new codes with higher rate than that of the mother code. The permeability rate is then defined as the ratio between surviving bits and the total mother coded bits. Rate compatible punctured coding is a restriction in that the coded bits of a high rate code are also included among the coded bits of a lower rate code. These channel codes are widely employed in an incremental manner in retransmission-based systems. There are many algorithms to decode convolutional codes as well as rate compatible punctured convolutional codes. Maximum likelihood decoding can be done using the Viterbi algorithm. Other decoding algorithms such as *soft output Viterbi algorithm* (SOVA) [HH89] and the BCJR algorithm [BCJR74] are also commonly used, they are denoted as *soft-input soft-output* (SISO) decoders. The BCJR algorithm is also known as the *maximum a posteriori* (MAP) algorithm, which maximizes the a posteriori probability. In this thesis, we use this decoder for simulation results.

2.4.2 Parallel Concatenated Convolutional Codes

Concatenated codes form a class of error-correcting codes that are obtained by cascading two codes; an inner code and an outer code. The concept of concatenated codes was first addressed in 1966 in [For66] as a solution to design powerful codes with reasonable computational complexity. The basic concatenated coding scheme proposed by Forney is now called a serially concatenated code. Turbo codes, as introduced first in [BGT93], implemented a parallel concatenation of two convolutional codes, with an interleaver between the two codes. The designation, *turbo code*, comes from the iterative decoder structure. It becomes the first practical code which closely approached the channel capacity.

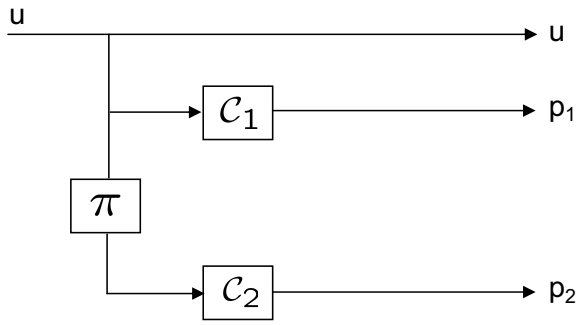

FIGURE 2.4: Parallel Concatenated Convolutional Codes.

Figure 2.4 shows a block diagram of a parallel concatenated convolutional code (PCCC) structure. This PCCC consists of two constituent encoders $\mathcal{C}_1$ and $\mathcal{C}_2$ linked by an interleaver π. Interleaving involves reordering the elements within a frame of data. A more general PCCC can have more than two constituent encoders and more than one interleaver. A key feature of PCCCs is the presence of interleavers between the different constituent encoders. By using an interleaver, we are able to increase the Hamming weight of each concatenated codeword and meanwhile reduce the number of sequences with low weight. PCCCs show very good performance at low and medium SNRs. However, it is well known that the performance of PCCCs is not be so good at very high SNRs, compared to serially concatenated convolutional codes.

A natural reliability value for the exchange of soft information is the *log-likelihood ratio* (LLR). Before detailing the iterative decoding process, we will briefly describe the LLR.

2.4.2.1 Log-Likelihood Ratios

The LLR for x with a priori probability $p(x)$ is defined as

$$L_a(x) = \log \frac{p(x=+1)}{p(x=-1)} \tag{2.20}$$

$L_a(x)$ is the *a priori* knowledge about the random variable x. For a transmission channel with transition probability $p(y|x)$, the a posteriori LLR value of x, conditioned on the received signal y, is

$$L(x|y) = \log \frac{p(x=+1|y)}{p(x=-1|y)} \tag{2.21}$$

The sign of $L(x|y)$ provides the hard decision on x, and the magnitude $|L(x|y)|$ tells the reliability of this decision. The larger $|L(x|y)|$ is, the more sure we are about the decision. Applying Baye's rule, we have

$$L(x|y) = \log \frac{p(x=+1)}{p(x=-1)} + \log \frac{p(y|x=+1)}{p(y|x=-1)} = L_a(x) + L_{ch}(y|x) \tag{2.22}$$

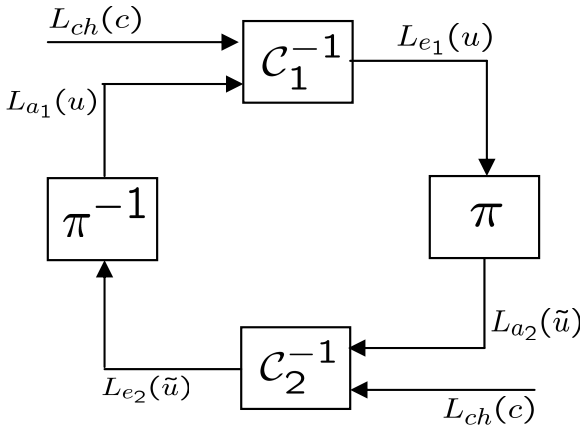

FIGURE 2.5: Iterative decoder of a PCCC.

For a Rayleigh fading channel, the channel LLR $L_{ch}(y|x)$is given by

$$L_{ch}(y|x) = \log \frac{p(y|x=+1)}{p(y|x=-1)} = \log \frac{\frac{1}{2\pi\sigma^2} \exp\left(\frac{-(y-h)^2}{2\sigma^2}\right)}{\frac{1}{2\pi\sigma^2} \exp\left(\frac{-(y+h)^2}{2\sigma^2}\right)} = \frac{2yh}{\sigma^2} \tag{2.23}$$

where h is the channel coefficient, as defined in Section 2.1.

2.4.2.2 Iterative Decoding

Figure 2.5 shows the structure of the iterative PCCC decoder. It contains a separate SISO decoder for each of the constituent encoders in the PCCC structure: Decoder $\mathcal{C}_1^{-1}$ is the SISO decoder corresponding to encoder $\mathcal{C}_1$ and decoder $\mathcal{C}_2^{-1}$ the one corresponding to encoder $\mathcal{C}_2$. The considered decoders use the BCJR algorithm.

Iterative (turbo) decoding of PCCCs involves an exchange of information between two components decoders $\mathcal{C}_1^{-1}$ and $\mathcal{C}_2^{-1}$. This exchange is enabled by linking the a priori probability soft input of one component decoder ($L_{a_1}(u)$ or $L_{a_2}(\tilde{u})$) to the extrinsic probability soft output provided by the other component decoder ($L_{e_1}(u)$ or $L_{e_2}(\tilde{u})$). Each SISO decoder computes the extrinsic information related to the information symbols (u), using the observation of the associated systematic and parity symbols (c) coming from the transmission channel ($L_{ch}(c)$), and the a priori. Since no a priori information is available from the decoding process at the beginning of the iterations, they are fixed to 0. In practice, the iterative decoding process is executed in a sequential manner. The decoding process starts arbitrarily with either decoder, $\mathcal{C}_1^{-1}$ for example. $\mathcal{C}_1^{-1}$ computes the a posteriori LLRs $L(u)$ and the extrinsic information $L_{e_1}(u)$. Next, $\mathcal{C}_2^{-1}$ is processed. $\mathcal{C}_2^{-1}$ is fed by the channel observation from the demodulator $L_{ch}(c)$ and the a priori information $L_{a_2}(\tilde{u})$ from $\mathcal{C}_1^{-1}$. $L_{a_2}(\tilde{u})$ is the interleaved version of $L_{e_1}(u)$ and $L_{e_1}(u) = L(u) - L_{a_1}(u)$. After $\mathcal{C}_1^{-1}$ processing is completed, $\mathcal{C}_2^{-1}$ starts processing. In

its turn, $\mathcal{C}_2^{-1}$ computes the a posteriori probability $L(\tilde{u})$ and forwards extrinsic information $L_{e_2}(\tilde{u}) = L(\tilde{u}) - L_{a_2}(\tilde{u})$ to $\mathcal{C}_1^{-1}$. In the next iteration, this extrinsic information is deinterleaved and serves as an a priori to $\mathcal{C}_1^{-1}$. This process is repeated until a fixed maximum number of iterations is reached or an early stopping criterion is fulfilled.

2.4.3 Bounds on the Frame Error Probability for Turbo Codes in Block Fading Channels

Coding for block fading channels has been addressed in [ML99] and [KH00]. The authors primarily considered the performance of convolutional codes based on a pairwise error probability and the union bound analysis. Unlike the performance of convolutional codes, the *frame error rate* (FER) performance of turbo codes exhibits a threshold behavior. This sub-section is devoted to a theoretic study of turbo codes. A threshold behavior analysis of the codes in the turbo code ensemble under *maximum likelihood decoding* (MLD) is conducted. It is well known that the optimal MLD is not possible for concatenated codes due to its high complexity. However, since the iterative decoding algorithm is a close approximation to MLD, it is important to know the MLD potential for this class of codes. In the following, we briefly present the performance analysis of a general mother turbo code on time-invariant (block fading) channels, as established by Jin and McEliece in [JJ02]. Likewise, results on punctured turbo codes are reviewed.

2.4.3.1 Performance of Turbo Codes

We consider a binary input memoryless channel with output alphabet Ω and transition probabilities $p(y|0)$ and $p(y|1)$, $y \in \Omega$. When a codeword $\mathbf{c} \in \mathcal{C} \subseteq \{0,1\}^n$ has been transmitted, the *Battacharyya noise* parameter is defined as

$$\nu = \sum_{y \in \Omega} \sqrt{p(y|0)p(y|1)} \tag{2.24}$$

if Ω is discrete and as

$$\nu = \int_{y \in \Omega} \sqrt{p(y|0)p(y|1)}dy \tag{2.25}$$

if Ω is a measurable subset of $\mathbb{R}$.

In [Div99], the performance threshold behavior of a block code is studied. For a linear block code $\mathcal{C}$ with weight enumerator A_d, the number of codewords of weight d, we have the well-known *union-Battacharyya bound* on the MLD frame error probability with a large codeword length n that satisfies

$$P_W^{\mathcal{C}}(\nu) \leq \begin{cases} \sum_{d=D_n}^{n} A_d \nu^d & -\log \nu > c_0, \\ 1, & -\log \nu \leq c_0 \end{cases} \tag{2.26}$$

where D_n is a sequence of numbers such that

$$D_n \to \infty \text{ and } \frac{D_n}{n^\epsilon} \, \forall \epsilon > 0 \tag{2.27}$$

For a given turbo code ensemble with rate R_c, there exists a code threshold c_0 such that for any binary input memoryless channel whose Battacharyya noise parameter ν is less than $\exp(-c_0)$, the average MLD frame error probability approaches zero at least as fast as n^{-L}, where L is the interleaver gain exponent [JJ02, DP95]. This code threshold of the union bound is then given by

$$c_0 = \limsup_{n\to\infty} \max_{D_n < d \leq n} \frac{\log A_d}{d} \tag{2.28}$$

For turbo codes with $L \geq 2$ constituent recursive convolutional encoders, we can rewrite (2.26) as follows

$$P_W^{\mathcal{C}}(\nu) \leq \begin{cases} O\left(n^{-L}\right) & -\log \nu > c_0, \\ 1, & -\log \nu \leq c_0 \end{cases} \tag{2.29}$$

Based upon earlier results, we can develop a union bound on the MLD frame error probability of turbo codes over block fading Rayleigh channels. Thus, the Battacharyya noise parameter ν is a function of the fading coefficient h, which is invariant for the whole codeword transmission period. Consequently, the FER union-Battacharyya bound is also a function of the fading coefficients. For instance, for a block fading Rayleigh channel, the Battacharyya noise parameter is given by

$$\nu = \exp(\gamma) \tag{2.30}$$

where the instantaneous SNR γ is defined in Section 2.1.

The MLD frame error probability for a block fading Rayleigh channel can then be bounded as

$$\begin{aligned} P_e &= \mathcal{E}\left[P_W^{\mathcal{C}}(\nu)\right] \\ &\leq p\left\{-\log \nu \leq c_0\right\} + O\left(n^{-L}\right) \end{aligned} \tag{2.31}$$

Figure 2.6 shows the union bound and simulation results for the frame error probability of a turbo code. We evaluate the performance of an eight-state turbo code, reported in [DP95], employing two RSC encoders with rate 1/3 associated through an S-random interleaver. The constituent codes have $(1, \frac{11}{13}, \frac{11}{13})_8$ as generator polynomials. The overall code rate is 1/5.

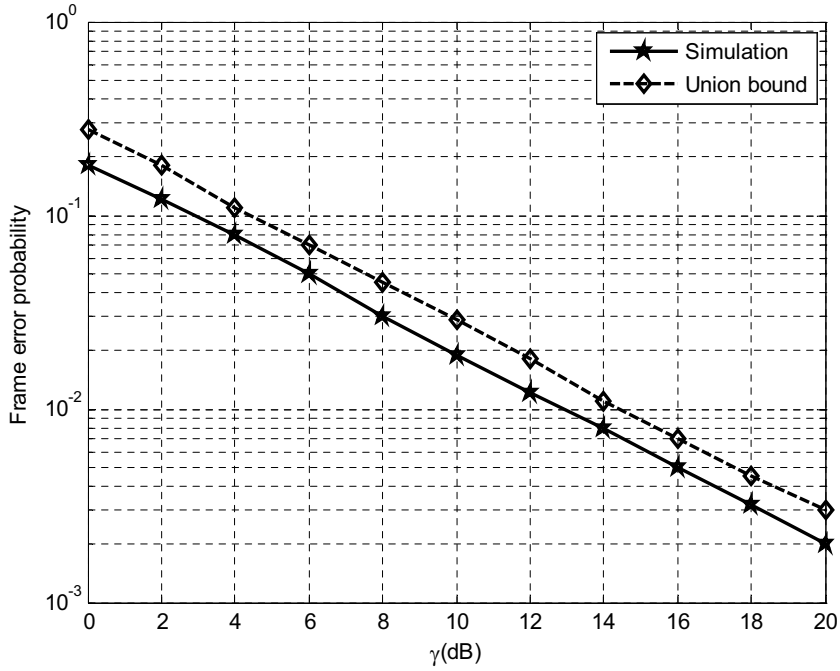

FIGURE 2.6: Frame error probability performance of a turbo code after 8 iterations for k = 128 bits. A Rayleigh block fading channel is assumed with BPSK modulation.

2.4.3.2 Performance of Punctured Turbo Codes

The asymptotic performance analysis of punctured turbo codes is given in [LSS03, SLS03]. The authors proved that, for punctured turbo code ensembles, if the permeability rate is α, the threshold of the punctured code is given by

$$c_0^P = \log \frac{\alpha}{\exp(-c_0) - (1-\alpha)} \tag{2.32}$$

where α is defined as the ratio between the number of surviving bits and the number of mother code bits.

2.5 Background on Retransmission Protocols

FEC is a powerful method to achieve good performance when no feedback is available at the transmitter. We now consider the alternative approach to reliable communications, namely, retransmission protocols. This approach, denoted as *automatic repeat request* (ARQ), provides reliability based on retransmissions and is used when a feedback channel is available. The feedback channel provides a means for the receiver to inform the transmitter of the success or failure of the transmission. A parity-bit or cyclic redundancy code (CRC) check of a received frame triggers retransmission requests. If decoding at the receiver is successful (according to the CRC check) no retransmission is

necessary. Therefore, an acknowledgment (ACK) is fed back to the transmitter. Otherwise, if decoding fails, the receiver feeds back a negative acknowledgment (NACK) and another transmission is performed. This process is repeated until an ACK message is received at the transmitter or a maximum retransmission number is achieved. From the application layer perspective, such retransmissions are *automatic*. The acronym ARQ is based on the Morse designation for retransmission request [FU98]. ARQ protocols can be divided into two categories: pure ARQ and hybrid ARQ. A particular hybrid ARQ emerged in the literature in order to achieve better performance, namely incremental redundancy hybrid ARQ.

In the following, we give more details about these protocols: hybrid ARQ and incremental redundancy hybrid ARQ. Finally, a brief introduction of the throughput efficiency performance is conducted since it is used as a convenient performance metric to evaluate point-to-point ARQ protocols as well as the cooperative ARQ protocols proposed later.

2.5.1 Hybrid Automatic Repeat Request Protocols

Hybrid ARQ (HARQ) is widely used in contemporary wireless systems such as *high speed packet access* (HSPA) and third generation (3GPP) *long term evolution* (LTE) [Sau06]. The key challenge of HARQ protocols is to combine the benefits of both channel coding and retransmission principle in order to achieve better performance [LC83]. It also involves the correcting capabilities of the used channel code. Incorporating channel coding reduces significantly the FER and consequently the required number of retransmissions. Therefore, this improves the throughput performance. In its simplest form, this better performance comes at the expense of a significantly increased transmitter and receiver complexity associated to the channel encoding/decoding process.

2.5.2 Incremental Redundancy Hybrid Automatic Repeat Request Protocols

The level of redundancy of the error correcting code adopted in an HARQ protocol has two opposite effects: it is an efficient way to combat wireless channel impairments; however, it suffers from higher channel utilization. The basic idea behind *incremental redundancy-HARQ* (IR-HARQ) is to adjust the redundancy level (the code rate) by incrementally transmitting redundancy bits until decoding is successful or the whole mother code is transmitted [SLS04]. Indeed, if the receiver fails to successfully decode a frame, a NACK message is sent to the transmitter. The latter sends additional new redundancy bits which are accumulated and combined by the receiver. This instance of the HARQ protocol exhibits higher performance by adapting the level of redundancy to the channel conditions. Figure 2.7 illustrates the transmission process of an example of an IR-HARQ protocol.

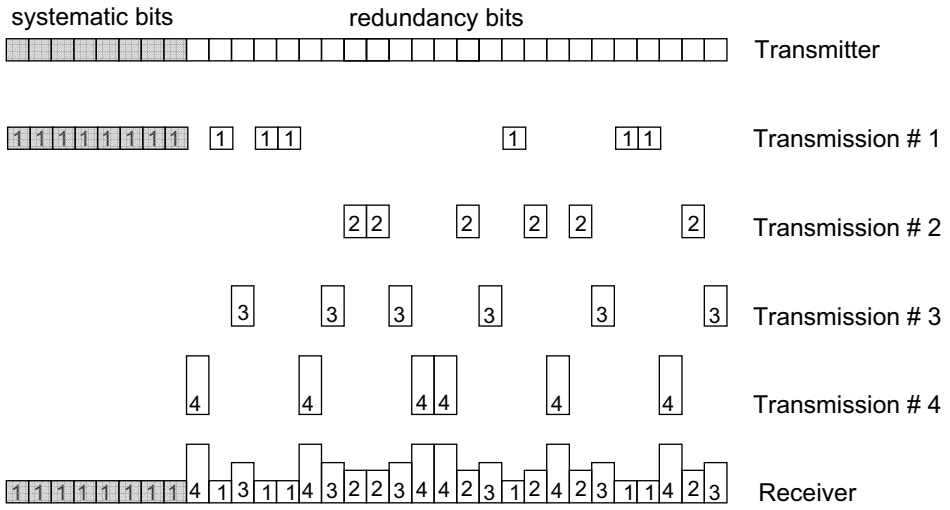

FIGURE 2.7: Incremental redundancy HARQ protocol.

The IR-HARQ protocol can be realized with RCPC codes by first using the highest rate code from the RCPC code family and sending additional bits as needed. Each transmission phase is determined by a *puncturing pattern*. The performance of such HARQ protocols is severely affected by the properties of the mother code used and the family of codes obtained by puncturing. The proposal of IR-HARQ protocols using turbo codes as well as the design of puncturing patterns are important issues addressed in [RM00, NS97, LI97].

Turbo codes are also a natural fit for IR-HARQ protocols, since two codewords or more are generated. In [NS97], authors propose a new turbo-based HARQ protocol, that uses the principles of turbo coding and iterative decoding. The proposed HARQ scheme does not require significant additional computational complexity or storage requirements at the receiver when a soft-output decoder is used to decode the transmissions. In [NS97], the authors explain that minor modifications in the turbo encoder and decoder structure are necessary to permit turbo combining. During the first transmission of a frame, a particular channel code is used, itself can also be a turbo code. If a negative ACK is received, indicating decoding failure at the receiver, the data is interleaved using a pseudo random interleaver and then encoded by an identical encoder and retransmitted. Now, the prior transmission and the retransmission can be effectively combined at the receiver. During every additional retransmission, should it be necessary, a different pseudo-random interleaving pattern is used. If the elementary channel code is a turbo one, the pseudo random interleavers used for the retransmissions are different from that used within the turbo encoder.

2.5.3 Throughput Efficiency Performance

The standard measure of the performance of an ARQ protocol is the *throughput efficiency* (η), defined in [Bab02] as

$$\eta = \varrho T \tag{2.33}$$

where ϱ is the *reliability*, defined as the ratio between the number of corrected information bits and the number of received information bits, and T is the *throughput* of the system, defined as the ratio between the average number of received information bits and the total number of bits sent over the channel per unit time, taking into account the rate of the channel code and the number of retransmissions. Therefore, the throughput efficiency is defined as the ratio between the number of information bits correctly transmitted per transmitter and channel time allocation. Otherwise, from both the renewal theorem [ZR96] and the renewal-reward theorem [CT01], the throughput efficiency can be written as

$$\eta = \frac{E[\mathcal{R}]}{E[D]} \tag{2.34}$$

where $E[\mathcal{R}]$ is the average reward, and $E[D]$ is the expected inter-renewal time. $E[\mathcal{R}]$ is used to quantify the average rate of the transmission, and $E[D]$ illustrates the average transmission delay.

2.6 Multi-Source Transmission

Since a limited amount of bandwidth is allocated for wireless transmission, multiple access techniques are essential to allow several sources to efficiently use the available resources. The objective of multiple access techniques is to allow the transmitting sources to share the finite bandwidth with the least possible degradation in the performance of the system. It allows the sources to transmit over the same multiple-access channel and to share its capacity. These techniques can be classified into orthogonal and non-orthogonal approaches. In the following, we will present four basic schemes: frequency division multiple access (FDMA), time division multiple access (TDMA), coded division multiple access (CDMA) and in more details interleaved division multiple access (IDMA), since it is the adopted technique to separate superposed signals when non-orthogonal channels are assumed.

For FDMA and TDMA techniques, the separation between transmitting sources is done, respectively, in the frequency and the temporal domains. TDMA and FDMA are *orthogonal* techniques where signals from different sources are orthogonal to each other, i.e., no interference has to be handled.

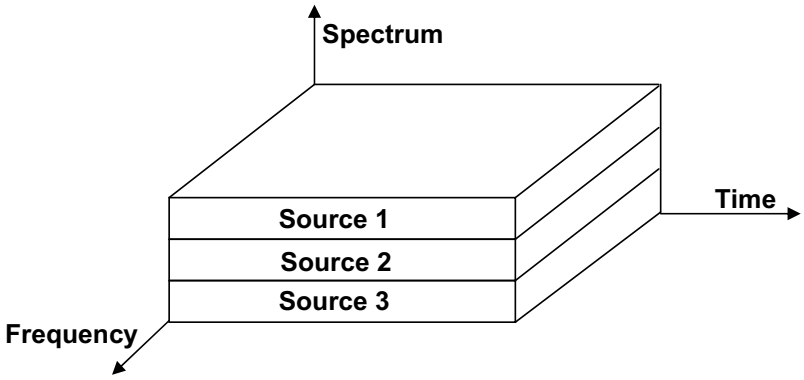

FIGURE 2.8: Non-orthogonal multiple access principle.

In FDMA, the division is done in the frequency domain, so that each source is allocated a part of the spectrum for all the time, in order to allow simultaneous transmissions. For instance, if the system accounts $q = 3$ sources, the channel bandwidth is divided into q sub-bandwidths.

In TDMA, the entire bandwidth is available to one source but only for a finite period of time, namely during one time slot. This separation in the temporal domain circumvents the problem of interference between the sources. However, TDMA requires careful time synchronization. TDMA is used in the digital 2G cellular systems such as the global system for mobile communications (GSM) and will be considered to illustrate orthogonal scenarios in the course of the thesis.

CDMA and IDMA are *non-orthogonal* techniques, where different codes or different interleavers are, respectively, used to identify each source. For these non-orthogonal techniques, each source is allocated the entire spectrum all of the time. Consequently, the transmission experiences interference between different sources.

In CDMA, all the sources occupy all the time the same bandwidth as shown in Figure 2.8. However they are assigned separate codes, which identify the different sources. Although the available resources are maximally exploited, and no time synchronization between the sources is required if totally orthogonal spreading sequences are used, a CDMA system experiences the interference problem. Then, the difficulty lies on the separation of the signals of the different sources at the receiver. A CDMA system utilizes a specific spreading code allocated to each source. The role of this specific code is twofold: to spread the narrow band signal and to separate the signals at the receiver.

2.6.1 Interleaved Division Multiple Access

This sub-section is devoted to present the details of the IDMA technique, the used technique to mitigate interference problemn when non-orthogonal channels are assumed. The IDMA technique, proposed in [PLWL03], can be considered as a special case of the

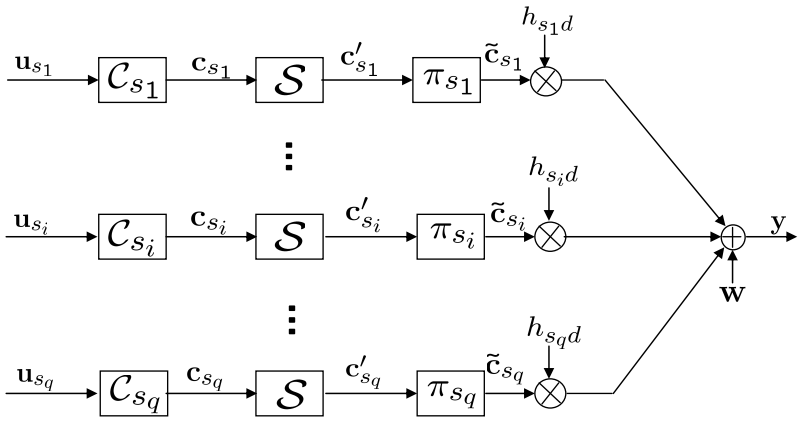

FIGURE 2.9: Transmitter block diagram of an IDMA system with q simultaneous sources.

CDMA technique, where the different sources are distinguished by means of interleavers. However, unlike the CDMA technique, if needed, a same spreading code is used for all the sources. IDMA inherits many advantages from CDMA, in particular, diversity against fading and mitigation of the interference problem. It clearly improves system performance through introducing chip-level interleavers. Furthermore, it allows a very simple chip-by-chip iterative multi-source detection strategy [PLWL04], resulting in a low receiver complexity.

2.6.1.1 IDMA Transmitter and Receiver Structures

We consider an IDMA system where q sources transmit simultaneously to a single destination. The structure of an IDMA transmitter is depicted in Figure 2.9.

The input information sequence $\mathbf{u}_{\mathrm{s}_i}$ of source s_i is encoded by encoder $\mathcal{C}_{\mathrm{s}_i}$ of rate R_{c_i} into codeword $\mathbf{c}_{\mathrm{s}_i}$. The sequences $\mathbf{c}_{\mathrm{s}_i}$ are then spread by using an $\mathcal{S}$-repetition code into sequences $\mathbf{c}'_{\mathrm{s}_i}$, where $\mathcal{S}$ is the spreading factor. The code rate after spreading is denoted by $R_{\mathrm{s}_i} = R_{c_i}/\mathcal{S}$ (This spreading operation may be omitted when a low rate channel code is used). Then $\mathbf{c}'_{\mathrm{s}_i}$ is scrambled by an interleaver π_{s_i}, producing $\tilde{\mathbf{c}}_{\mathrm{s}_i}$. Following the CDMA convention, we call the $\tilde{\mathbf{c}}_{\mathrm{s}_i}$ *chip* sequences. The key principle of IDMA is that the interleavers π_{s_i} should be different for different sources.

The received signal $\mathbf{y}$ at the destination is the superposition of the chip sequences weighted by the channel coefficients of s_i-to-d links, $i = 1, ..., q$. The received signal from q sources can be written as

$$\mathbf{y} = \sum_{i=1}^{q} h_{\mathrm{s}_i \mathrm{d}} \mathbf{x}_{\mathrm{s}_i} + \mathbf{w} \tag{2.35}$$

where $h_{\mathrm{s}_i \mathrm{d}}$ is the block fading channel coefficient over the s_i-to-d link, $\mathbf{x}_{\mathrm{s}_i}$ is the modulated sequence of the $\tilde{\mathbf{c}}_{\mathrm{s}_i}$ and $\mathbf{w}$ is a vector of AWGN with variance σ^2.

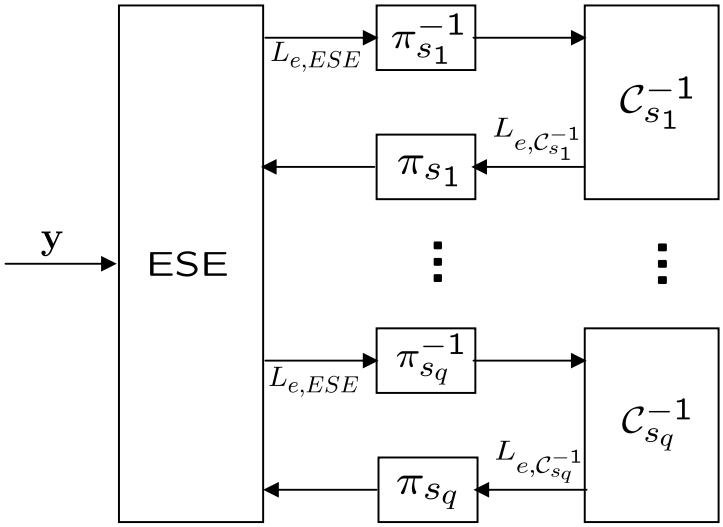

FIGURE 2.10: Receiver block diagram of an IDMA system with q simultaneous sources.

In the receiver, illustrated in Figure 2.10, two main blocks are used: an *elementary signal estimator* (ESE) that exchanges extrinsic information with q *a posteriori probability* (APP) decoders, $\mathcal{C}_{\mathrm{s}_i}^{-1}$, $i = 1, ..., q$. A global iterative process is then applied to recover the information of all sources. Due to the use of interleavers π_{s_i}, the ESE operation can be carried out by a chip-by-chip detection algorithm [PLWL06], with only one sample $y(j)$ is used at a time. The outputs of the ESE and $\mathcal{C}^{-1}$ are extrinsic LLRs about $x_{\mathrm{s}_i}(j)$. The a posteriori LLR generated by decoders $\mathcal{C}_{\mathrm{s}_i}^{-1}$ for source s_i is given by

$$L_{e,\mathcal{C}_{\mathrm{s}_i}^{-1}}\left(x_{\mathrm{s}_i}(j)\right) = \log\left(\frac{\Pr\left(x_{\mathrm{s}_i}(j) = +1\right)}{\Pr\left(x_{\mathrm{s}_i}(j) = -1\right)}\right) \tag{2.36}$$

The ESE computes the extrinsic information $L_{e,\mathrm{ESE}}\left(x_{\mathrm{s}_i}(j)\right)$ using the chip-by-chip detection algorithm, briefly described in the following subsection.

2.6.1.2 The Elementary Signal Estimator Function

The received signal samples $y(j)$ can be written as

$$y(j) = h_{\mathrm{s}_i\mathrm{d}} x_{\mathrm{s}_i}(j) + \zeta_{\mathrm{s}_i}(j) \tag{2.37}$$

where

$$\begin{aligned} \zeta_{\mathrm{s}_i}(j) &= y(j) - h_{\mathrm{s}_i\mathrm{d}} x_{\mathrm{s}_i}(j) \\ &= \sum_{i' \neq i} h_{\mathrm{s}_{i'}\mathrm{d}} x_{\mathrm{s}_{i'}}(j) + w(j) \end{aligned} \tag{2.38}$$

is the distortion (including interference plus noise) in $y(j)$ with respect to source s_i.

From the central limit theorem, $\zeta_{\mathrm{s}_i}(j)$ can be approximated as a Gaussian variable with mean $\mathcal{E}\left(\zeta_{\mathrm{s}_i}(j)\right)$ and variance $\mathrm{Var}\left(\zeta_{\mathrm{s}_i}(j)\right)$. The ESE detection algorithm based on (2.35)- (2.38), assuming that the a priori statistics $\mathcal{E}\left(\zeta_{\mathrm{s}_i}(j)\right)$ and $\mathrm{Var}\left(\zeta_{\mathrm{s}_i}(j)\right)$ are available, is given in Algorithm 2.1 below.

Algorithm 2.1 Chip-by-Chip Algorithm:

Step (i): Initialization $L_{e,\mathcal{C}_{\mathrm{s}_i}^{-1}}\left(x_{\mathrm{s}_i}(j)\right) = 0,\ \forall i,j.$

Step (ii): Estimation of Interference Mean and Variance

1. $\mathcal{E}\left(x_{\mathrm{s}_i}(j)\right) = \tanh\left(L_{e,\mathcal{C}_{\mathrm{s}_i}^{-1}}\left(x_{\mathrm{s}_i}(j)\right)/2\right),\ \forall i,j$
2. $\mathrm{Var}\left(x_{\mathrm{s}_i}(j)\right) = 1 - \left(\mathcal{E}\left(x_{\mathrm{s}_i}(j)\right)\right)^2,\ \forall i,j$
3. $\mathcal{E}\left(\zeta_{\mathrm{s}_i}(j)\right) = \sum_{i'\neq i} h_{\mathrm{s}_{i'}\mathrm{d}}\mathcal{E}\left(x_{\mathrm{s}_{i'}}(j)\right),\ \forall j$
4. $\mathrm{Var}\left(\zeta_{\mathrm{s}_i}(j)\right) = \sum_{i'\neq i}\left|h_{\mathrm{s}_{i'}\mathrm{d}}\right|^2 \mathrm{Var}\left(x_{\mathrm{s}_i}(j)\right) + \sigma^2,\ \forall j$

Step (iii): LLR Generation $L_{e,\mathrm{ESE}}\left(x_{\mathrm{s}_i}(j)\right) = \frac{2h_{\mathrm{s}_{i'}\mathrm{d}}}{\mathrm{Var}\left(\zeta_{\mathrm{s}_i}(j)\right)}\left(y(j) - \mathcal{E}\left(\zeta_{\mathrm{s}_i}(j)\right)\right),\ \forall i,j$

The major asset of IDMA over CDMA is a lower multi-source detection complexity. For instance, the complexity of a CDMA soft interference cancellation detector is polynomial with the number of sources, e.g., the well-known minimum mean square error (MMSE) algorithm in [WP99] has complexity of $O(q^2)$ due to matrix operations. However, the IDMA lends itself to a simple chip-by-chip detection algorithm whose complexity grows only linearly with the number of users [PLWL03].

2.7 Transmission of Correlated Sources Over a Multiple Access Channel

In general, sources in a wireless environment can be correlated. An example for this is sensor networks. Due to their vicinity, neighbouring sensors measure data that is statistically dependent. In sensor network applications, the observations collected by the sensors are intrinsically correlated, for instance in scenarios where distributed sensing of a random field is performed (e.g., geological exploration, environmental sensing, electromagnetic sensing, etc) [AKC08]. The design of efficient transmission schemes of correlated signals, observed at different sources, to one or more collectors is one of the main challenges in these networks. In its simplest forms, the design problem at hand can be summarized as follows: two or more independent sources have to transmit correlated signals to a collector node by using the minimum possible energy, i.e., by properly exploiting the implicit correlation among the sources. Joint source-channel coding is a technique by which the available rate is allocated between source coding rate and

channel coding rate based on a performance measure that jointly considers the effects of source and channel coding.

In the case of orthogonal AWGN channels, the separation between source and channel coding is known to be optimal [Sha48]. This means that the ultimate performance limits can be achieved by first compressing each source up to Slepian-Wolf limit [SW04], and then utilizing independent capacity-achieving channel codes (one per source). This separate optimization of source and channel coding, as shown by Shannon, is well suited for the point-to-point case. However, it can generate a significant performance loss in more general scenarios, e.g., for correlated sources [GF01]. An example of the latter is considered in [CGS80], where the authors provide bounds on the capacity region for the multiple access channel with arbitrarily correlated sources; they provide sufficient conditions for the correlated sources to be sent over the channel with an arbitrarily small probability of error. All these results with others in [CT91] and in [Due91] show the sub-optimality of the separation-based coding strategy.

[AH83] extends techniques presented in [CGS80], to more general models with discrete sources and channels and lossless transmission. Sufficient conditions for lossy transmission of correlated sources over a multiple access channel with side information are given in [RVS08] and [VS06]. Joint source-channel coding schemes for transmission of correlated sources over a multiple access channel are also discussed in [GV97] and [LU06].

In point-to-point wireless transmission, the availability of side information (correlation) at the receiver side has been demonstrated to increase the reliability of the transmission. In this thesis, we try to extend this in the context of wireless cooperative communication networks. We will focus on the design of cooperative physical layer schemes that can make use of side information at the relay/destination nodes. We further restrict ourselves to uncoded transmission, which is practically relevant since power is a scarce resource in inexpensive sensor nodes and hence a coding/decoding stage may be infeasible. In Chapter 5, we study the performance of a cooperative multiple access system, with noisy separated channels, where correlated sources communicate to a unique destination with the help of one or multiple relays, in the presence of Gaussian or block faded channels.

2.8 Chapter Summary

In this chapter, we presented an overview of the point-to-point communication, introducing several concepts used later in the cooperative context. First, wireless channel properties were addressed in order to better understand the channel environment limits. Thereafter, a background about some information theoretic tools, used to analyze the performance of the wireless communication channel, was presented. Furthermore,

we gave a quick overview of two main error control techniques (channel coding and retransmission protocols), a starting point of the proposals conducted in the course of the thesis. The turbo codes were detailed, since they have good performance in the point-to-point communications. Thus, it will be interesting to explore their performance in the cooperative systems. Moreover, in the following, we will consider two scenarios of transmission: orthogonal and non-orthogonal multi-source transmissions. Therefore, we summarized the different main techniques used for multiple access communications. In particular, we detailed the IDMA technique that will be adopted later to separate superposed source signals in the proposed cooperative systems. Finally, we presented the source correlation problem and suggested its extension to cooperative networks.

Chapter 3

Cooperative HARQ Protocols for Turbo Coded Cooperation

Cooperative communication has emerged as an efficient concept that draws some of the benefits of multiple antenna devices over wireless fading channels, such as spatial diversity gain. In Section 3.1, we give a brief overview of the basic concepts of cooperative communications. In particular, we review key results of the relay channel, the simplest cooperative scheme, introduced by van der Meulen in [vdM71]. For the relay channel, Cover and El Gamal [CG79] described two fundamental cooperative strategies where the relay either decodes (decode-and-forward), or compresses (compress-and-forward) the received source information before forwarding it to the destination. We further present several cooperative strategies proposed in the prior works. In addition, in Sub-section 3.1.4, we give a brief review of cooperative HARQ protocols found in the literature. In Section 3.2, we detail the coded cooperation scheme as well as the turbo coded cooperation scheme, used as a starting point to design proposed cooperative HARQ protocols, since only few works extended the idea of cooperative HARQ to the case of user cooperation. Almost previous works explore exclusively the case of one source node assisted by one or multiple relay nodes.

In this chapter, we explore cooperative HARQ protocols over user cooperation system, a configuration that has not yet fully explored. In Section 3.3, we propose and evaluate three different HARQ protocols for a two-source wireless network with turbo coded cooperation, which consider both link reliability and system efficiency. Finally, performance comparison and discussions of proposed cooperative HARQ protocols are included at the end of this chapter. The results are given for two different scenarios: the orthogonal transmission (Section 3.4) and the non-orthogonal transmission (Section 3.5).

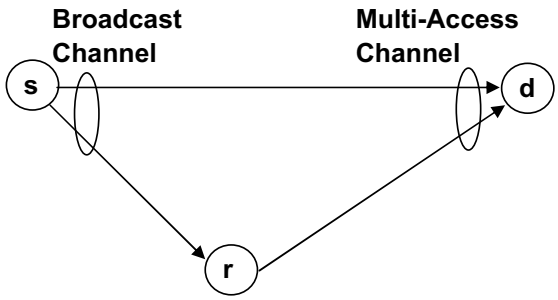

FIGURE 3.1: The relay channel model.

3.1 Background on Cooperative Communications

3.1.1 The Relay Channel

The relay channel can be traced back to the pioneering paper by van der Meulen [vdM71]. The author presented this channel as a three-terminal network which consists of a source, a relay and a destination. The relay assists the source by forwarding extra information to the destination. The relay channel model is shown in Figure 3.1. It presents the simplest cooperation pattern, which is also the basic building block for *multihop routing*, whereby a frame is sequentially routed from a source to the destination through a series of hops (relays).

The relay channel was further investigated by Cover and El Gamal in [CG79], where upper and lower bounds to the capacity were derived and two different strategies of forwarding at the relay node were detailed: decode-and-forward, and compress-and-forward. The key result of this pioneering work showed that, in many instances, the overall capacity is better than the individual capacity between the source and the destination. As illustrated in Figure 3.1, the source broadcasts its encoded information to the destination and the relay. The relay receives a noisy version of the source information. The relay then transmits a processed version of the source codewords to the destination, based on what it has received. Therefore, the relay channel can be decomposed into a broadcast channel and a multiple access channel. The original work by Cover and El Gamal [CG79] assumes that the relay operates in the full-duplex setup. The relay is considered to simultaneously transmit and receive in the same frequency. However, since the full-duplex setup may be impractical with current RF technology, we assume, in the course of this thesis, that all transmitting sources operate in the half-duplex setup. Therefore, the relaying node receives the source information in one time slot, and then transmits in a different time slot.

3.1.2 Cooperative Strategies

According to the forwarding strategy adopted at the relaying node, the cooperative strategies are generally grouped into three classes: *amplify-and-forward* (AF), *decode-and-forward* (DF) and *compress-and-forward* (CF) strategies.

3.1.2.1 Amplify-and-Forward

Amplify-and-forward is conceptually the most trivial cooperative strategy. As the name implies, in the AF scheme, the relay simply retransmits a scaled version of the signal it has received subject to the power constraint at the relay. Although the fact that amplifying the signal will also amplify the noise at the relay, the destination still receives two independently-faded versions of the information and is thus able to make better decisions. A potential challenge in this scheme is that processing analog values may be technologically non-trivial. Laneman and Wornell first proposed amplify-and-forward as a cooperative strategy in [LW00], since it is a simple strategy to analyze, and it has been very useful in the understanding of cooperative communication systems.

3.1.2.2 Decode-and-Forward

Under the *decode-and-forward* strategy, the relay attempts to decode the received signal, and then retransmits an estimate of the detected symbols. The DF strategy performs very well, in the case of successful decoding at the relay. However, in [LTW04], it is shown that this protocol achieves diversity order one, the same as non-cooperative transmission, and actually performs worse than non-cooperative transmission for a wide range of conditions. For instance, when the relay fails to correctly decode the received signal an error propagation phenomenon is observed. Consequently, using the DF strategy is not beneficial. To avoid the problem of error propagation by the relay, Laneman, Wornell, and Tse [LTW04] proposed an adaptive decode-and-forward method. Unlike the fixed DF scheme, when the channel between the source to the relay has high instantaneous SNR, the relay detects and forward the source information, but when the channel has low SNR value, the relay keeps silent.

3.1.2.3 Compress-and-Forward

In the *compress-and-forward* strategy, the relay is no longer required to decode the information transmitted by the source but simply to describe its observation to the destination. The CF strategy is used when the relay cannot decode the information sent by the source, but still can help by compressing and forwarding it to the destination. The relay quantizes the received signal and sends a compressed version of it to the destination. The challenge here comes essentially from the fact that in order to lower the requirements on the transmission rate from relay to destination, the CF scheme has

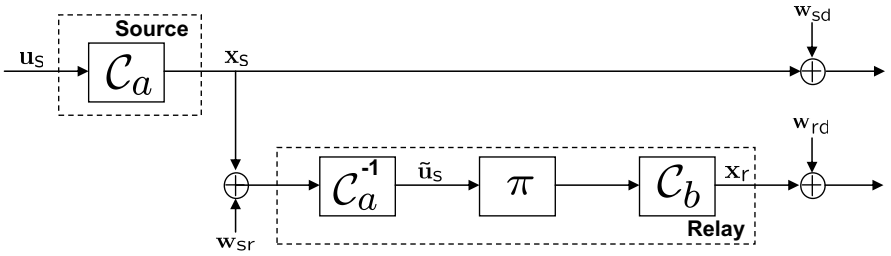

FIGURE 3.2: The distributed turbo code block diagram.

to consider the correlation between the two observations (from the source as well as from the relay). Unlike the DF scheme, CF remains beneficial even when the source-to-relay link is not error-free. Furthermore, as opposed to DF, in CF, the relay does not use any knowledge of the codebook used by the source.

In [KGG05], a comparison of DF and CF schemes is addressed according to the relay location. It was shown that the achievable rate of DF is higher when the relay is close to the source while CF outperforms DF in terms of achievable rate when the relay gets closer to the destination.

3.1.3 Distributed Turbo Codes for the Relay Channel

The distributed turbo code (DTC) scheme was first proposed in [VZ03] under the assumption of error-free source-to-relay channel. Figure 3.2 describes schematically the distributed turbo codes for the relay channel. The overall turbo codeword is transmitted over two phases. In the first phase, the source encodes the information bits $\mathbf{u}_s$ by the encoder $\mathcal{C}_a$ into codeword $\mathbf{x}_s$, which is broadcasted to both the relay and the destination. During this transmission phase, the relay attempts to decode the received codeword and generates an estimate $\tilde{\mathbf{u}}_s$ of the source information. This estimate is then interleaved and re-encoded by the encoder $\mathcal{C}_b$ before being forwarded, in the second transmission phase, to the destination. The system of Figure 3.2 can be seen as a distributed turbo code, and the destination receives two sub-codewords of the original frame and jointly decodes them by an iterative decoding in the same manner as for a conventional turbo code.

In [VZ03], the distributed turbo code is designed based on RSC codes both at the source and at the relay. The authors mainly compared a repetition code, where the destination performs a maximum ratio combing (MRC) and Viterbi decoding, with two distributed turbo codes of overall rates equal to 1/3 (1/2-rate at the source and 1-rate at the relay) and 1/4 (1/2-rate at the source and 1/2-rate at the relay), respectively. The results in the paper, are reported in Figure 3.3. We notice that the distributed turbo codes performance is clearly better than that of the repetition code with relaying. This gain is mainly obtained from the iterative decoding process. A further important

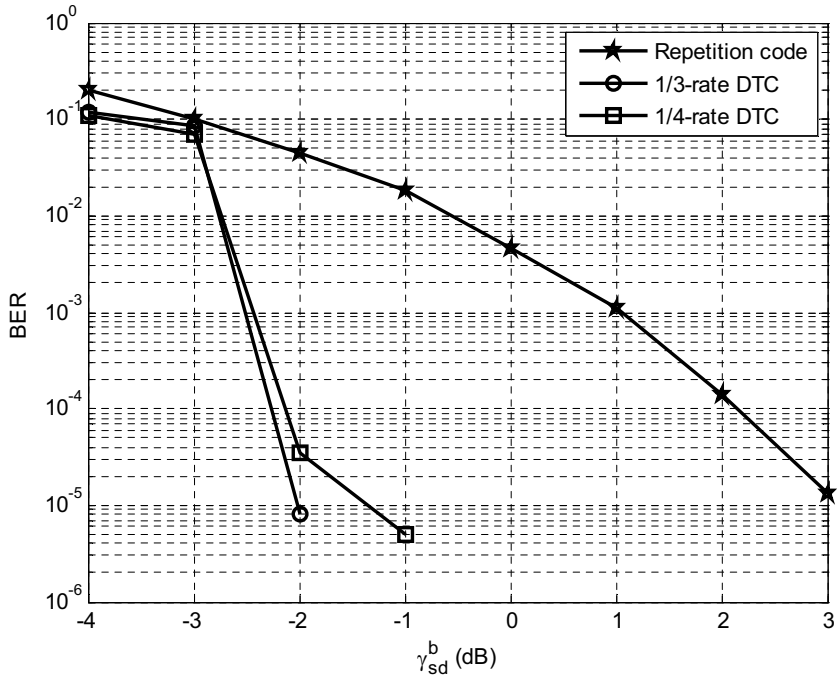

FIGURE 3.3: Performance comparison between repetition code, 1/3-rate DTC and 1/4-rate DTC over AWGN channel with $\gamma^b_{sd} = \gamma^b_{rd}$ dB.

concluding remark from the paper is that the relay does not need to transmit the systematic bits which have been transmitted through the direct link. This conclusion is made because the 1/3-rate DTC and the 1/4-rate DTC (identical to the 1/3-rate DTC with the unique difference is that the systematic bits are retransmitted from the relay during the second phase) achieve nearly the same performance especially for the convergence behavior.

3.1.4 Cooperative HARQ Protocols

Hybrid automatic repeat request is a common technique used to make a wireless link reliable. Recently, conventional HARQ protocols have been extended to cooperative relaying systems [ZHF04, NAGS05, YZQ06, YZQ07, SSBNC06, Nar08, LL08, AFH08, LSBM10]. Unlike the traditional environment, where the retransmission demand is responded by the source node; in cooperation HARQ systems, the relay nodes are also able to respond the retransmission demand and retransmit the packets. These new protocols have been called cooperative HARQ protocols. The pioneering works were proposed to address the main advantages of the cooperative HARQ protocol. First, it was shown, in [ZHF04, YZQ06, YZQ07], that cooperative HARQ yields higher reliability than conventional HARQ protocols, since it offers spatial diversity and path loss reduction by relaying. Second, in [NAGS05] it was shown that cooperative HARQ is more efficient than non-ARQ cooperation, since it overcomes throughput degradation due to the fixed

cooperative phase. Further works on cooperative HARQ protocols were dedicated to evaluate the performance of such systems in terms of outage behavior [LTW04, LSBM10], throughput [ZV05, SSBNC06, SSBN06] and DMT [NAGS05, AGS05, TDK07, AGS08]. Finally, other works studied these protocols from an optimization point of view by maximizing the throughput as a function of the rate or the relay location [Nar08, LL08]. However, all these works explore exclusively the case of one source node assisted by one or multiple relay nodes. Only few works extended the idea of cooperative HARQ to the case of user cooperation [AFH08, ZWW09]. In [AFH08], IR was combined with rate compatible punctured convolutional codes for the coded cooperation model in order to adapt both the level of cooperation and the code rate to channel conditions. In [ZWW09], two HARQ protocols for the two-source cooperating system employing Alamouti space-time codes were investigated. A more general configuration with a multiple-source cooperative case combined with network coding was proposed in [SLW09]: in the relays retransmission slot, if both sources need the assistance of the relay at the same time, a signal superposition modulation, is adopted before retransmission. The relay superposes s_1 frame with s_2, with the power level of $1-\gamma^2$ and γ^2 where $0 \leq \gamma \leq 1$, respectively.

In the traditional relaying scheme, where there is a limited number of relay nodes, the sources have to compete with each other by queuing to enjoy the possible diversity gain offered by the relay, since it can assist only one source at a time. However, in multiple-source systems, we can overcome the shortage of relays and consequently we avoid user competition by favorising rather user cooperation. In this work, we explore cooperative HARQ protocols over user cooperation system. The proposed protocols combine the HARQ protocol [NS97] at data link layer and the turbo coded cooperation at physical layer [JHHN04].

3.2 The Coded Cooperation

In this section, we introduce a particular user cooperation scheme, called *coded cooperation*, in which cooperative communication is integrated with channel coding. After reviewing system and channel models, we describe the coded cooperation scheme. In the sequel, the *turbo coded cooperation* is detailed where the implementation of the coded cooperation is based on turbo codes. The turbo coded cooperation is the cooperative scheme used to design all cooperative HARQ proposed in Section 3.3. Finally, simulation results are provided for a variety of channel conditions.

3.2.1 System and Channel Models

We consider the wireless relay network depicted in Figure 3.4. Two sources s_1 and s_2 cooperate to transmit statistically independent data to a single destination d. Source s_i

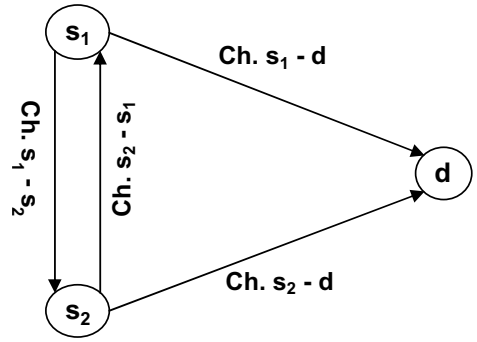

FIGURE 3.4: A three-node cooperative wireless network: Each source acts as a relay for its partner.

($i = 1, 2$) can either transmit its own local information (transmission mode) or help the partner node by relaying its information (relaying mode). We denote by $\mathbf{u}_{iL}$ the local data at source s_i. Both sources are equipped with two encoders $\mathcal{C}_a$ and $\mathcal{C}_b$ of rates R_a and R_b, respectively. The sources transmit on orthogonal channels (i.e., TDMA), which allows the destination, and the other node in the relaying mode, to separately detect each source.

All channels are modeled as Rayleigh block fading with additive white Gaussian noise. We denote by $\gamma_{\mathrm{s}_i\mathrm{d}}$ and $\gamma_{\mathrm{s}_i\mathrm{s}_j}$ the instantaneous SNR of the s_i-to-d channel and of the s_i-to-s_j channel, respectively. We define $\gamma_{\mathrm{s}_i\mathrm{d}} = \rho \cdot |h_{\mathrm{s}_i\mathrm{d}}|^2$, where $\rho = E_s/N_0$ is the received SNR (E_s is the received signal energy and N_0 is the single-sided noise power density). $h_{\mathrm{s}_i\mathrm{d}}$ are zero-mean, circularly symmetric complex Gaussian random variables, and are assumed to be constant over the transmission of a frame $\mathbf{u}_{1L}$, i.e., over all transmission phases. This channel model is considered in order to investigate the ability of the distributed spatial diversity to enhance link level performance in scenarios where temporal diversity is limited or unavailable. At the destination, the received symbol y^d_{iL} from source s_i is given by:

$$y^d_{iL} = h_{\mathrm{s}_i\mathrm{d}} x_{iL} + w \tag{3.1}$$

where $x_{iL} \in \{\pm 1\}$ denotes the BPSK modulated symbol. Similar expressions are obtained for the inter-source channels.

3.2.2 Coded Cooperation Scheme

In the following, we briefly describe the coded cooperation (CCoop) scheme when no HARQ is used. Without loss of generality, we focus on the information generated at source s_1. The transmission of source data $\mathbf{u}_{iL}$, of length K bits, is performed over two time slots, also called phases. In the first phase, referred to as the *broadcast phase*, source s_1 encodes $\mathbf{u}_{1L}$ by $\mathcal{C}_a$ into codeword $\mathbf{x}_{1L}$, of length $N_a = K/R_a$ bits. $\mathbf{x}_{1L}$ is augmented with a cyclic redundancy code (CRC) in order to facilitate error detection

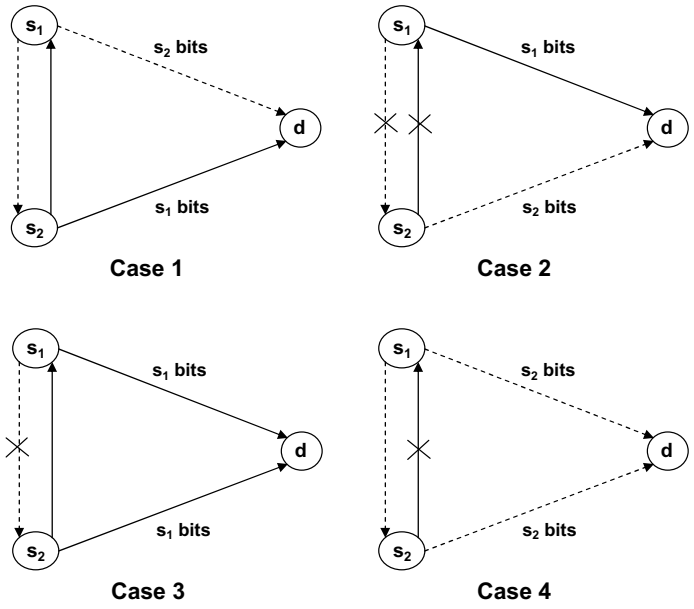

FIGURE 3.5: The four possible cases of cooperation depending whether each source decodes successfully or not its partner information.

and transmitted over the wireless channel. For simplicity, in the remainder of the thesis, when referring to a codeword $\mathbf{x}$, we shall assume that it includes a CRC and throughout this manuscript, all results are given for a perfect CRC. Due to the broadcast nature of the wireless channel both the destination and s_2 receive a noisy observation of $\mathbf{x}_{1L}$, denoted by $\mathbf{y}_{1L}^{d}$ and $\mathbf{y}_{1L}^{s_2}$, respectively. If decoding is successful at s_2 (i.e., s_2 is able to regenerate $\mathbf{u}_{1L}$), s_2 switches to the relaying mode; in the second phase, referred to as the *cooperation phase*, $\mathbf{u}_{1L}$ is then encoded by $\mathcal{C}_b$ into $\mathbf{x}_{2R}$, of length $N_b = K/R_b$ bits, and forwarded to the destination. The received observation of $\mathbf{x}_{2R}$ is denoted by $\mathbf{y}_{2R}^{d}$. On the other hand, if decoding is not successful, s_2 operates in the transmission mode (non-cooperative); in the second phase $\mathbf{u}_{2L}$ is then encoded by encoder $\mathcal{C}_b$ into $\tilde{\mathbf{x}}_{2L}$ and forwarded to the destination. The received vector is denoted by $\tilde{\mathbf{y}}_{2L}^{d}$. A similar operation is performed at node s_1 during the second phase. Correspondingly, we define the vectors $\mathbf{x}_{1R}$, $\mathbf{y}_{1R}^{d}$, $\tilde{\mathbf{x}}_{1L}$ and $\tilde{\mathbf{y}}_{1L}^{d}$. Notice that $\mathbf{x}_{2R} = \tilde{\mathbf{x}}_{1L}$ and $\mathbf{x}_{1R} = \tilde{\mathbf{x}}_{2L}$.

With reference to source s_1 four cases are possible, as illustrated in Figure 3.5:

- Case 1 ($\Theta = 1$) decoding at sources s_1 and s_2 is successful: two codewords, $\mathbf{x}_{1L}$ and $\mathbf{x}_{2R}$, are generated for $\mathbf{u}_{1L}$. Notice that $\mathbf{x}_{1L}$ and $\mathbf{x}_{2R}$ form a codeword of a distributed code, where the first subcodeword is generated by s_1 and the second subcodeword is generated by s_2. The destination can estimate $\mathbf{u}_{1L}$ by exploiting jointly the corresponding received sequences $\mathbf{y}_{1L}$ and $\mathbf{y}_{2R}$. The overall codeword, $\mathbf{x} = (\mathbf{x}_{1L}, \mathbf{x}_{2R})$, is of length $N = N_a + N_b$.

- Case 2 ($\Theta = 2$) decoding at sources s_1 and s_2 fails: two codewords are transmitted for $\mathbf{u}_{1L}$, namely $\mathbf{x}_{1L}$ and $\tilde{\mathbf{x}}_{1L}$, both generated by s_1. Therefore, a distributed (over

TABLE 3.1: CRC error detection coverage

Number of CRC bits	Error detection coverage
4	0.9375
7	0.992188
12	0.999756
16	0.99998
32	0.9999999997

time) code is obtained. Here, no cooperative diversity is exploited. The overall codeword, $\mathbf{x} = (\mathbf{x}_{1L}, \tilde{\mathbf{x}}_{1L})$, is of length $N = N_a + N_b$.

- Case 3 ($\Theta = 3$) decoding at source s_1 fails, decoding at source s_2 is successful: in this case both s_1 and s_2 dedicate the second phase to transmit $\mathbf{u}_{1L}$. Therefore, three codewords are generated for $\mathbf{u}_{1L}$, namely $\mathbf{x}_{1L}$, $\tilde{\mathbf{x}}_{1L}$ and $\mathbf{x}_{2R}$. The destination receives the corresponding noisy observations $\mathbf{y}^{\mathrm{d}}_{1L}$, $\tilde{\mathbf{y}}^{\mathrm{d}}_{1L}$ and $\mathbf{y}^{\mathrm{d}}_{2R}$, and optimally combines $\tilde{\mathbf{y}}^{\mathrm{d}}_{1L}$ and $\mathbf{y}^{\mathrm{d}}_{2R}$ before jointly exploiting them with $\mathbf{y}^{\mathrm{d}}_{1L}$ to perform decoding. This optimal combining is an maximum ratio combining. The overall codeword, $\mathbf{x} = (\mathbf{x}_{1L}, \tilde{\mathbf{x}}_{1L}, \mathbf{x}_{2R})$, is of length $N = N_a + N_b$.

- Case 4 ($\Theta = 4$) decoding at source s_1 is successful, decoding at source s_2 fails: a single codeword, $\mathbf{x}_{1L}$, is allocated to $\mathbf{u}_{1L}$. The destination attempts to estimate $\mathbf{u}_{1L}$ by decoding $\mathbf{y}^{d}_{1L}$. The overall codeword, $\mathbf{x} = \mathbf{x}_{1L}$, is of length $N = N_a$.

Notice that with some abuse of language we call the second phase the *cooperation* phase. However, in this phase source s_i may work either in the transmission mode or in the relaying mode, depending on the CRC check. We denote by $\alpha = N_a/N$ the cooperation level, giving the ratio of the N total channel symbols allocated to the broadcast phase [HN06].

This coded cooperation as shown in [NHH04, JHHN04] achieves diversity and sizable gains over non-cooperative networks. The coded cooperation scheme is based on the DF strategy, while it avoids the problem of error propagation, by reverting to the non-cooperative mode, when the inter-source channel is not error-free.

3.2.2.1 The Cyclic Redundancy Code

The CRC is a key element of the coded cooperation scheme. Therefore, this subsection presents a brief discussion about the error-detection capabilities of CRCs. Table 3.1 gives the error detection coverage ratio for several common number of CRC bits [Wic95]. We notice that considering a perfect CRC does not significantly affect the overall performance, since high error detection coverage can be obtained by using well-known CRC. Furthermore, we can point out that the use of CRC does not represent additional

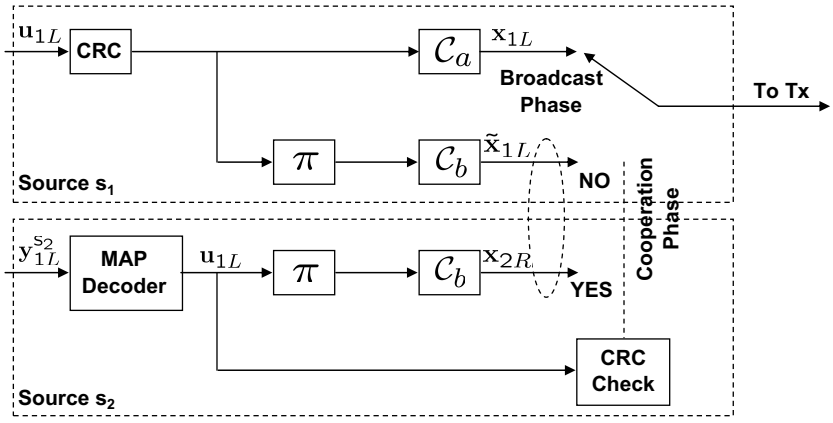

FIGURE 3.6: The turbo coded cooperation scheme with reference to source s_1.

required overhead bits, affecting the system throughput, since most current and future wireless systems already incorporate CRC into channel code schemes [SSCL01].

3.2.3 Turbo Coded Cooperation Scheme

Turbo codes are a natural fit for cooperative communications, since two codewords are generated (at the source and at the relay). As seen in Sub-section 3.1.3, this principle, called *distributed turbo coding* and introduced in [VZ03], combines channel coding with cooperation. The relay decodes, interleaves and re-encodes the message prior to forwarding. The overall network can be regarded as a distributed (over space) turbo code. This approach benefits from cooperative diversity, coding and turbo processing gains. This work was later extended to a two-user wireless network in [NHH04, JHHN04], called *turbo coded cooperation* (TCCoop). The implementation of coded cooperation using turbo codes is shown in Figure 3.6. The scheme presented above has a general fixed cooperation level of $\alpha = \frac{R_a R_b}{R_a + R_b}$. It is possible to have a flexible cooperation level, as well as better performance, by using different permeability rates of fixed mother turbo codes. With reference to source s_1 four cases are possible, as illustrated in the previous section. The unique difference between coded cooperation and turbo coded cooperation lies within the cooperation phase, where $\mathbf{u}_{1L}$, before being encoded by $\mathcal{C}_b$ into $\mathbf{x}_{2R}$ (for the relaying mode) or $\tilde{\mathbf{x}}_{1L}$ (for the transmitting mode), is first interleaved. The sources and the destination have the same random interleaver, shown as π in Figure 3.6.

3.2.4 Performance Evaluation

In this section, we present the simulation results of the coded cooperation scheme using two particular coding strategies: RCPC codes and turbo codes. We evaluate the bit error rate (BER) under a fixed cooperation level α and different channel conditions, and compare them with the non cooperative scheme. In all cases, the information frame

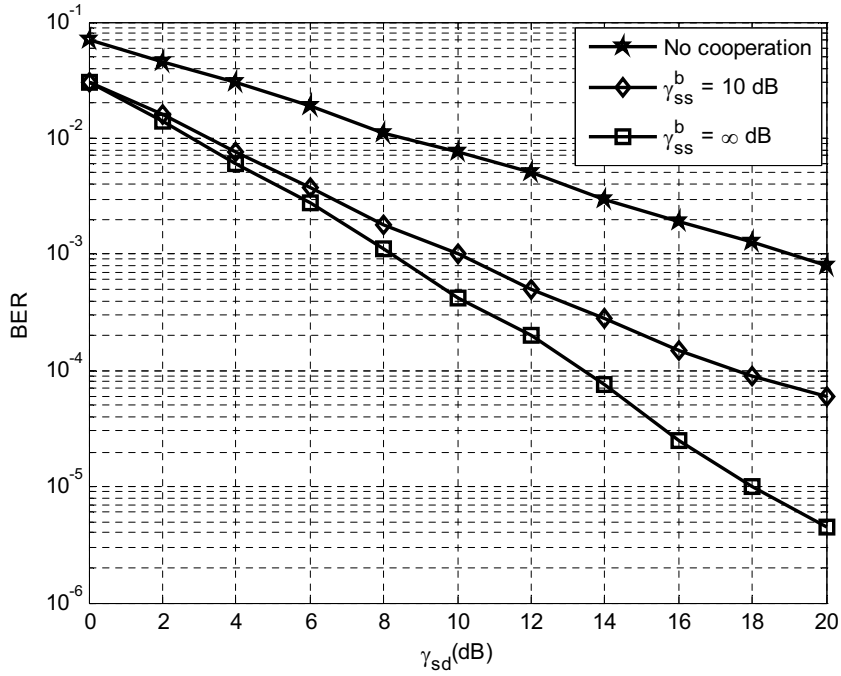

FIGURE 3.7: BER curves of the coded cooperation scheme using RCPC codes for equal time allocation ($\alpha = 1/2$) over Rayleigh block fading channel.

length is $K = 128$ bits, symmetric s_i-to-d channels ($\gamma_{s_1 d} = \gamma_{s_2 d} = \gamma_{sd}$) and reciprocal inter-source channels ($\gamma_{s_1 s_2} = \gamma_{s_2 s_1} = \gamma_{ss}$) are considered. A perfect CRC is assumed.

3.2.4.1 Rate Compatible Punctured Convolutional Codes

Many coding strategies are possible to implement a coded cooperation system, e.g., we may adopt RCPC codes to design the two encoders $\mathcal{C}_a$ and $\mathcal{C}_b$. We use the family of RCPC codes with memory $m = 4$, puncturing period $P = 8$, overall code rate $R = 1/4$ and generator polynomials in octal form $(23, 35, 27, 33)_8$ reported in [Hag88]. The cooperation level is fixed to $\alpha = 1/2$, i.e., equal time allocation is assumed. Consequently, the transmission phases (broadcast and cooperation phases) have the same code rate $R_a = R_b = 1/2$. In Figure 3.7, we give BER simulation results over a Rayleigh block fading channel as a function of γ_{sd}^b expressed in dB, for $\gamma_{ss}^b = 10$ dB and for perfect inter-source channel. Adding cooperation to the non-cooperative RCPC code scheme, with similar rate, bandwidth and power, when $\gamma_{ss}^b = 10$, yields 9 dB gain at BER=10^{-3}. This gain is exclusively due to the cooperative diversity. For the perfect (error-free) inter-source channel ($\gamma_{ss}^b = \infty$), the cooperative diversity gain is limited to 11 dB at BER=10^{-3}.

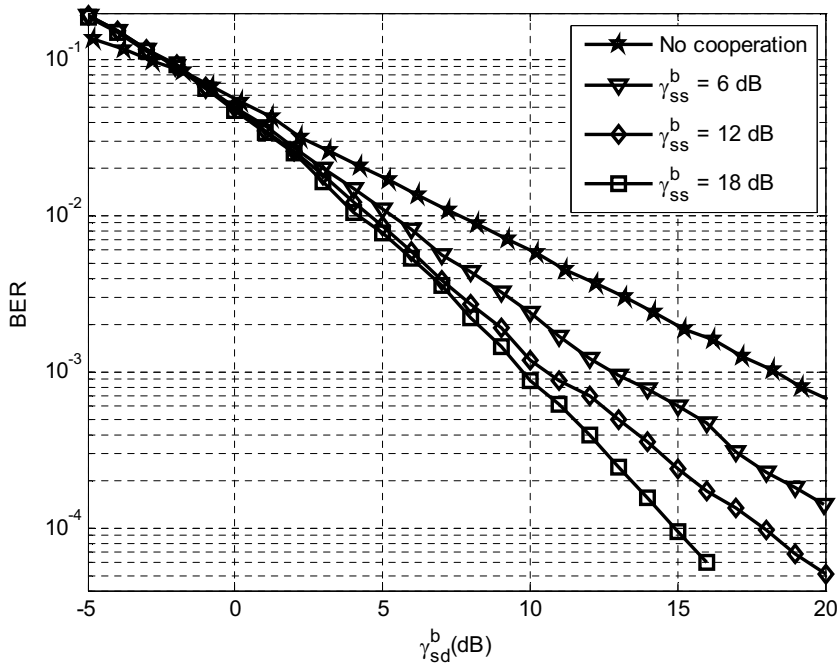

FIGURE 3.8: BER curves of the coded cooperation scheme using turbo codes for a fixed cooperation level $\alpha = 2/3$ over Rayleigh block fading channel.

3.2.4.2 Turbo Codes

For the example here, we consider the rate-1/2 convolutional encoder with generator polynomials $(1, 15/13)_8$ in octal form for $\mathcal{C}_a$ and the rate-1 convolutional encoder with generator polynomial $(17/13)_8$ for $\mathcal{C}_b$. A random interleaver is used. The cooperation level is then fixed to $\alpha = 2/3$. The broadcast phase and the cooperation phase have, respectively, $R_a = 1/2$ and $R_b = 1$ as code rates.

In Figure 3.8 BER curves are given for $\gamma_{ss}^b = 6$ dB, for $\gamma_{ss}^b = 12$ dB and for $\gamma_{ss}^b = 18$ dB, as a function of γ_{sd}^b. The turbo coded cooperation scheme improves the BER performance compared to the original non-cooperative turbo coded system. The gain at BER=10^{-3} is from 5 dB for the case of $\gamma_{ss}^b = 6$ dB to 7.5 dB for the case of $\gamma_{ss}^b = 18$ dB. A higher diversity is obtained if the inter-source transmission experiences a better channel conditions. Indeed, in each case ($\gamma_{ss}^b = 6$ dB, $\gamma_{ss}^b = 12$ dB and $\gamma_{ss}^b = 18$ dB) the slope of the curve changes, since the level of cooperation is improved.

3.3 Cooperative HARQ Protocols for Turbo Coded Cooperation

The goal of HARQ protocols in the two-source network of Figure 3.4, based on the turbo coded cooperation scheme, must be twofold: first to increase throughput, by avoiding transmissions when unnecessary; second to improve error rate performance.

With this aim, the first contribution of the thesis is to propose three basic hybrid ARQ protocols, called *destination-level HARQ* (DL-HARQ), *relay-level HARQ* (RL-HARQ) and *two-level HARQ* (TL-HARQ), respectively. They are addressed in the following.

3.3.1 Destination-Level HARQ Protocol

Compared to non-cooperation, coded cooperation may suffer from a throughput degradation, since two phases are always occupied for a single packet. The second phase brings degradation in throughput if the packets from both sources are correctly decoded after the first phase. In this case, the additional phase is not required (cooperation phase). Compared to the previously presented cooperative HARQ in Sub-section 3.1.4, a similar HARQ protocol could be defined for the two-source system in order to circumvent this drawback. The decision of retransmission can be performed at the destination: if decoding is successful, an ACK is fed back to s_1 and s_2 and the transmission of $\mathbf{u}_{1L}$ and $\mathbf{u}_{2L}$ is limited to the first phase. Otherwise, if decoding of either $\mathbf{u}_{1L}$ or $\mathbf{u}_{2L}$ fails, the destination feds back a NACK and the cooperation phase is performed. The second transmission phase for s_1 depends also tightly on decoding results of s_2, and is adjusted as following:

- If a NACK message is fed back to both sources, only CRC results at partner node dictate second transmission strategy, as described for the turbo coded cooperation scheme.
- If only decoding of s_1 fails at the destination after the first phase, no additional information is transmitted for s_2. Therefore, the second phase will be fully dedicated to s_1: s_2 does not need its partner cooperation anymore; then, the s_1-to-d link will be allocated to s_1. On the other hand, if possible (depending on CRC), s_2 cooperates with s_1 by transmitting $\mathbf{x}_{2R}$.

3.3.2 Relay-Level HARQ Protocol

It has been proved that the diversity gain in coded cooperation systems is conditioned by the quality of the inter-source channels [JHHN04]. Indeed, diversity gain cannot be obtained unless successful decoding is accomplished at the partner node. An immediate suggestion from HARQ protocols to be designed for this system model is then to strengthen the inter-source link. Another problem of coded cooperation is that, depending on channel conditions, the resulting coding scheme is asymmetric, i.e., it favors one source over the other. Consider for instance the case where s_1 decodes successfully and s_2 does not. In this case, the three codewords $\mathbf{x}_{2L}$, $\mathbf{x}_{1R}$ and $\tilde{\mathbf{x}}_{2L}$, distributed (over space) turbo code, will be transmitted for $\mathbf{u}_{2L}$, while only one codeword, $\mathbf{x}_{1L}$, will be transmitted for $\mathbf{u}_{1L}$. RL-HARQ can be used to circumvent these two drawbacks. In this

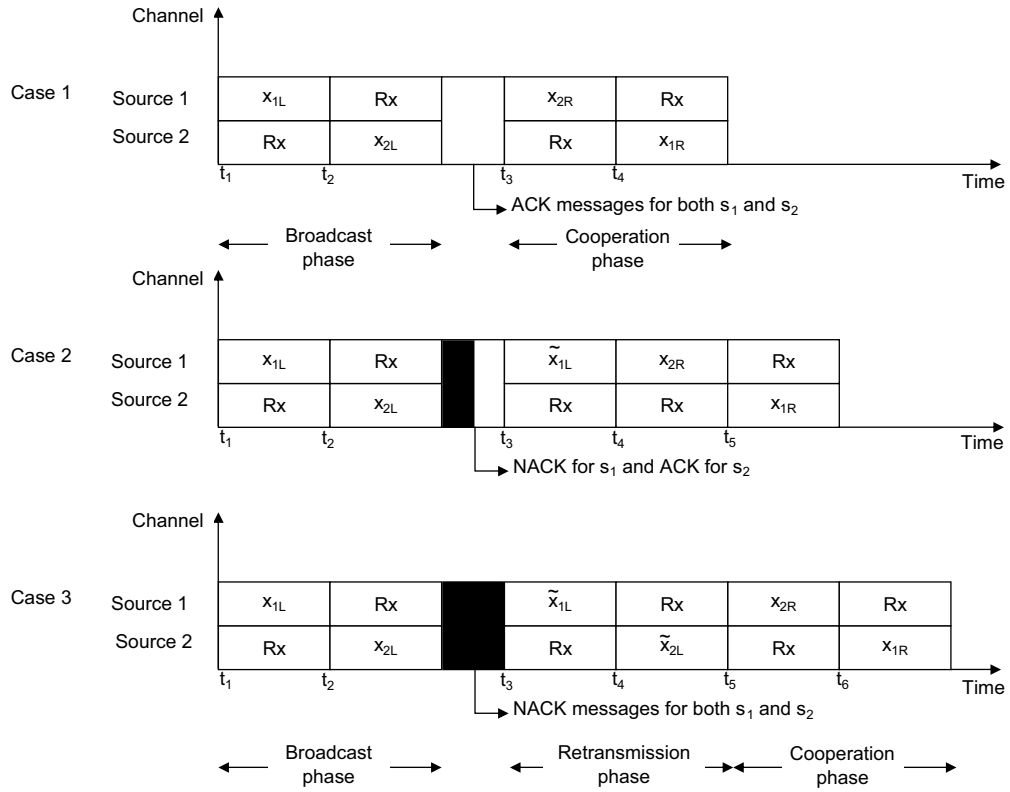

FIGURE 3.9: Relay-Level HARQ protocol.

protocol, the retransmission decision is taken by the partner node, in order to make the cooperation phase more efficient: alike the principle of turbo coded cooperation, since two codewords, $\mathbf{x}_{1L}$ and $\tilde{\mathbf{x}}_{1L}$, are available at partner node among two successive transmissions, a distributed (over time) turbo code is present, therefore ensuring improved inter-source channel quality and higher symmetry. Since the sources operate more frequently in relaying mode, higher diversity is achieved. Here, upon reception of $\mathbf{y}_{2L}^{\mathrm{s}_1}$ ($\mathbf{y}_{1L}^{\mathrm{s}_2}$) at s_1 (s_2), CRC results are fed back and exchanged between both sources. The protocol is depicted in Figure 3.9.

Three cases are possible:

- Case 1 ($\Omega = 1$) decoding at nodes s_1 and s_2 is successful: both s_1 and s_2 transmit ACK messages informing that the packets were correctly received, and that relaying can be performed at both nodes, by transmitting $\mathbf{x}_{1R}$ and $\mathbf{x}_{2R}$.

- Case 2 ($\Omega = 2$) decoding at node s_1 is successful, decoding at node s_2 fails: s_2 stores the corrupted packet in a temporary buffer and feeds back a NACK, while s_1 feeds back an ACK. A *retransmission phase* is then allocated for s_1, which transmits $\tilde{\mathbf{x}}_{1L}$. Therefore, s_2 can attempt to estimate $\mathbf{u}_{1L}$ from $\mathbf{y}_{1L}^{\mathrm{s}_2}$ and $\tilde{\mathbf{y}}_{1L}^{\mathrm{s}_2}$ applying turbo decoding.. Note that even if unsuccessful decoding persists at s_2, the destination

will benefit from the retransmission phase to accomplish turbo decoding using the two coded versions of $\mathbf{u}_{1L}$ ($\mathbf{x}_{1L}$ and $\tilde{\mathbf{x}}_{1L}$).

- Case 3 ($\Omega = 3$) decoding at nodes s_1 and s_2 fails: each source stores the erroneous packet in a temporary buffer and sends a NACK message to request retransmission. A *retransmission phase* is then allocated for s_1 and s_2, which transmit $\tilde{\mathbf{x}}_{1L}$ and $\tilde{\mathbf{x}}_{2L}$, respectively. At partner node, turbo decoding using the two transmission attempts is performed. Then, the cooperation phase is performed as described for the turbo coded cooperation scheme in the previous section; four sub-cases emerge according to decoding results (CRC results) at partner node after the retransmission phase.

Note that due to the retransmission phase, the proposed HARQ protocol guarantees that iterative decoding for both sources at the destination is always possible even if only one source transmits in the relaying mode during the cooperation phase. Therefore, performance improvement is expected.

3.3.3 Two-Level HARQ Protocol

Both DL-HARQ and RL-HARQ protocols can be combined to increase the throughput of the system and to improve error rate performance. The designation TL-HARQ comes from the fact that the protocol works at two levels: first, the destination feeds back ACK or NACK messages to the sources to determine whether the cooperation phase is required or not. The first ARQ level avoids degrading system throughput when packets are correctly decoded. In a second level, if a NACK was received, both sources feed back information on their own decoding to request retransmission from the partner node, if required. The goal of the second ARQ level is to improve the inter-source channels: allowing a higher degree of cooperation between sources and a high symmetry will result in better performance. To illustrate the proposed protocol, we detail several possible (but not exhaustive) cases:

- decoding of both $\mathbf{u}_{1L}$ and $\mathbf{u}_{2L}$ is successful at the destination: the destination feedbacks an ACK message to both users, informing that the cooperation phase is not required, and that transmission of the next information packet can be performed.

- $\mathbf{u}_{1L}$ is corrupted at both destination and s_2: both the destination and s_1 feedback a NACK message regarding $\mathbf{u}_{1L}$. A retransmission phase is then allocated for s_1, which transmits $\tilde{\mathbf{x}}_{1L}$. s_2 attempts to decode $\mathbf{u}_{1L}$ from $\mathbf{x}_{1L}$ (from the broadcast phase) and $\tilde{\mathbf{x}}_{1L}$ (from the retransmission phase) using iterative decoding. The cooperation phase is then performed as described in the previous sub-section.

- $\mathbf{u}_{1L}$ is corrupted at the destination but decoded correctly at s_2: the destination feedbacks a NACK regarding $\mathbf{u}_{1L}$, s_2 feedbacks an ACK. Since partner node feedback is positive, no retransmission phase is required for s_1 and the cooperation phase is then performed.

3.4 Performance Evaluation

It was emphasized above that cooperative retransmission protocols utilize spatial diversity, due to both cooperation and retransmissions. In addition, other important aspects of cooperative retransmission protocols are its spectral-efficient and energy-efficient nature. Therefore, to give a complete performance evaluation, two metrics quantifying the reliability and the efficiency of the system have to be considered. Consequently, in this section, we give BER results and throughput efficiency performance of the proposed HARQ protocols and compare them with the original turbo coded cooperation scheme. Furthermore, the energy efficiency aspect is taken into account through the computation of the effective system rate and involving it as a parameter of the expression of the energy per bit to noise ration (γ^b). As an example here we considered the rate-1/2 convolutional encoder with generator polynomials $(1, 15/13)_8$ for $\mathcal{C}_a$ and the rate-1 convolutional encoder with generator polynomial $(17/13)_8$ for $\mathcal{C}_b$. The information block length is $K = 128$ bits and a random interleaver is used.

In order to highlight the roles of cooperative and ARQ diversity gains, as opposed to the temporal diversity, we adopt the long-term static constraint, where all the ARQ rounds corresponding to a certain message take place over the channel realization. This approach was adopted in many previous related works [ZHF04, NAGS05, TDK07, ZWW09]. Furthermore, we assume that the feedback channels are error free and at most one retransmission attempt is allowed. Indeed, increasing the number of retransmission attempts is not appropriate to the adopted system and channel models. Increasing retransmission from the same partner node, i.e., over the same channel coefficient, is not relevant. Therefore, multiple retransmissions is not appropriate to a two-source cooperative system, unlike the case of multiple-relay networks [AFH08, ZWW09].

3.4.1 Bit Error Rate

In Figure 3.10 BER curves are given for $\gamma^b_{ss} = 6$ dB as a function of γ^b_{sd}, where $\gamma^b = \gamma/R$, being R the rate of the system. Note that the rate of the system depends on the code rate, the cooperative case and the average number of retransmission attempts. The cooperative retransmission protocols improve BER performance compared to the original turbo coded cooperation system. The DL-HARQ yields 1.5 dB gain at BER=10^{-3} with respect to the TCCoop system, thanks to a better system rate (less retransmission attempts). Notice that in this case the slope of the curve does not change, since the

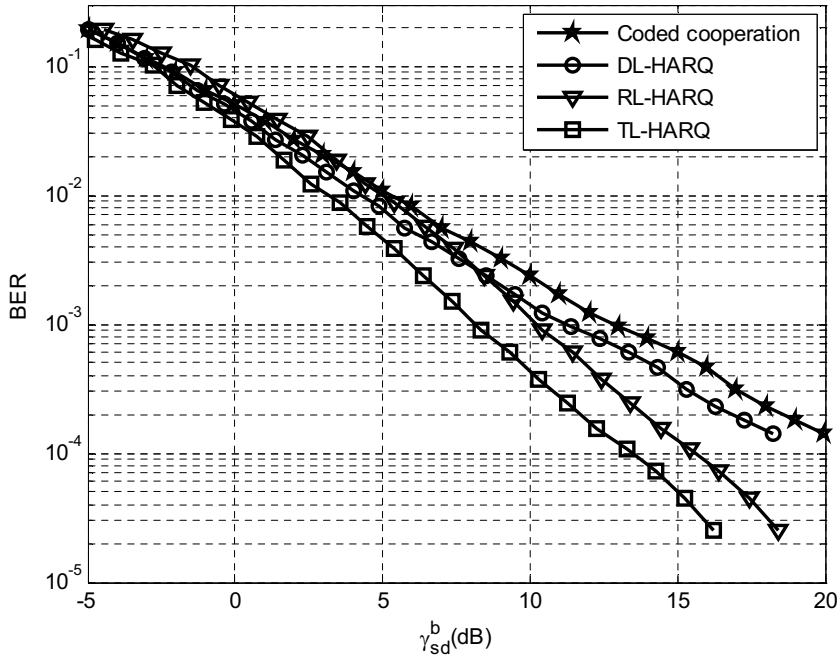

FIGURE 3.10: Bit error rate curves of cooperative HARQ for turbo coded cooperation, where $\alpha = 2/3$, Rayleigh block fading channel is assumed and $\gamma^b_{ss} = 6$ dB.

level of cooperation does not significantly improve with DL-HARQ. On the other hand a higher diversity is obtained if RL-HARQ is used (the quality of the inter-source channel is improved), thus improving BER for high γ^b_{sd}. The TL-HARQ protocol gives the best results: it achieves the diversity gain of the RL-HARQ protocol but it provides some extra coding gain, about 2 dB.

Asymptotically, the turbo coded cooperation scheme as well as DL-HARQ, RL-HARQ and TL-HARQ protocols achieve the same diversity. To highlight this result, in Figure 3.11 we plot BER curves of TCCoop scheme, DL-HARQ, RL-HARQ and TL-HARQ protocols for $\gamma^b_{ss} = \gamma^b_{sd}$ dB. From Figure 3.11, we note that all protocols achieve full diversity of two since the slope of their corresponding curves do not change. This result is confirmed by the analytical analysis given in Section 4.2 of Chapter 4, where we determine the diversity order of the studied cooperative HARQ protocols by examining the asymptotic behavior of their respective outage probabilities in the high-SNR regime.

3.4.2 Throughput Efficiency

The throughput efficiency performance for the case of a fixed inter-source channel quality ($\gamma^b_{ss} = 6$ dB) is reported in Figure 3.12. We recall that the *throughput efficiency* (η) is defined as (see Sub-section 2.5.3)

$$\eta = \varrho T \tag{3.2}$$

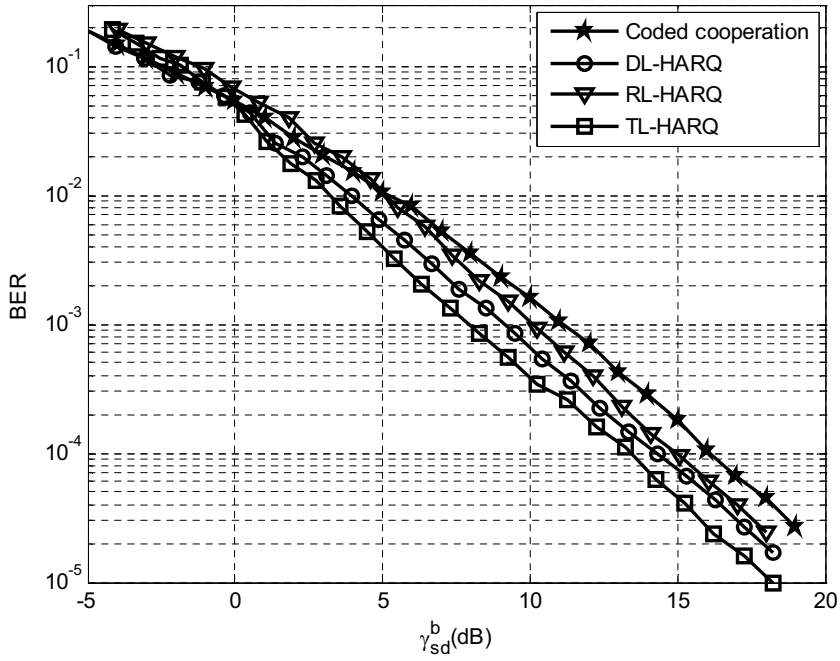

FIGURE 3.11: Bit error rate curves of cooperative HARQ for turbo coded cooperation, where $\alpha = 2/3$, Rayleigh block fading channel is assumed and $\gamma^b_{ss} = \gamma^b_{sd}$ dB.

The *throughput efficiency* of the coded cooperation system without ARQ is limited to $\eta \leq 1/3$, since two phases are always allocated for the transmission of a packet, hence $R = 1/3$. A throughput efficiency degradation is observed for the RL-HARQ with respect to the turbo coded cooperation scheme, since retransmissions to the partner node can occur even if the packet can be correctly decoded at destination in the broadcast phase. Notice that in this case the reliability ϱ is improved (see Figure 3.10), but not enough to compensate the degradation in throughput T. This phenomenon is more visible when the inter-source channel is of bad quality. On the other hand, the DL-HARQ protocol avoids the throughput degradation by allowing the cooperation phase only when it is necessary. In this case η tends to 1/2 since for high γ^b_{sd} only the broadcast phase is required, hence $R = 1/2$. However, as shown in Figure 3.10 the error rate is higher than the one of the RL-HARQ. The best results are achieved by the TL-HARQ protocol, since it combines the benefits of the DL-HARQ protocol (i.e., increased throughput with respect to the turbo coded cooperation scheme) and of the RL-HARQ (higher reliability).

The throughput efficiency performance for the case of an increasing inter-source channel quality ($\gamma^b_{ss} = \gamma^b_{sd}$), is given in Figure 3.13. The same observations are valid for $\gamma^b_{ss} = \gamma^b_{sd}$. However, the throughput efficiency degradation observed for the RL-HARQ with respect to the turbo coded cooperation scheme when $\gamma^b_{ss} = 6$ dB, is compensated at the high-SNR regime since the inter-source channel becomes good enough to settle for only one transmission between both sources. Furthermore, a minimum inter-source channel quality ($\gamma^b_{ss} = 0$ dB) is needed in order to bring a throughput efficiency gain of

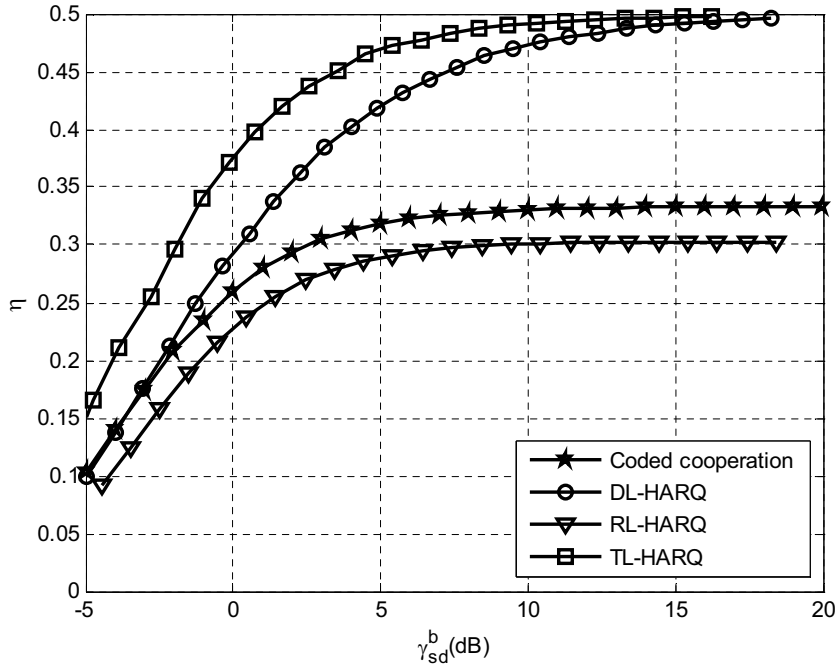

FIGURE 3.12: Throughput efficiency of cooperative HARQ for turbo coded cooperation, where $\alpha = 2/3$, Rayleigh block fading channel is assumed and $\gamma_{ss}^{b} = 6$ dB.

the TL-HARQ with respect to the DL-HARQ.

3.5 Multi-Source Transmission with Interleave Division Multiple Access

Orthogonal scenarios with TDMA were considered in the previous sections. However, a throughput degradation characterizes TCCoop scheme due to a supplementary cooperation phase. This drawback may be circumvented by reducing the transmission time of this critical phase. Non-orthogonal schemes where several sources are allocated the same bandwidth and time slot are more appropriate. In this section, we consider the multi-source cooperative network based on the turbo coded cooperation scheme where both sources transmit to a destination with simultaneous multiple-access. As explained in Chapter 2 (Secion 2.6), several transmitting techniques can be used to deal with multiple-access interference at the destination. In our work, we consider the use of IDMA for multi-source detection. This choice is dictated by the low complexity of the IDMA receiver. Separation between q sources is obtained by the use of a different interleaver for each source. The complexity of the IDMA receiver is $O(q)$ [PLWL03] while that of CDMA system is $O(q^2)$ [WP99]. For a coded cooperation system, the nodes act either as a source transmitting its local information or as a relay helping the partner by forwarding its information. Therefore, to still operate in the half-duplex setup, the

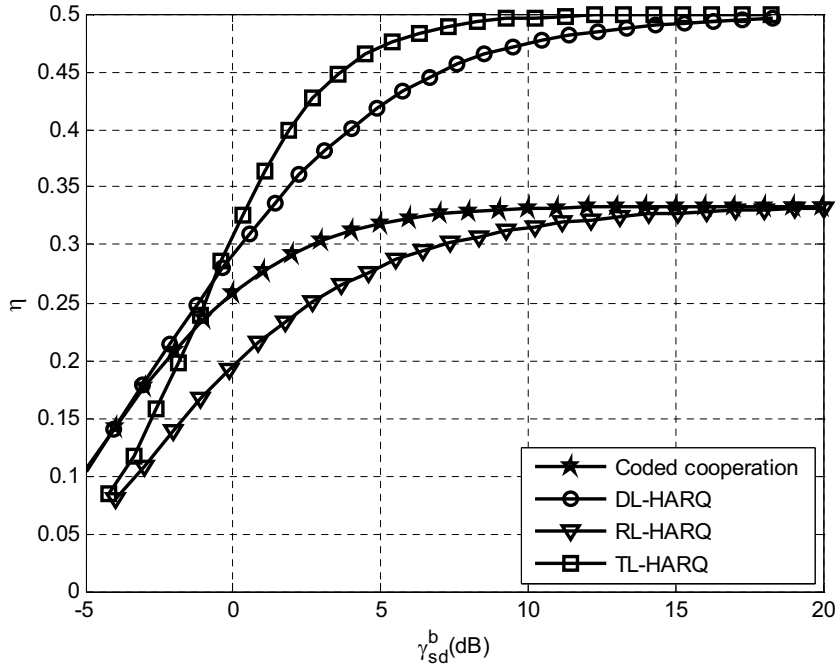

FIGURE 3.13: Throughput efficiency of cooperative HARQ for turbo coded cooperation, where $\alpha = 2/3$, Rayleigh block fading channel is assumed and $\gamma_{ss}^{b} = \gamma_{sd}^{b}$ dB.

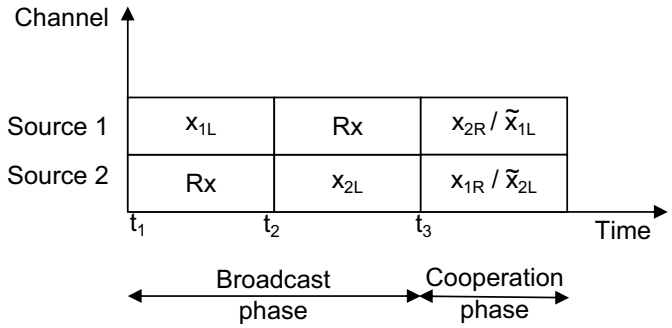

FIGURE 3.14: The transmission time is yet divided into two phases: orthogonal broadcast phase (two time slots) and a non-orthogonal cooperation phase (a unique time slot allocated for both sources).

sources have to transmit in an orthogonal way for the first transmission phase (broadcast phase). The multi-source transmission with IDMA is limited to the second phase (cooperation phase). The transmission time is illustrated in Figure 3.14.

From the first orthogonal phase, the destination receives the noisy observation of each source codeword transmitted over the direct link. On the other hand, during the cooperation phase, since both sources transmit simultaneously, a multi-source detector at the destination is required to distinguish between signals from both sources. We assume perfect frame synchronization. Two main blocks are used: an ESE that exchanges extrinsic information with two turbo-decoders, one for each source, in an outer iterative process. Thanks to the use of interleavers, the ESE operation can be carried out by a

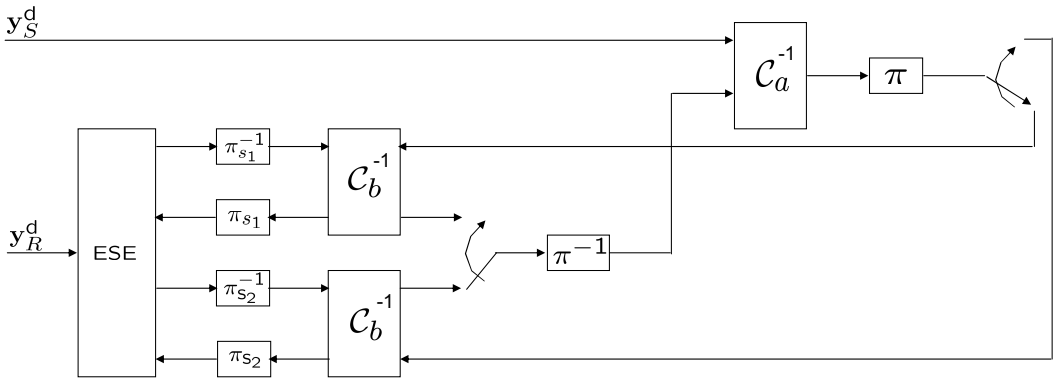

FIGURE 3.15: IDMA receiver at the destination for turbo coded cooperative scheme for one source.

low complexity chip-by-chip detection algorithm (described in Sub-section 2.6.1) that manages the multiple access interference. The ESE computes the extrinsic information for the considered source by assuming that the signal of the partner is a Gaussian noise. The extrinsic information is then used as input information for the turbo coded cooperation protocol. Hence, an inner iterative process is performed to obtain the distributed turbo decoding for each source. We denote by global iteration an iteration between the IDMA receiver and decoder $\mathcal{C}_a$, and local iteration an iteration within the IDMA receiver. The structure of the distributed turbo code receiver with multi-source detection at the destination node is depicted in Figure 3.15. Here, we consider a single local iteration for each global iteration with a total number of iterations of 8.

To illustrate the effect of using the IDMA mode, we give BER results and throughput efficiency performance of the proposed HARQ protocols as well as the original turbo coded cooperation scheme using both multiple-access techniques (TDMA and IDMA). The simulation example here is the same considered in Section 3.4.

In Figure 3.16 BER curves are given for $\gamma_{ss}^b = 3$ dB as a function of γ_{sd}^b, where $\gamma^b = \gamma/R$, being R the rate of the system. The rate of the system here depends not only on the code rate and the average number of retransmission attempts, but also on the multiple-access technique. For instance, for an orthogonal TCCoop when both sources operate under the perfect cooperation case with $\alpha = 2/3$, the overall rate equals $1/3$, it corresponds to 6 different time slots allocated to transmit two local frames of two sources. On the other hand, for a non-orthogonal TCCoop, both local frames at cooperating sources take 5 different time slots to reach the destination; then, the overall rate is $R = 2/5$. The most significant remark to be made from this figure is that the BER performance of TCCoop system is slightly affected when operating over non-orthogonal channels. For instance, a low degradation persist after 8 iterations of IDMA process aiming on source signal separation (interference cancellation).

The throughput performance is reported in Figure. 3.17. The throughput efficiency

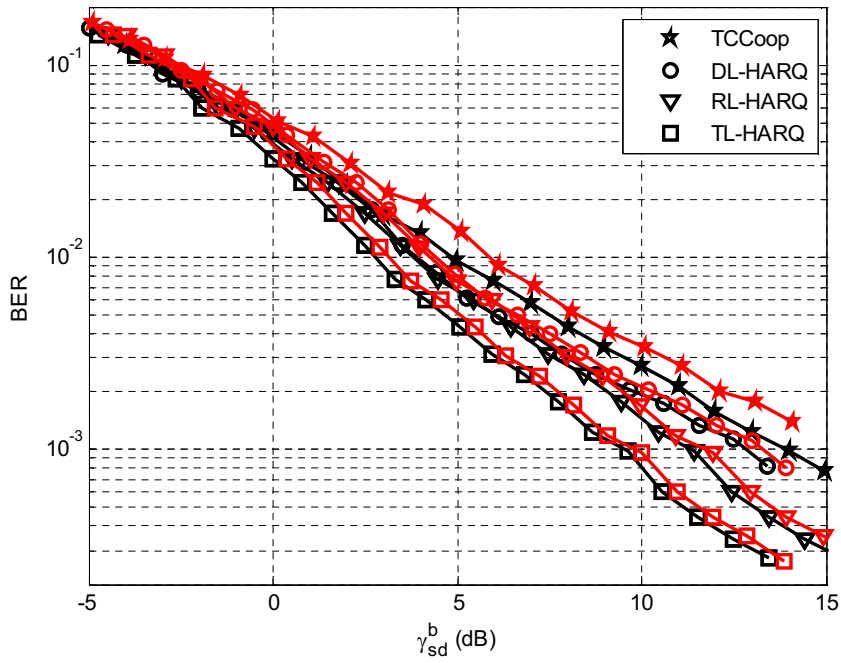

FIGURE 3.16: Bit error rate curves of cooperative HARQ for turbo coded cooperation, where $\alpha = 2/3$, Rayleigh block fading channel is assumed and $\gamma_{ss}^{b} = 3$ dB, using TDMA (*black curves*) and IDMA (*red curves*) multiple-access techniques.

of the turbo coded cooperation system over orthogonal channels is limited to $\eta \leq 1/3$, since two phases are always allocated for the transmission of a packet, hence $R = 1/3$. A sizable throughput efficiency increase is obtained with the non-orthogonal channel based on IDMA technique. In this case, the throughput efficiency is limited to $R = 2/5$ since better transmission delay is obtained when the same time slot is allocated to both sources to perform the cooperation phase. The BER degradation observed over non-orthogonal channel with respect to the orthogonal one is largely compensated by the throughput gain. For DL-HARQ and TL-HARQ protocols, the throughput efficiency limit for high γ_{sd}^{b} is the same, since it corresponds to the first transmission phase which still operates on an orthogonal way. However, for low and medium SNR regime, a significant improvement on the system efficiency is noted. Moreover, The RL-HARQ protocol benefits also from the overall system throughput preservation when non-orthogonal channels are assumed for the cooperation phase.

3.6 Chapter Summary

In this chapter, we presented background knowledge about basic cooperative communication systems. We started by introducing the relay channel. Then, we presented the different cooperative strategies. Furthermore, we gave a quick overview of distributed turbo codes for the relay channel. In addition, we detailed the well-known cooperative

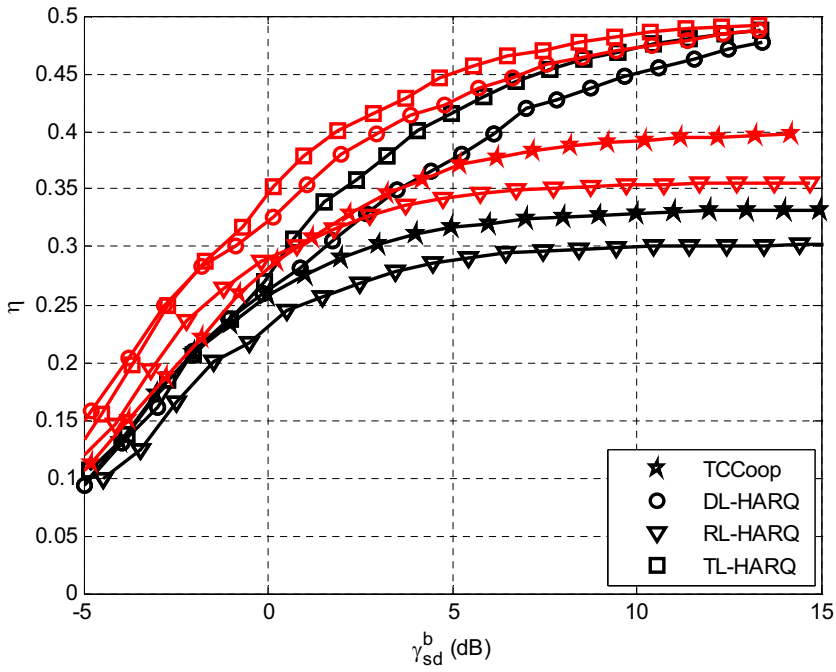

FIGURE 3.17: Throughput efficiency of cooperative HARQ for turbo coded cooperation, where $\alpha = 2/3$, Rayleigh block fading channel is assumed and $\gamma_{ss}^{b} = 3$ dB, using TDMA (*black curves*) and IDMA (*red curves*) multiple-access techniques.

scheme for wireless user cooperation, called coded cooperation, in which cooperation is integrated with channel coding and is controlled by an error detection code in order to avoid error propagation. The extension of distributed turbo codes to the coded cooperation scheme was also described, by presenting the turbo coded cooperation scheme. Moreover, this chapter was dedicated to develop three different extensions to the turbo coded cooperation scheme: three cooperative HARQ protocols differing on where decision of retransmission is performed. This consists on the first main contribution of the thesis.

A first HARQ protocol, DL-HARQ, was proposed to avoid throughput degradation due to the cooperation phase, when unnecessary. A second HARQ protocol, RL-HARQ, was then designed to improve inter-source channel quality, thus increasing the diversity of the system. However, RL-HARQ brings a significant degradation in throughput. Finally, a third protocol, TL-HARQ, combining the benefits of DL-HARQ (higher throughput) and RL-HARQ (higher reliability) was proposed. Numerical results demonstrated that the TL-HARQ protocol achieved the best performance both in terms of error rate and throughput efficiency. Significant improvements were observed with respect to the non-ARQ scheme and the DL-HARQ and RL-HARQ protocols. Sizable gains in terms of throughput efficiency were noted when we assumed non-orthogonal channels during the cooperation phase and half-duplex mode operation. Using the IDMA technique for

superposed signal separation, we achieve asymptotically up to 20 % of throughput efficiency gain for DL-HARQ and TL-HARQ protocols. This gain largely compensate the non significant BER degradation observed over the non-orthogonal channel with respect to the orthogonal one.

Chapter 4

Performance Analysis of Coded Cooperation with HARQ

In the previous chapter, we explored cooperative HARQ protocols for user cooperation system. In this chapter we analyze the outage behavior of the HARQ protocols introduced in the previous chapter, in order to evaluate them according to different parameters: channel conditions, rate and time allocation. The outage probability has been shown to be a lower bound on frame error rate (FER) for sufficiently large frame length [KH00], [ML99]. Therefore, the outage analysis gives a coarse performance evaluation since it does not depend on the used channel code. Furthermore, we determine the asymptotic diversity order of the proposed protocols. The outage analysis does not consider system efficiency, which is one of the dominant factors determining performance. Therefore, to better compare the proposed cooperative protocols, we analyze them in terms of the diversity-multiplexing tradeoff (DMT). The DMT is a measure of performance adopted to establish the gain offered by the proposed protocols, characterizing the tradeoff between the reliability and the efficiency. The outage behavior and the DMT analysis of the previously proposed cooperative HARQ protocols represent the second main contribution of the thesis.

In [LES06], the frame error probability of the coded cooperation system based on the pairwise error probability was analyzed, and the authors defined the *cooperation gain* as the performance improvement with respect to the non-cooperative case. In this chapter, we extend the analysis in [LES06] to the cooperative HARQ context using turbo processing, acting out as the third main contribution of the thesis. Bounds on frame error probability derived here give a companion analysis to that established by the outage analysis, taking into account also the used channel code. We define two parameters to assess the benefits of the DL-HARQ and the TL-HARQ protocols: the *cooperation gain*, with respect to the non-cooperative point-to-point IR-HARQ, and the *retransmission*

gain, with respect to the conventional turbo coded cooperative system when no retransmission is allowed. These gains are introduced to quantify the performance improvement of the considered systems in terms of reliability (frame error probability) and efficiency (throughput efficiency), and to determine the geometric conditions under which using cooperative HARQ protocols is useful.

4.1 Outage Probability

In this section, we analyze the probability of outage of the proposed cooperative HARQ protocols and compare them with that of coded cooperation. We consider derivations for source s_1 only. Due to the symmetry of the system, identical expressions are obtained for s_2 by simply reversing s_1 and s_2 roles. As a reference, we first consider the direct transmission of a source message to the destination, where no retransmissions neither cooperation occur (see Section 2.2). The outage probability for Rayleigh block fading can be evaluated as [OSW94]

$$P_{\text{out}} = \Pr\left(\gamma_{\mathrm{s}_1\mathrm{d}} < 2^R - 1\right) = 1 - \exp\left(-\frac{2^R - 1}{\Gamma_{\mathrm{s}_1\mathrm{d}}}\right) \tag{4.1}$$

where $\Gamma_{\mathrm{s}_1\mathrm{d}} = \rho\mathcal{E}[|h_{\mathrm{s}_1\mathrm{d}}|^2]$ denotes the mean value of the SNR of the s_1-to-d channel.

4.1.1 Coded Cooperation Scheme

Seen as an adaptive decode-and-forward scheme, the outage events of the coded cooperation scheme can be formulated into four cases ($\Theta \in \{1, 2, 3, 4\}$), as described in Section 3.2 of Chapter 3:

- Case 1 ($\Theta = 1$) decoding at nodes s_1 and s_2 is successful: two codewords, $\mathbf{x}_{1L}$ and $\mathbf{x}_{2R}$ are transmitted over broadcast and cooperation phases. Notice that $\mathbf{x}_{1L}$ and $\mathbf{x}_{2R}$ form a codeword of a distributed code, where the first subcodeword is generated by s_1 and the second subcodeword is generated by s_2.

- Case 2 ($\Theta = 2$) decoding at nodes s_1 and s_2 fails: two codewords are transmitted for $\mathbf{u}_{1L}$, namely $\mathbf{x}_{1L}$ and $\tilde{\mathbf{x}}_{1L}$, both generated by s_1. Therefore, a distributed (over time) code is obtained.

- Case 3 ($\Theta = 3$) decoding at node s_1 fails, decoding at node s_2 is successful: in this case both s_1 and s_2 dedicate the second phase to transmit $\mathbf{u}_{1L}$. Therefore, three codewords are generated for $\mathbf{u}_{1L}$, namely $\mathbf{x}_{1L}$, $\tilde{\mathbf{x}}_{1L}$ and $\mathbf{x}_{2R}$.

- Case 4 ($\Theta = 4$) decoding at node s_1 is successful, decoding at node s_2 fails: a single codeword, $\mathbf{x}_{1L}$, is allocated to $\mathbf{u}_{1L}$.

For cases $\Theta = 1$ and $\Theta = 2$, the second phase is dedicated to the transmission of only one codeword for $\mathbf{u}_{1L}$ ($\mathbf{x}_{1R}$ or $\tilde{\mathbf{x}}_{1L}$ from either the partner node or the node itself, respectively). Therefore, the total mutual information is the *sum* of the mutual information received in each phase. On the other hand, for case $\Theta = 3$ two identical codewords are transmitted for $\mathbf{u}_{1L}$ in the second phase ($\mathbf{x}_{1R}$ and $\tilde{\mathbf{x}}_{1L}$). In this case the destination must optimally combine them before the joint decoding process. This can be seen as a chase combining operation. Thus, the instantaneous SNR rather than the mutual information is accumulated to compute the contribution of the second phase over participating links. Finally, for the case that only the first phase is dedicated to the transmission of $\mathbf{u}_{1L}$ (case $\Theta = 4$), the threshold rate defining the outage computation is reduced to R/α, the rate allocated to the first phase. We recall that R is the transmission rate and α is the cooperation level, giving the ratio of the N total channel symbols allocated to the broadcast phase, as defined in Section 3.2.

Following this discussion, the outage event can be written as

$$\mathcal{O}_1 \equiv \left\{ \underbrace{\alpha \log(1+\gamma_{\mathrm{s_1d}})}_{\text{Broadcast Phase}} + \underbrace{(1-\alpha)\log(1+\bar{\mathcal{I}}_{\mathrm{s_2s_1}}(R/\alpha)\gamma_{\mathrm{s_1d}} + \mathcal{I}_{\mathrm{s_1s_2}}(R/\alpha)\gamma_{\mathrm{s_2d}})}_{\text{Cooperation Phase}} < R \right\} \quad (4.2)$$

where $\mathcal{I}_{s_i s_j}(x)$ is an indicator function of the outage status of the s_i-to-s_j link, with reference to the received rate x. $\mathcal{I}_{s_i s_j}(x) = 0$ when the link is in outage and $\mathcal{I}_{s_i s_j}(x) = 1$ when it is not.

The outage probability is given by [HSN06]

$$P_{\mathrm{out},1}^{\mathrm{CCoop}} = \Pr(\mathcal{O}_1) = F(R) + G(R) \quad (4.3)$$

where

$$F(x) = \exp\left(\frac{1-2^{x/\alpha}}{\Gamma_{\mathrm{s_2s_1}}}\right)\left[1-\exp\left(\frac{1-2^{x/\alpha}}{\Gamma_{\mathrm{s_1d}}}\right) - \exp\left(\frac{1-2^{x/\alpha}}{\Gamma_{\mathrm{s_1s_2}}}\right)\Psi_1(x)\right] \quad (4.4)$$

$$G(x) = \left[1-\exp\left(\frac{1-2^{x/\alpha}}{\Gamma_{\mathrm{s_2s_1}}}\right)\right]\left[1-\exp\left(\frac{1-2^{x}}{\Gamma_{\mathrm{s_1d}}}\right) - \exp\left(\frac{1-2^{x/\alpha}}{\Gamma_{\mathrm{s_1s_2}}}\right)\Psi_2(x)\right] \quad (4.5)$$

$$\Psi_1(x) = \int_0^{2^{x/\alpha}-1} \frac{1}{\Gamma_{\mathrm{s_1d}}} \exp\left(-\frac{\gamma_{\mathrm{s_1d}}}{\Gamma_{\mathrm{s_1d}}} - \frac{a(x)}{\Gamma_{\mathrm{s_2d}}}\right) d\gamma_{\mathrm{s_1d}} \quad (4.6)$$

$$\Psi_2(x) = \int_0^{2^{x}-1} \frac{1}{\Gamma_{\mathrm{s_1d}}} \exp\left(-\frac{\gamma_{\mathrm{s_1d}}}{\Gamma_{\mathrm{s_1d}}} - \frac{b(x)}{\Gamma_{\mathrm{s_2d}}}\right) d\gamma_{\mathrm{s_1d}} \quad (4.7)$$

$$a(x) = \frac{2^{x/(1-\alpha)}}{(1+\gamma_{\mathrm{s_1d}})^{\alpha/(1-\alpha)}} - 1 \quad (4.8)$$

$$b(x) = \frac{2^{x/(1-\alpha)}}{(1+\gamma_{\mathrm{s_1d}})^{\alpha/(1-\alpha)}} - 1 - \gamma_{\mathrm{s_1d}} \tag{4.9}$$

4.1.2 Destination-Level HARQ Protocol

For this protocol, the first-round rate R is relative to the first transmission phase. The total received rate is then αR, when the cooperation phase (retransmission phase) is required. Similarly to the coded cooperation case, the two transmissions can be viewed as time sharing between two independent channels, where the first channel is used a fraction α of the time and the remaining fraction is reserved to the optional cooperation phase. Following the discussion in Subsection 3.3.1, as the second phase depends not only on CRC results at partner node but also on decoding results of s_2 at the destination after the first transmission phase, the outage event is given by

$$\begin{aligned}\mathcal{O}_1 \equiv \{&\alpha \log(1+\gamma_{\mathrm{s_1d}}) \\ &+ (1-\alpha)\log(1+(\mathcal{I}_{\mathrm{s_2d}}(R) + \bar{\mathcal{I}}_{\mathrm{s_2d}}(R)\bar{\mathcal{I}}_{\mathrm{s_2s_1}}(R))\gamma_{\mathrm{s_1d}} + \mathcal{I}_{\mathrm{s_1s_2}}(R)\gamma_{\mathrm{s_2d}}) < \alpha R\}\end{aligned} \tag{4.10}$$

where $\mathcal{I}_{\mathrm{s_2d}}(x)$ is defined in the same manner as $\mathcal{I}_{\mathrm{s_i s_j}}(x)$.

The outage probability relative to this protocol is given by

$$P_{\mathrm{out},1}^{\text{DL-HARQ}} = \left[1 - \exp\left(\frac{1-2^R}{\Gamma_{\mathrm{s_2d}}}\right)\right] F(\alpha R) + G(\alpha R) \tag{4.11}$$

where $F(x)$ and $G(x)$ are defined in (4.4) and (4.5), respectively.

4.1.3 Relay-Level HARQ Protocol

Following the discussion in Sub-section 3.3.2, the instantaneous channel capacity depends on whether decoding is successful or not at partner node s_2 after the first transmission phase, and after the retransmission phase, if required, exploiting jointly codewords $\mathbf{x}_{1L}$ and $\tilde{\mathbf{x}}_{1L}$. The retransmission phase is also viewed as an extra information by the destination, since the radio link is broadcast-oriented. However, if it is present, it is considered as an extra channel utilization. Since the transmission process performed in the retransmission phase is the same as that performed in the cooperation phase, the system is viewed as a repetition-based relaying scheme. Therefore, a normalization (bandwidth expansion) factor is required to fairly express the equivalent channel capacity [SSS08].

According to cases $\Omega = 1, 2$, and 3, explained in Sub-section 3.3.2, the equivalent channel capacity expression is evaluated to

- $\Omega = 1$: $C = \alpha \log(1+\gamma_{\mathrm{s_1d}}) + (1-\alpha)\log(1+\gamma_{\mathrm{s_2d}})$
- $\Omega = 2$: $C = \log(1+\gamma_{\mathrm{s_1d}})$

- $\Omega = 3$: we distinguish between four subcases (see Sub-section 3.3.2):
  - $\Theta = 1 : C = \alpha \log(1 + \gamma_{\mathrm{s_1 d}}) + (\frac{1-\alpha}{2}) \log(1 + \gamma_{\mathrm{s_1 d}} + \gamma_{\mathrm{s_2 d}})$
  - $\Theta = 2 : C = \alpha \log(1 + \gamma_{\mathrm{s_1 d}}) + (\frac{1-\alpha}{2}) \log(1 + 2\gamma_{\mathrm{s_1 d}})$
  - $\Theta = 3 : C = \alpha \log(1 + \gamma_{\mathrm{s_1 d}}) + (\frac{1-\alpha}{2}) \log(1 + 2\gamma_{\mathrm{s_1 d}} + \gamma_{\mathrm{s_2 d}})$
  - $\Theta = 4 : C = \log(1 + \gamma_{\mathrm{s_1 d}})$

The outage event can then be written as

$$\mathcal{O}_1 \equiv \{\alpha \log(1 + \gamma_{\mathrm{s_1 d}}) + \mathcal{D}_{\mathrm{BE}}(1 - \alpha) \log(1 + \mathcal{D}_{\mathrm{Rtx}}\gamma_{\mathrm{s_1 d}} + \mathcal{D}_1\gamma_{\mathrm{s_1 d}} + \mathcal{D}_2\gamma_{\mathrm{s_2 d}}) < R\} \quad (4.12)$$

where $\mathcal{D}_{\mathrm{BE}}$, $\mathcal{D}_{\mathrm{Rtx}}$, $\mathcal{D}_1$ and $\mathcal{D}_2$ are defined as follows:

- $\mathcal{D}_{\mathrm{BE}}$ refers to the bandwidth expansion factor and is defined as $\mathcal{D}_{\mathrm{BE}} = \frac{\bar{\mathcal{I}}_{\mathrm{s_1 s_2}}(R/\alpha)}{2} + \mathcal{I}_{\mathrm{s_1 s_2}}(R/\alpha)$.
- $\mathcal{D}_{\mathrm{Rtx}} = \bar{\mathcal{I}}_{\mathrm{s_1 s_2}}(R/\alpha)$ expresses the condition that retransmission to partner node is required (first decoding at partner node is unsuccessful). Hence, the contribution of the $\mathrm{s_1}$-to-d link has to be considered as an extra participating SNR (chase combining operation).
- $\mathcal{D}_1 = \bar{\mathcal{I}}_{\mathrm{s_2 s_1}}(R/\alpha)\bar{\mathcal{I}}_{\mathrm{s_2 s_1}}(R)$ is a variable indicating conditions under which the $\mathrm{s_1}$-to-d link is dedicated to $\mathrm{s_1}$ during the cooperation phase.
- $\mathcal{D}_2 = \mathcal{I}_{\mathrm{s_1 s_2}}(R/\alpha) + \bar{\mathcal{I}}_{\mathrm{s_1 s_2}}(R/\alpha)\mathcal{I}_{\mathrm{s_1 s_2}}(R)$ is a variable indicating conditions under which the $\mathrm{s_2}$-to-d link is reserved to cooperate with $\mathrm{s_1}$.

The outage probability derivation relative to this protocol is straightforward applying the appropriate equivalent channel capacities under the appropriate conditions (relative to $\mathcal{I}_{\mathrm{s}_i\mathrm{s}_j}(x)$ and $\mathcal{I}_{\mathrm{s}_i\mathrm{d}}(x)$ values).

4.1.4 Two-Level HARQ Protocol

The outage analysis relative to this protocol is the same as that developed for the RL-HARQ protocol, except that we have to consider two main assumptions:

- The first-round rate is R, the same as defined for DL-HARQ. It corresponds to the first transmission phase (broadcast phase), since transmission can be stopped after this phase if correct decoding at the destination occurs for both sources.
- Retransmission to partner node and the cooperation phase are determined by two levels: by the decoding results at the destination after the broadcast phase, and, if necessary (unsuccessful decoding), by the CRC results at partner node.

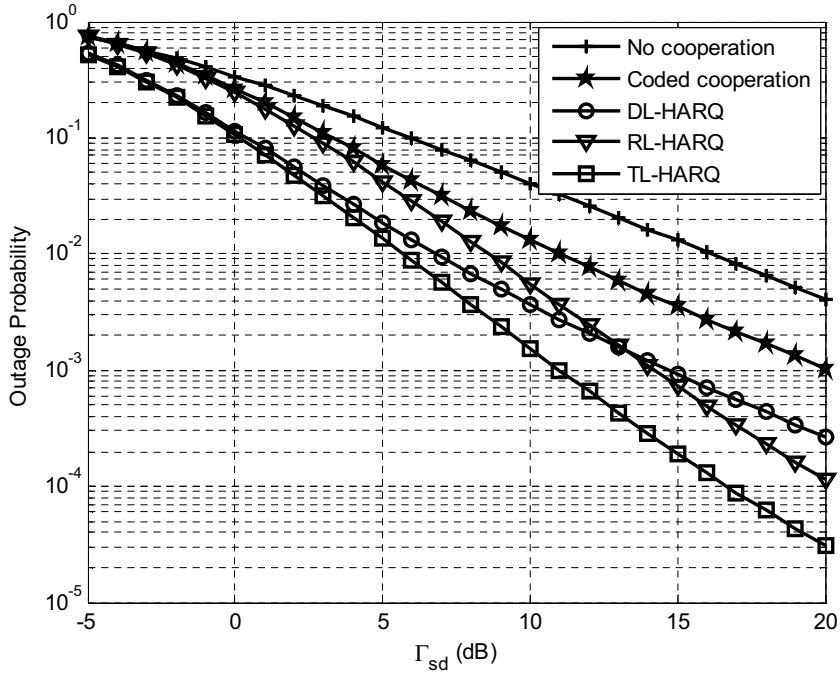

FIGURE 4.1: Outage probability curves for several coded cooperation schemes with $\Gamma_{\mathrm{s_1s_2}} = 6$ dB, $\Gamma_{\mathrm{s_1d}} = \Gamma_{\mathrm{s_2d}} = \Gamma_{\mathrm{sd}}$ and $\alpha = 2/3$.

Taking into account this, the outage event is given by

$$\begin{aligned}\mathcal{O}_1 \equiv \Big\{ & \alpha \log(1+\gamma_{\mathrm{s_1d}}) + \mathcal{D}'_{\mathrm{BE}}(1-\alpha) \\ & \log(1+\mathcal{D}'_{\mathrm{Rtx}}\gamma_{\mathrm{s_1d}} + \mathcal{D}'_1\gamma_{\mathrm{s_1d}} + \mathcal{D}'_2\gamma_{\mathrm{s_2d}}) < \alpha R \Big\}\end{aligned} \tag{4.13}$$

where

$$\mathcal{D}'_{\mathrm{BE}} = \frac{\bar{\mathcal{I}}_{\mathrm{s_1s_2}}(R)}{2} + \mathcal{I}_{\mathrm{s_1s_2}}(R) \tag{4.14a}$$

$$\mathcal{D}'_{\mathrm{Rtx}} = \bar{\mathcal{I}}_{\mathrm{s_1s_2}}(R) \tag{4.14b}$$

$$\mathcal{D}'_1 = \mathcal{I}_{\mathrm{s_2d}}(R) + \bar{\mathcal{I}}_{\mathrm{s_2d}}(R)\bar{\mathcal{I}}_{\mathrm{s_2s_1}}(R)\bar{\mathcal{I}}_{\mathrm{s_2s_1}}(\alpha R) \tag{4.14c}$$

$$\mathcal{D}'_2 = \mathcal{I}_{\mathrm{s_1s_2}}(R) + \bar{\mathcal{I}}_{\mathrm{s_1s_2}}(R)\mathcal{I}_{\mathrm{s_1s_2}}(\alpha R) \tag{4.14d}$$

4.1.5 Numerical Results

In Figure 4.1 we give the outage probabilities of the cooperative protocols proposed and analyzed in the previous sections. A first phase rate of 1/2 bit/s/Hz, and symmetric s_i-to-s_j ($\Gamma_{\mathrm{s_1s_2}} = \Gamma_{\mathrm{s_2s_1}} = 6$ dB) and s_i-to-d ($\Gamma_{\mathrm{s_1d}} = \Gamma_{\mathrm{s_2d}}$) channels, are assumed. The cooperation level (or time resource allocation) is fixed to $\alpha = 2/3$; this leads to an overall rate of 1/3. This value minimizes the outage probability for the coded cooperation scheme [HSN06]. The DL-HARQ improves the non-HARQ coded cooperation thanks to a better system rate. Notice that in this case the slope of the curve does not change,

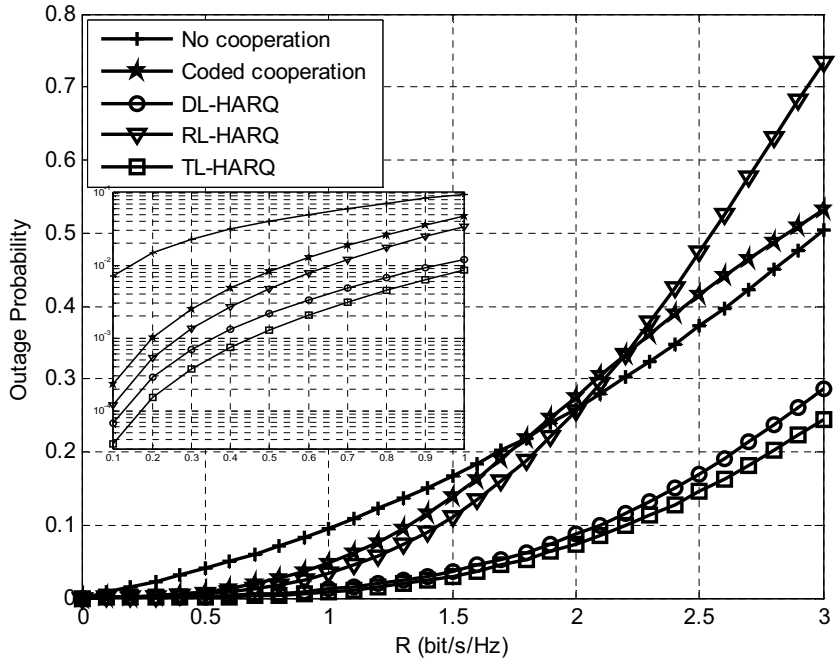

FIGURE 4.2: Outage probability versus rate for several coded cooperation schemes. All channels have mean SNR $\Gamma = 10$ dB. $\alpha = 2/3$.

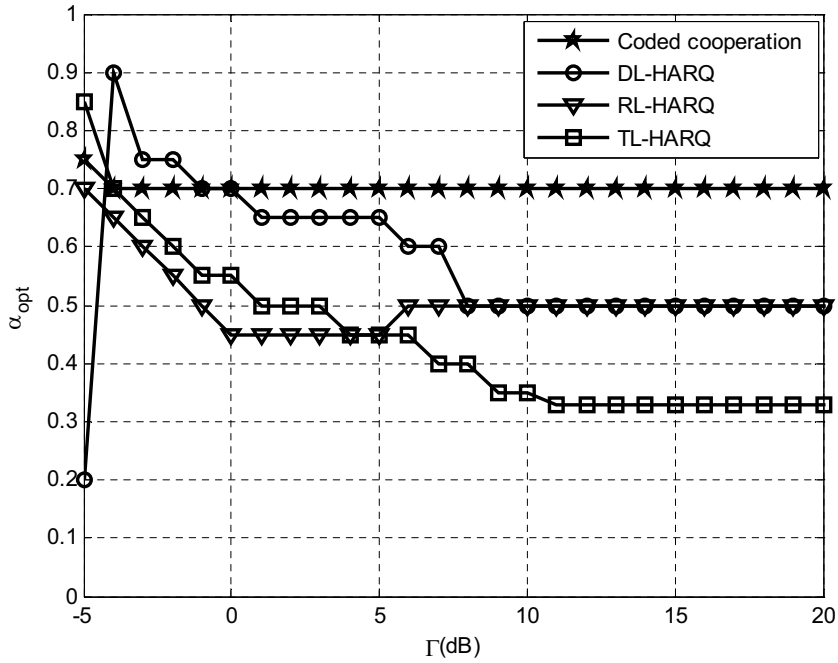

FIGURE 4.3: Optimal time allocation for several coded cooperation schemes, as a function of $\Gamma_{\mathrm{sd}} = \Gamma_{\mathrm{s}_i\mathrm{s}_j} = \Gamma$.

since the level of cooperation has not been significantly improved. A higher diversity is obtained if RL-HARQ is used (the quality of the inter-source channel is improved), thus improving performance for high $\Gamma_{\mathrm{s}_i\mathrm{d}}$. This performance improvement brought by

RL-HARQ is obtained by retransmitting over the inter-source channel; note that the use of more channel resources was taken into account into the derivation of the outage probability where for each case, we consider the appropriate rate depending on the number of retransmission attempts. The TL-HARQ protocol gives the best results: it achieves the diversity gain of the RL-HARQ protocol and it provides some extra coding gain.

Figure 4.2 reports the outage probability as a function of R for $\alpha = 2/3$ and $\Gamma_{\mathrm{s}_i\mathrm{d}} = \Gamma_{\mathrm{s}_i\mathrm{s}_j} = 10$ dB. In the low-rate regime ($R < 1$), all HARQ protocols give a significant improvement with respect to coded cooperation and non-cooperation, with TL-HARQ giving the best performance. However, for high rates ($R > 1$), coded cooperation and RL-HARQ perform worse than non-cooperation. Notice that CCoop scheme and RL-HARQ protocol require higher utilization of the channel with respect to DL-HARQ and TL-HARQ protocols. As a result, the transmission rate is decreased. Therefore, this is not suitable when a high rate is required. On the other hand, DL-HARQ and TL-HARQ yield a significant gain, thanks to the control of retransmission at the destination. Similar results were observed for poorer channels. The outage behavior depicted in Figure 4.2 are congruent with simulation results given in Figure 3.10.

To analyze the effect of the cooperation level α on the performance of the system, we plot in Figure 4.3 the optimal value of α, α_{opt}, that minimizes the probability of outage, for an overall transmission rate 1/3. In the figure, $\Gamma_{\mathrm{s}_i\mathrm{s}_j} = \Gamma_{\mathrm{s}_i\mathrm{d}} = \Gamma$. For the coded cooperation scheme, $\alpha_{\mathrm{opt}} = 0.7$ for $\Gamma \geq 0$ dB. This indicates that it is generally better to allocate a higher portion of the total rate R to the first phase, which improves the chances of successful decoding at partner node. On the other hand, for the RL-HARQ protocol, equal time allocation ($\alpha_{\mathrm{opt}} = 0.5$) between the broadcast phase and the retransmission/cooperation phases is optimal for a wide range of channel conditions. Allowing a retransmission attempt to the partner node strengthens this critical link, which increases the level of cooperation in the second phase. Likewise, the DL-HARQ protocol is characterized by $\alpha_{\mathrm{opt}} = 0.5$. Finally, for the TL-HARQ protocol, $\alpha_{\mathrm{opt}} \sim 0.33$ for high-SNR regime ($\Gamma \geq 11$ dB), favoring the cooperation phase.

4.2 Asymptotic Analysis and Diversity Order

To determine the diversity order of the cooperative HARQ protocols presented in the previous sections, we follow the approach in [HSN06]: we examine the asymptotic behavior of their respective outage probabilities in the high-SNR regime. To make easier this study, we can re-parameterize the average SNRs $\Gamma_{\mathrm{s}_i\mathrm{d}}$ and $\Gamma_{\mathrm{s}_i\mathrm{s}_j}$ as $\Gamma_{\mathrm{s}_i\mathrm{d}} \Rightarrow \Gamma_{\mathrm{T}}\Gamma_{\mathrm{s}_i\mathrm{d}}$ and $\Gamma_{\mathrm{s}_i\mathrm{s}_j} \Rightarrow \Gamma_{\mathrm{T}}\Gamma_{\mathrm{s}_i\mathrm{s}_j}$, respectively, where Γ_{T} is the ratio of the source transmit power to the received noise, and $\Gamma_{\mathrm{s}_i\mathrm{d}}$ and $\Gamma_{\mathrm{s}_i\mathrm{s}_j}$ are now finite constants including large-scale path loss and shadowing effects [HSN06]. In addition to that, we assume that Γ_{T} is the

TABLE 4.1: Asymptotic analysis of outage probabilities.

Cooperative Scheme	Outage Probability Expression
CCoop	$P_{\text{out},1} = \frac{1}{\Gamma_T^2}\left[\frac{(2^{R/\alpha}-1)^2}{\Gamma_{\text{s}_1\text{d}}\Gamma_{\text{s}_1\text{s}_2}} + \frac{\Lambda(R,\alpha)}{\Gamma_{\text{s}_1\text{d}}\Gamma_{\text{s}_2\text{d}}}\right] + O\left(\frac{1}{\Gamma_T^3}\right)$
DL-HARQ	$P_{\text{out},1} = \frac{1}{\Gamma_T^2}\left[\frac{(2^{R/\alpha}-1)(2^{R/}-1)}{\Gamma_{\text{s}_1\text{d}}\Gamma_{\text{s}_1\text{s}_2}} + \frac{\Delta(R,\alpha)}{\Gamma_{\text{s}_1\text{d}}\Gamma_{\text{s}_2\text{d}}}\right] + O\left(\frac{1}{\Gamma_T^3}\right)$
RL-HARQ	$P_{\text{out},1} = \frac{1}{\Gamma_T^2}\frac{\Lambda(R,\alpha)}{\Gamma_{\text{s}_1\text{d}}\Gamma_{\text{s}_2\text{d}}} + O\left(\frac{1}{\Gamma_T^3}\right)$
TL-HARQ	$P_{\text{out},1} = \frac{1}{\Gamma_T^2}\frac{\Delta(R,\alpha)}{\Gamma_{\text{s}_1\text{d}}\Gamma_{\text{s}_2\text{d}}} + O\left(\frac{1}{\Gamma_T^3}\right)$

same for both sources. These assumptions allow us to express the outage probability as a function of $1/\Gamma_{\text{T}}$. Then, considering the high-SNR regime ($\Gamma_T \to \infty$), the diversity order is given by the smallest exponent of $1/\Gamma_{\text{T}}$.

The outage probability expression as a function of $1/\Gamma_{\text{T}}$ is obtained by expanding each exponential term using Taylor's series representation in the outage probability expressions of the studied systems. Thus, for terms of the form $\exp\left(\frac{1-2^r}{\Gamma_{\text{T}}\Gamma_{\text{s}_i\text{s}_j}}\right)$ and $1-\exp\left(\frac{1-2^r}{\Gamma_{\text{T}}\Gamma_{\text{s}_i\text{s}_j}}\right)$ ($r = R/\alpha, R, \alpha R$), we can write

$$\begin{aligned} \exp\left(\frac{1-2^r}{\Gamma_{\text{T}}\Gamma_{i,j}}\right) &= 1 - \frac{2^r-1}{\Gamma_{\text{T}}\Gamma_{i,j}} + \frac{(2^r-1)^2}{2\Gamma_{\text{T}}^2\Gamma_{i,j}^2} + O\left(\frac{1}{\Gamma_{\text{T}}^3}\right) \\ 1-\exp\left(\frac{1-2^r}{\Gamma_{\text{T}}\Gamma_{i,j}}\right) &= \frac{2^r-1}{\Gamma_{\text{T}}\Gamma_{i,j}} - \frac{(2^r-1)^2}{2\Gamma_{\text{T}}^2\Gamma_{i,j}^2} + O\left(\frac{1}{\Gamma_{\text{T}}^3}\right) \end{aligned} \tag{4.15}$$

Then, by collecting like-order terms and simplifying results, we obtain their respective functions using Γ_{T} parametrization. In Table 4.1 we give the outage probability expressions. In the table, $\Lambda(R,\alpha)$ and $\Delta(R,\alpha)$ are the integral of $a(R)$ from 0 to $2^{R/\alpha}-1$, and the integral of $b(\alpha R)$ from 0 to $2^{\alpha R}-1$, respectively. As $1/\Gamma_{\text{T}} \to \infty$, the outage probability is a function of $1/\Gamma_{\text{T}}^2$ for all cases, i.e., all described cooperative schemes achieve full diversity (diversity order of 2). To highlight this result given through the asymptotical analysis, we plot outage probability curves where $\Gamma_{\text{s}_i\text{s}_j} = \Gamma_{\text{s}_i\text{d}}$ in Figure 4.4. From this figure, we note that all protocols achieve the full diversity since, at high SNR, the slopes of all curves are the same. The outage behavior depicted in Figure 4.4 are congruent with simulation results given in Figure 3.11.

4.3 Diversity-Multiplexing Tradeoff

By examining the asymptotic behavior of the corresponding outage probabilities of the proposed HARQ protocols as well as of the original CCoop scheme, in the high-SNR regime, it turns out that all of them have the same diversity order. In this section, we derive lower bounds on the DMT for the case of long-term quasi-static channels. The

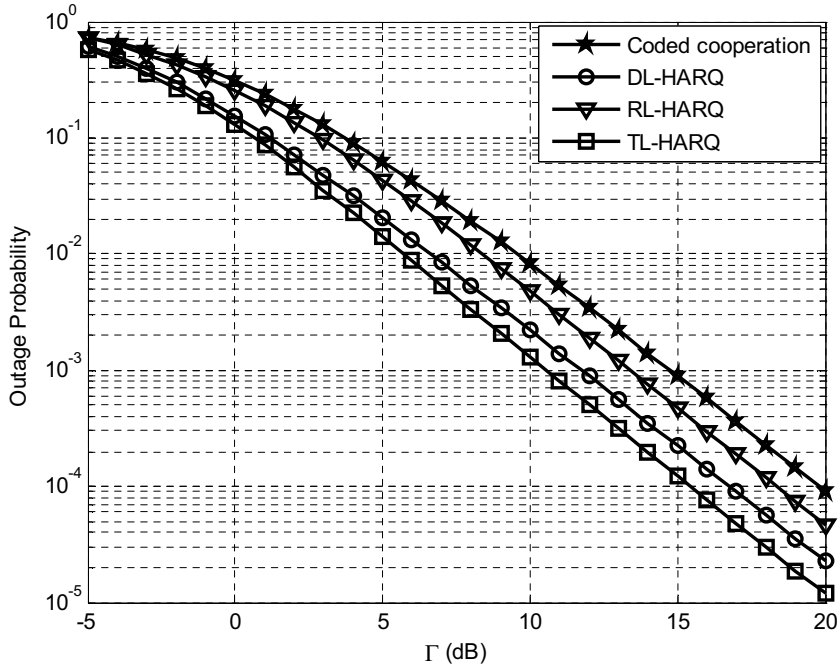

FIGURE 4.4: Outage probability for equal channels SNR and an overall rate of 1/3: Same diversity.

DMT framework, originally developed in [ZT03] for point-to-point MIMO systems, is adopted to stress the difference between the different protocols, since all of them achieve full diversity.

4.3.1 Coded Cooperation Tradeoff Curve

Theorem 4.1. *For a long-term static fading channel, the achievable diversity-multiplexing tradeoff for the coded cooperation scheme is lower bounded by* $d_{CCoop}(r,\alpha)$*, where*

$$d_{CCoop}(r,\alpha) = \begin{cases} 2 - \frac{r}{\min(\alpha,1-\alpha)} & r \in [0, \min(\alpha, 1-\alpha)] \\ \frac{1-r}{\max(\alpha,1-\alpha)} & r \in [\min(\alpha, 1-\alpha), 1] \end{cases} \quad \text{for } \alpha \leq \frac{2}{3},$$

$$d_{CCoop}(r,\alpha) = \begin{cases} 2 - \frac{r}{1-\alpha} & r \in [0, 1-\alpha] \\ \frac{1-r}{\alpha} & r \in [1-\alpha, 2\alpha-1] \\ 2 - \frac{2r}{\alpha} & r \in [2\alpha-1, 1] \end{cases} \quad \text{otherwise.} \tag{4.16}$$

Proof. Our proof has two main steps. First, from the outage events formulated in Section 4.1, we can define the corresponding events for large ρ. The exponential order of the dominant component is then the DMT expression [AGS05]. We assume that $|h_{\mathrm{s}_i\mathrm{d}}|^2$ can be expressed as $|h_{\mathrm{s}_i\mathrm{d}}|^2 \doteq \rho^{-\mu_{\mathrm{s}_i\mathrm{d}}}$. Given a multiplexing gain $r \in [0,1]$, and letting R grow with ρ according to $R = r\log(\rho)$, the outage event $\mathcal{O}_1^+$ at the destination for large

TABLE 4.2: Capacity Expressions For High SNR Regime.

$\mathcal{I}_{\mathrm{s_1 s_2}}$	$\mathcal{I}_{\mathrm{s_2 s_1}}$	$C^+(\mu_{\mathrm{s_1 d}}, \mu_{\mathrm{s_2 d}})$
1	1	$\alpha(1-\mu_{\mathrm{s_1 d}})^+ + (1-\alpha)(1-\mu_{\mathrm{s_2 d}})^+ < r$
0	0	$(1-\mu_{\mathrm{s_1 d}})^+ < r$
1	0	$\alpha(1-\mu_{\mathrm{s_1 d}})^+ + (1-\alpha)(1-\min(\mu_{\mathrm{s_1 d}}, \mu_{\mathrm{s_2 d}}))^+ < r$
0	1	$\alpha(1-\mu_{\mathrm{s_1 d}})^+ < r$

ρ (for s_1), becomes

$$\mathcal{O}_1^+ \equiv \left\{(\mu_{\mathrm{s_1 d}}, \mu_{\mathrm{s_2 d}}) \in \mathbb{R}_+^2 : C^+(\mu_{\mathrm{s_1 d}}, \mu_{\mathrm{s_2 d}}) < r\right\} \tag{4.17}$$

where $C^+(\mu_{\mathrm{s_1 d}}, \mu_{\mathrm{s_2 d}})$, for cases $\Theta = 1, 2, 3$, and 4, is given in Table 4.2.

For each case, the corresponding exponential order is the solution of

$$\Pr\left\{\mathcal{O}_1^+(\Theta = i)\right\} \doteq \rho^{d_i(r,\alpha)} \tag{4.18}$$

where $d_i(r,\alpha) = \inf_{(\mu_{\mathrm{s_1 d}}, \mu_{\mathrm{s_2 d}}) \in \mathcal{O}_1^+(\Theta = i)} (\mu_{\mathrm{s_1 d}} + \mu_{\mathrm{s_2 d}})$. Furthermore, for $r \in [0,1]$, we can easily show that

$$\Pr\left\{\mathcal{I}_{s_i s_j}(R/\alpha) = 0\right\} \doteq \rho^{(1-\frac{r}{\alpha})^+}, \quad \Pr\left\{\mathcal{I}_{s_i s_j}(R/\alpha) = 1\right\} \doteq 1. \tag{4.19}$$

Therefore, from the cases detailed above, we can conclude that

$$\begin{aligned} d_{\mathrm{CCoop}}(r,\alpha) &= \min\Bigg\{ d_1(r,\alpha), 2 - \frac{2r}{\alpha} + d_2(r,\alpha), \\ &\qquad \left(1 - \frac{r}{\alpha}\right)^+ + (1-r)^+, 2\left(1 - \frac{r}{\alpha}\right)^+ \Bigg\} \\ &= \min\left\{ d_1(r,\alpha), 2\left(1 - \frac{r}{\alpha}\right)^+ \right\} \end{aligned} \tag{4.20}$$

where $d_1(r,\alpha)$ is the solution of (4.18) and is given by (see Appendix A)

$$d_1(r,\alpha) = \begin{cases} 2 - \frac{r}{\min(\alpha, 1-\alpha)} & r \in [0, \min(\alpha, 1-\alpha)] \\ \frac{1-r}{\max(\alpha, 1-\alpha)} & r \in [\min(\alpha, 1-\alpha), 1] \end{cases} \tag{4.21}$$

Finally, comparing both $d_1(r,\alpha)$ and $2(1-\frac{r}{\alpha})^+$ in the ranges $[0, 1-\alpha]$ and $[1-\alpha, \alpha]$ (for $\alpha \leq 1/2$), and in the range $[0, \alpha]$ (for $\alpha \geq 1/2$), we obtain the expression in (4.16). □

4.3.2 Destination-Level HARQ Tradeoff Curve

Theorem 4.2. *For the case of long-term static fading channel with two transmission rounds, including the broadcast phase and the optional cooperation phase, and for an effective rate r_e, the achievable diversity-multiplexing tradeoff for the DL-HARQ is lower*

bounded by $d_{\textit{DL-HARQ}}(r_e,\alpha)$*, where*

$$d_{\textit{DL-HARQ}}(r_e,\alpha)=2-(1+\alpha)r_e \qquad \textit{for}\ \alpha\le\tfrac{\sqrt{5}-1}{2},$$
$$d_{\textit{DL-HARQ}}(r_e,\alpha)=\begin{cases}2-\frac{\alpha}{1-\alpha}r_e & r_e\in[0,\frac{1-\alpha}{\alpha}]\\ \frac{1-\alpha r_e}{\alpha} & r_e\in(\frac{1-\alpha}{\alpha},\frac{2\alpha-1}{\alpha^2}]\\ 2-(1+\alpha)r_e & r_e\in(\frac{2\alpha-1}{\alpha^2},1]\end{cases} \qquad \textit{otherwise.} \tag{4.22}$$

Proof. We recall that the lower bound of the tradeoff expression is given by the minimum of the exponential orders of the outage probabilities relative to all conditional cases with regard to $\mathcal{I}_{s_is_j}(R)$ and $\mathcal{I}_{\mathrm{s_2d}}(R)$. Here, we analyze the two dominating cases:

- Case $\mathcal{I}_{\mathrm{s_2d}}(R)=\mathcal{I}_{\mathrm{s_is_j}}(R)=1$: We have $\Pr\{\mathcal{I}_{\mathrm{s_2d}}(R)=1\}=\Pr\{\mathcal{I}_{\mathrm{s_is_j}}(R)=1\}\doteq 1$. The corresponding outage probability is given by

$$\begin{aligned}\Pr\{\mathcal{O}_1^+\}&=\Pr\{\mathcal{I}_{\mathrm{s_2d}}(R)=\mathcal{I}_{s_is_j}(R)=1\}\\ &\quad\cdot\Pr\{\mathcal{O}_1^+|\mathcal{I}_{\mathrm{s_2d}}(R)=\mathcal{I}_{s_is_j}(R)=1\}\\ &\doteq\rho^{-d_{\mathrm{A}}(r,\alpha)}\end{aligned} \tag{4.23}$$

  where $d_{\mathrm{A}}(r,\alpha)=\inf_{(\mu_{\mathrm{s_1d}},\mu_{\mathrm{s_2d}})\in\mathcal{O}_1^+}(\mu_{\mathrm{s_1d}}+\mu_{\mathrm{s_2d}})$, and
  $\mathcal{O}_1^+\equiv\{(\mu_{\mathrm{s_1d}},\mu_{\mathrm{s_2d}})\in\mathbb{R}_+^2:\alpha(1-\mu_{\mathrm{s_1d}})^+ +(1-\alpha)(1-\min(\mu_{\mathrm{s_1d}},\mu_{\mathrm{s_2d}}))^+<\alpha r\}$.

- Case $\mathcal{I}_{\mathrm{s_2d}}(R)=\mathcal{I}_{\mathrm{s_2s_1}}(R)=1$ and $\mathcal{I}_{\mathrm{s_1s_2}}(R)=0$: We have $\Pr\{\mathcal{I}_{\mathrm{s_2d}}(R)=1\}=\Pr\{\mathcal{I}_{s_2\mathrm{s_1}}(R)=1\}\doteq 1$ and $\Pr\{\mathcal{I}_{\mathrm{s_1s_2}}(R)=0\}\doteq\rho^{-(1-r)^+}$. The corresponding outage probability is given by

$$\begin{aligned}\Pr\{\mathcal{O}_1^+\}&=\Pr\{\mathcal{I}_{\mathrm{s_2d}}(R)=\mathcal{I}_{\mathrm{s_2s_1}}(R)=1,\mathcal{I}_{\mathrm{s_1s_2}}(R)=0\}\\ &\quad\cdot\Pr\{\mathcal{O}_1^+|\mathcal{I}_{\mathrm{s_2d}}(R)=\mathcal{I}_{\mathrm{s_2s_1}}(R)=1,\mathcal{I}_{\mathrm{s_1s_2}}(R)=0\}\\ &\doteq\rho^{-(1-r)^+-(1-\alpha r)^+}\end{aligned} \tag{4.24}$$

  where $\mathcal{O}_1^+\equiv\{(\mu_{\mathrm{s_1d}},\mu_{\mathrm{s_2d}})\in\mathbb{R}_+^2:(1-\mu_{\mathrm{s_1d}})^+<\alpha r\}$.

Finally, the tradeoff curve is defined as $d_{\text{DL-HARQ}}(r,\alpha)=\min\{d_{\mathrm{A}}(r,\alpha);2-(1+\alpha)r\}$. The expression of $d_{\mathrm{A}}(r,\alpha)$ is evaluated in Appendix B.1, and is obtained to be

$$d_{\mathrm{A}}(r,\alpha)=2-2\alpha r \qquad \text{for}\ \alpha\le\tfrac{1}{2},$$
$$d_{\mathrm{A}}(r,\alpha)=\begin{cases}2-\frac{\alpha}{1-\alpha}r & r\in[0,\frac{1-\alpha}{\alpha}]\\ \frac{1-\alpha r}{\alpha} & r\in(\frac{1-\alpha}{\alpha},1]\end{cases} \qquad \text{otherwise.} \tag{4.25}$$

To determine the exponential order of the outage probability for the DL-HARQ, all possible comparisons between $d_{\mathrm{A}}(r,\alpha)$ and $2-(1+\alpha)r$ for different values of α and r over defined rate ranges have to be done:

- For $\alpha\le 1/2$: $2-(1+\alpha)r\le 2-2\alpha r$, $\forall\alpha\le 1$.

- For $\alpha > 1/2$:
  - For $r \in [0, \frac{1-\alpha}{\alpha}]$: Let us compare $2-(1+\alpha)r$ and $2-\frac{\alpha}{1-\alpha}r$. We have, $2-(1+\alpha)r \leq 2-\frac{\alpha}{1-\alpha}r, \forall \alpha \in [\frac{1}{2}, \frac{\sqrt{5}-1}{2}]$.
  - For $r \in (\frac{1-\alpha}{\alpha}, 1)$: Let us compare $2-(1+\alpha)r$ and $\frac{1-\alpha r}{\alpha}$. We have $2-(1+\alpha)r \leq \frac{1-\alpha r}{\alpha}, \forall r \geq \frac{2\alpha-1}{\alpha^2}$. To get the exact comparison result, we have to compare first $\frac{1-\alpha}{\alpha}$ and $\frac{2\alpha-1}{\alpha^2}$:
    1. For $\alpha \in [\frac{1}{2}, \frac{\sqrt{5}-1}{2}]$, we have $\frac{2\alpha-1}{\alpha^2} \leq \frac{1-\alpha}{\alpha}$. Then $\min\left\{2-(1+\alpha)r, \frac{1-\alpha r}{\alpha}\right\} = 2-(1+\alpha)r, \quad \forall \alpha \in [\frac{1-\alpha}{\alpha}, 1] \subset [\frac{2\alpha-1}{\alpha^2}, 1]$.
    2. For $\alpha \in (\frac{\sqrt{5}-1}{2}, 1]$, we have $\frac{1-\alpha}{\alpha} < \frac{2\alpha-1}{\alpha^2}$. Then $\min\left\{2-(1+\alpha)r; \frac{1-\alpha r}{\alpha}\right\} = \begin{cases} \frac{1-\alpha r}{\alpha} & \forall \alpha \in [\frac{1-\alpha}{\alpha}, \frac{2\alpha-1}{\alpha^2}] \\ 2-(1+\alpha)r & \forall \alpha \in (\frac{2\alpha-1}{\alpha^2}, 1] \end{cases}$.

On the other hand, following the discussion in [GCD06] and [TDK07], we have $\eta(\rho) = \frac{R(\rho)}{1+\rho^{-d_{\text{DL-HARQ}}(r,\alpha)}} \doteq R(\rho)$, which results in $r_e = r$. Now, considering this result and those from the comparisons above, we obtain the expression in (4.22). □

4.3.3 Relay-level HARQ

Theorem 4.3. *For the RL-HARQ protocol, and for an effective rate r_e, the achievable diversity-multiplexing tradeoff is lower bounded by $d_{RL\text{-}HARQ}(r_e, \alpha)$, where*

$$\begin{aligned} d_{RL\text{-}HARQ}(r_e,\alpha) &= \left[\tfrac{(1+\alpha)-2r_e}{1-\alpha}\right]^+ && \text{for } \alpha \leq \tfrac{1}{3}, \\ d_{RL\text{-}HARQ}(r_e,\alpha) &= \begin{cases} 2-\frac{2}{1-\alpha}r_e & r_e \in [0, \frac{1-\alpha}{2}] \\ \left[\frac{(1+\alpha)-2r_e}{2\alpha}\right]^+ & r_e > \frac{1-\alpha}{2} \end{cases} && \text{otherwise.} \end{aligned} \tag{4.26}$$

Proof. (Sketch) The dominant component of the outage probability of the RL-HARQ protocol evaluated in Section 4.1 is related to the probabilities $\Pr\left\{\mathcal{I}_{s_i s_j}(R)=1\right\} \doteq 1$. The corresponding outage probability, for large ρ, is evaluated as

$$\begin{aligned} \Pr\left\{\mathcal{O}_1^+\right\} &\doteq \rho^{-d(r,\alpha|\mathcal{I}_{s_i s_j}(R)=1)} \doteq \rho^{d_{\text{B}}(r,\alpha)}, \\ d_{\text{B}}(r,\alpha) &= \inf_{(\mu_{\text{s}_1\text{d}},\mu_{\text{s}_2\text{d}})\in\mathcal{O}_1^+} (\mu_{\text{s}_1\text{d}} + \mu_{\text{s}_2\text{d}}) \end{aligned} \tag{4.27}$$

where $\mathcal{O}_1^+ \equiv \left\{(\mu_{\text{s}_1\text{d}}, \mu_{\text{s}_2\text{d}}) \in \mathbb{R}_+^2 : \alpha(1-\mu_{\text{s}_1\text{d}})^+ + \frac{1-\alpha}{2}(1-\min(\mu_{\text{s}_1\text{d}}, \mu_{\text{s}_2\text{d}}))^+ < r\right\}$, and $d_{\text{B}}(r,\alpha)$ is given in Appendix B.2. Finally, using the results of [GCD06] and [TDK07] showing that $r_e \doteq r$, we obtain (4.26). □

4.3.4 Two-level HARQ

Theorem 4.4. *For the TL-HARQ protocol, the achievable diversity-multiplexing tradeoff is lower bounded by $d_{TL\text{-}HARQ}(r_e, \alpha)$, where*

$$\begin{aligned} d_{TL\text{-}HARQ}(r_e,\alpha) &= 2 - \tfrac{4\alpha}{1+\alpha} r_e \quad r_e \in [0,1] && \text{for } \alpha \leq \tfrac{1}{3}, \\ d_{TL\text{-}HARQ}(r_e,\alpha) &= \begin{cases} 2 - \tfrac{2\alpha}{1-\alpha} r_e & r_e \in [0, \tfrac{1-\alpha}{2\alpha}] \\ \tfrac{1+\alpha}{2\alpha} - r_e & r_e \in (\tfrac{1-\alpha}{2\alpha}, 1] \end{cases} && \text{otherwise.} \end{aligned} \tag{4.28}$$

Proof. (Sketch) The dominant contribution is given by $\mathcal{I}_{\mathrm{s_2d}}(R) = \mathcal{I}_{s_i s_j}(\alpha R) = 1$. Therefore, the tradeoff curve is given by

$$\begin{aligned} d_{\text{TL-HARQ}}(r,\alpha) &= d(r,\alpha | \mathcal{I}_{\mathrm{s_2d}}(R) = \mathcal{I}_{s_i s_j}(\alpha R) = 1) \\ &= d_{\mathrm{C}}(r,\alpha) = \inf_{(\mu_{\mathrm{s_1d}}, \mu_{\mathrm{s_2d}}) \in \mathcal{O}_1^+} (\mu_{\mathrm{s_1d}} + \mu_{\mathrm{s_2d}}) \end{aligned} \tag{4.29}$$

where $\mathcal{O}_1^+ \equiv \left\{ (\mu_{\mathrm{s_1d}}, \mu_{\mathrm{s_2d}}) \in \mathbb{R}_+^2 : \alpha(1-\mu_{\mathrm{s_1d}})^+ + \frac{1-\alpha}{2}(1 - \min(\mu_{\mathrm{s_1},d}, \mu_{\mathrm{s_2d}}))^+ < \alpha r \right\}$, and $d_{\mathrm{C}}(r,\alpha)$ is evaluated in Appendix B.3. Using this and the fact that $r_e \doteq r$, we obtain (4.28). □

In Figure 4.5(a) and Figure 4.5(b), we examine the DMT curves of the proposed protocols for $\alpha = 2/3$ and $\alpha = 1/3$. For both values of α, coded cooperation shows better system performance compared to non-cooperation. Interestingly, not all HARQ protocols provide some gain. For $\alpha = 2/3$, the diversity gain for RL-HARQ is, for any rate, smaller than that offered by the coded cooperation scheme. This is due to the fact that retransmissions can occur even if the packet is correctly decoded at the destination in the broadcast phase: the rate will be unnecessarily decreased. A similar diversity loss is also observed compared to non-cooperation for high transmission rates ($R > 0.5$). The TL-HARQ protocol performs better than coded cooperation for $R > 0.5$, but shows some loss for $R < 0.5$. On the other hand, the DL-HARQ protocol performs best for all rates. For $\alpha = 1/3$, DL-HARQ and TL-HARQ show a significant gain with respect to coded cooperation and non-cooperation, with TL-HARQ performing the best. Notice that the DL-HARQ and TL-HARQ DMT curves improve significantly with respect to $\alpha = 2/3$. In the sequel, we will concentrate only on the analysis of DL-HARQ and TL-HARQ protocols, since the RL-HARQ witness a significant degradation in terms of system efficiency. This was observed from the throughput efficiency simulation, the outage performance as a function of the rate and from the DMT analysis.

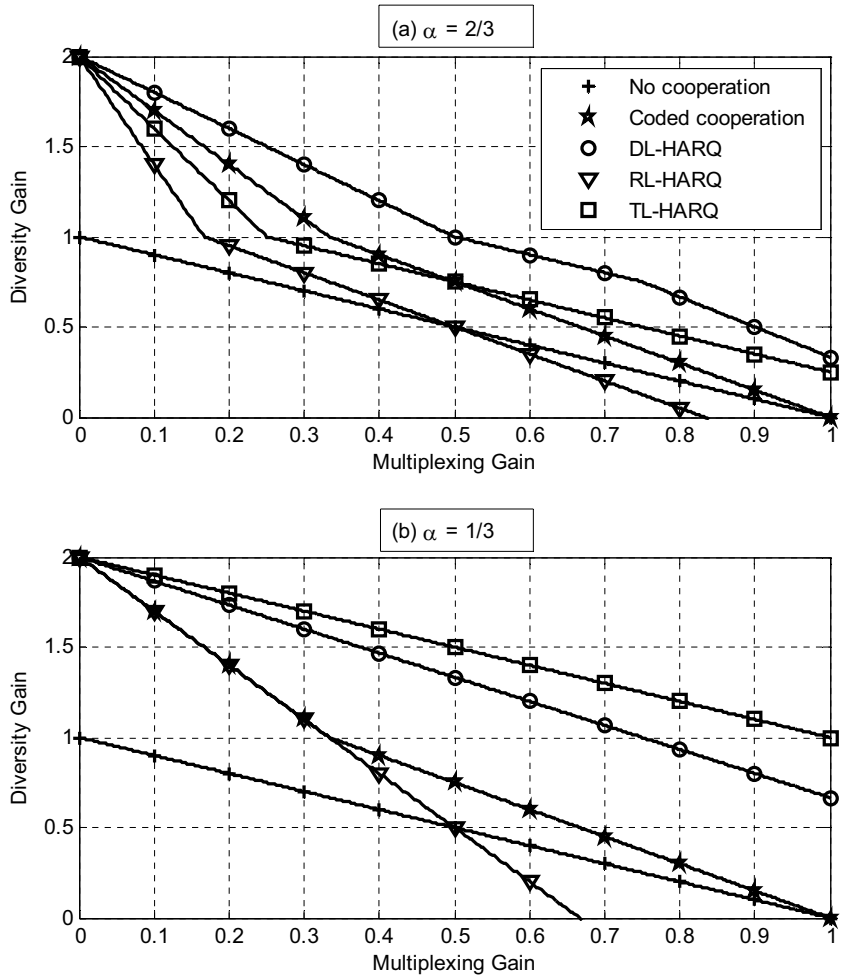

FIGURE 4.5: Diversity-multiplexing tradeoff curves of several coded cooperation schemes.

4.4 Bounds on the Frame Error Probability for Cooperative HARQ Protocols based on Turbo Coded Cooperation

The system of Figure 3.4 can be seen as a (distributed) turbo code. At each phase, the turbo code is punctured and only part of the parity bits are transmitted. After two transmission phases, the whole mother codeword is available at the destination. In [SLS03, LSS06], it was shown that the performance of a turbo code punctured with permeability rates α and $1-\alpha$ and transmitted over two parallel channels with Bhattacharyya noise parameters ρ_1 and ρ_2, respectively, is the same as the performance of the mother code over a channel with an effective Bhattacharyya noise parameter equal to $\alpha\rho_1 + (1-\alpha)\rho_2$, with $\rho_i = \exp(-\nu_{\mathrm{s}_i\mathrm{d}}\gamma_{\mathrm{s}_i\mathrm{d}})$, for $i = 1, 2$. Using results in Sub-section2.4.3 and results for distributed turbo codes [SLS03, LSS06], we can derive a bound on the frame error probability for the system in Figure 3.4. We recall that transmission is

performed over two phases (three phases for the TL-HARQ protocol). After the first transmission phase, decoding of the punctured turbo code with permeability rate α is performed at both sources as well as at the destination. The frame error probability for source s_1 and s_2 data (at source s_2 and s_1, respectively), can be bounded by

$$P_{e,\mathrm{s}_1\mathrm{s}_2}^{\varphi_1} \leq 1 - e^{-c_0^P \gamma_{\mathrm{s}_1\mathrm{s}_2}^{-1}} = \varepsilon_{\mathrm{s}_1\mathrm{s}_2}^{\varphi_1} \tag{4.30}$$

and

$$P_{e,\mathrm{s}_2\mathrm{s}_1}^{\varphi_1} \leq 1 - e^{-c_0^P \gamma_{\mathrm{s}_2\mathrm{s}_1}^{-1}} = \varepsilon_{\mathrm{s}_2\mathrm{s}_1}^{\varphi_1}, \tag{4.31}$$

respectively.

At the destination, the probability of error for s_i can be upper bounded as

$$P_{e,\mathrm{s}_i\mathrm{d}}^{\varphi_1} \leq 1 - e^{-c_0^P \gamma_{\mathrm{s}_i\mathrm{d}}^{-1}} = \varepsilon_{\mathrm{s}_i\mathrm{d}}^{\varphi_1}, \qquad i = 1, 2. \tag{4.32}$$

With reference to source s_1, four cases are possible for the second phase:

- Case 1: Decoding at sources s_1 and s_2 is successful. Both sources perform cooperation and the whole mother turbo code of source s_1 is transmitted. The frame error probability corresponds then to that of a turbo code punctured with permeability rates α and $1-\alpha$ and transmitted over two parallel channels with SNR $\gamma_{\mathrm{s}_1\mathrm{d}}$ and $\gamma_{\mathrm{s}_2\mathrm{d}}$, respectively, and can be bounded as

$$\begin{aligned} P_{e,\mathrm{s}_1\mathrm{d}}^{\varphi_2,\mathrm{C}_1} &\leq 1 - \omega_1 - \int_0^{-\log\omega_1} e^{-\nu_{\mathrm{s}_1\mathrm{d}}} \Upsilon_1(\nu_{\mathrm{s}_1\mathrm{d}}) d\nu_{\mathrm{s}_1\mathrm{d}} \\ &= \varepsilon_{\mathrm{s}_1\mathrm{d}}^{\varphi_2,\mathrm{C}_1} \end{aligned} \tag{4.33}$$

  where

$$\omega_1 = \left[\frac{\max(e^{-c_0} - (1-\alpha), 0)}{\alpha}\right]^{\gamma_{\mathrm{s}_1\mathrm{d}}^{-1}} \tag{4.34}$$

  and

$$\Upsilon_1(\nu_{\mathrm{s}_1\mathrm{d}}) = \left[\frac{\max(e^{-c_0} - \alpha e^{-\nu_{\mathrm{s}_1\mathrm{d}}\gamma_{\mathrm{s}_1\mathrm{d}}}, 0)}{1-\alpha}\right]^{\gamma_{\mathrm{s}_2\mathrm{d}}^{-1}}. \tag{4.35}$$

- Case 2: Decoding at both sources fails. Two codewords are transmitted for $\mathbf{u}_{1L}$, namely $\mathbf{x}_{1L}$ and $\tilde{\mathbf{x}}_{1L}$, both generated by s_1. Therefore, a distributed (over time) code is obtained. The corresponding frame error probability can be bounded as

$$P_{e,\mathrm{s}_1\mathrm{d}}^{\varphi_2,\mathrm{C}_2} \leq 1 - e^{-c_0 \gamma_{\mathrm{s}_1\mathrm{d}}^{-1}} = \varepsilon_{\mathrm{s}_1\mathrm{d}}^{\varphi_2,\mathrm{C}_2}. \tag{4.36}$$

- Case 3: Decoding at node s_1 fails, decoding at node s_2 is successful. The bound on the frame error probability for this case is given by

$$\begin{aligned} P_{e,\mathrm{s_1d}}^{\varphi_2,\mathrm{C_3}} &\leq 1 - e^{-\omega_2} - \int_0^{\omega_2} e^{-\nu_{\mathrm{s_1d}}} \Upsilon_2(\nu_{\mathrm{s_1d}}) d\nu_{\mathrm{s_1d}} \\ &= \varepsilon_{\mathrm{s_1d}}^{\varphi_2,\mathrm{C_3}} \end{aligned} \tag{4.37}$$

with

$$\begin{aligned} \omega_2 &= \frac{c_0}{\gamma_{\mathrm{s_1d}}}, \\ \Upsilon_2(\nu_{\mathrm{s_1d}}) &= \left[\frac{\max(e^{-c_0} e^{\nu_{\mathrm{s_1d}} \gamma_{\mathrm{s_1d}}} - \alpha, 0)}{1-\alpha} \right]^{\gamma_{\mathrm{s_2d}}^{-1}}. \end{aligned} \tag{4.38}$$

- Case 4: Decoding at node s_1 is successful, decoding at node s_2 fails. A single codeword, $\mathbf{x}_{1L}$, is allocated to $\mathbf{u}_{1L}$. The destination attempts to estimate $\mathbf{u}_{1L}$ by decoding the received punctured turbo code. The frame error probability of s_1, $P_{e,\mathrm{s_1d}}^{\varphi_2,\mathrm{C_4}}$, is then bounded as for $P_{e,\mathrm{s_1d}}^{\varphi_1}$, given in (4.32).

Due to the symmetry of the system, similar expressions are obtained for source s_2, by simply reversing s_1 and s_2 roles.

Using (4.30), (4.31), (4.33) (4.36) and (4.37), and upper bounding the probability of no error by $1 - P_e \leq 1$, the frame error probability of the turbo coded cooperation system for source s_1 can be bounded as

$$\begin{aligned} P_{e,\mathrm{s_1d}}^{\mathrm{CCoop}} &= (1 - P_{e,\mathrm{s_1s_2}}^{\varphi_1})(1 - P_{e,\mathrm{s_2s_1}}^{\varphi_1}) P_{e,\mathrm{s_1d}}^{\varphi_2,\mathrm{C_1}} + P_{e,\mathrm{s_1s_2}}^{\varphi_1} P_{e,\mathrm{s_2s_1}}^{\varphi_1} P_{e,\mathrm{s_1d}}^{\varphi_2,\mathrm{C_2}} \\ &\quad + (1 - P_{e,\mathrm{s_1s_2}}^{\varphi_1}) P_{e,\mathrm{s_2s_1}}^{\varphi_1} P_{e,\mathrm{s_1d}}^{\varphi_2,\mathrm{C_3}} + P_{e,\mathrm{s_1s_2}}^{\varphi_1} (1 - P_{e,\mathrm{s_2s_1}}^{\varphi_1}) P_{e,\mathrm{s_1d}}^{\varphi_2,\mathrm{C_4}} \\ &\leq \varepsilon_{\mathrm{s_1d}}^{\varphi_2,\mathrm{C_1}} + \varepsilon_{\mathrm{s_1s_2}}^{\varphi_1} \varepsilon_{\mathrm{s_2s_1}}^{\varphi_1} \varepsilon_{\mathrm{s_1d}}^{\varphi_2,\mathrm{C_2}} + \varepsilon_{\mathrm{s_2s_1}}^{\varphi_1} \varepsilon_{\mathrm{s_1d}}^{\varphi_2,\mathrm{C_3}} + \varepsilon_{\mathrm{s_1s_2}}^{\varphi_1} \varepsilon_{\mathrm{s_1d}}^{\varphi_2,\mathrm{C_4}} \\ &= \varepsilon_{e,\mathrm{s_1d}}^{\mathrm{CCoop}}. \end{aligned} \tag{4.39}$$

Following the discussion in Section 3.3.1, as the second phase depends not only on CRC results at partner node but also on decoding results of s_2 at the destination after the first transmission phase, the frame error probability of the DL-HARQ protocol is given by

$$\begin{aligned} P_{e,1}^{\text{DL-HARQ}} = P_{e,\mathrm{s_2d}}^{\varphi_1} \Big[&(1 - P_{e,\mathrm{s_1s_2}}^{\varphi_1})(1 - P_{e,\mathrm{s_2s_1}}^{\varphi_1}) P_{e,\mathrm{s_1d}}^{\varphi_2,\mathrm{C_1}} + P_{e,\mathrm{s_1s_2}}^{\varphi_1} P_{e,\mathrm{s_2s_1}}^{\varphi_1} P_{e,\mathrm{s_1d}}^{\varphi_2,\mathrm{C_2}} \\ &+ (1 - P_{e,\mathrm{s_1s_2}}^{\varphi_1}) P_{e,\mathrm{s_2s_1}}^{\varphi_1} P_{e,\mathrm{s_1d}}^{\varphi_2,\mathrm{C_3}} + P_{e,\mathrm{s_1s_2}}^{\varphi_1} (1 - P_{e,\mathrm{s_2s_1}}^{\varphi_1}) P_{e,\mathrm{s_1d}}^{\varphi_2,\mathrm{C_4}} \Big] \\ + (1 - P_{e,\mathrm{s_2d}}^{\varphi_1}) \Big[&(1 - P_{e,\mathrm{s_1s_2}}^{\varphi_1}) P_{e,\mathrm{s_1d}}^{\varphi_2,\mathrm{C_3}} + P_{e,\mathrm{s_1s_2}}^{\varphi_1} P_{e,\mathrm{s_1d}}^{\varphi_2,\mathrm{C_2}} \Big], \end{aligned} \tag{4.40}$$

which can be upper bounded as

$$\begin{aligned} P_{e,1}^{\text{DL-HARQ}} &\leq \varepsilon_{\text{s}_2\text{d}}^{\varphi_1}\left[\varepsilon_{\text{s}_1\text{d}}^{\varphi_2,\text{C}_1}+\varepsilon_{\text{s}_1\text{s}_2}^{\varphi_1}\varepsilon_{\text{s}_2\text{s}_1}^{\varphi_1}\varepsilon_{\text{s}_1\text{d}}^{\varphi_2,\text{C}_2}+\varepsilon_{\text{s}_2\text{s}_1}^{\varphi_1}\varepsilon_{\text{s}_1\text{d}}^{\varphi_2,\text{C}_3}+\varepsilon_{\text{s}_1\text{s}_2}^{\varphi_1}\varepsilon_{\text{s}_1\text{d}}^{\varphi_2,\text{C}_4}\right] \\ &\quad+\varepsilon_{\text{s}_1\text{d}}^{\varphi_2,\text{C}_3}+\varepsilon_{\text{s}_1\text{s}_2}^{\varphi_1}\varepsilon_{\text{s}_1\text{d}}^{\varphi_2,\text{C}_2} \\ &= \varepsilon_{e,\text{s}_1\text{d}}^{\text{DL-HARQ}}. \end{aligned} \tag{4.41}$$

For the TL-HARQ protocol several cases must be considered, arising from the decoding results at the destination after the first transmission phase, and, if necessary (unsuccessful decoding), by the decoding results at partner node. Notice that the additional transmission to the partner node, if requested, is also overheard by the destination node due to the broadcast nature of the wireless link. The bound on the frame error probability of the TL-HARQ protocol for source s_1 is derived by taking into account all possible transmission cases and is given by

$$\begin{aligned} P_{e,1}^{\text{TL-HARQ}} &\leq \varepsilon_{\text{s}_2\text{d}}^{\varphi_1}\left[\varepsilon_{\text{s}_1\text{d}}^{\varphi_2,\text{C}_1}+\varepsilon_{\text{s}_1\text{s}_2}^{\varphi_1}\varepsilon_{\text{s}_1\text{s}_2}^{\varphi_2}\varepsilon_{\text{s}_1\text{d}}^{\varphi_2,\text{C}_2}\right]+\varepsilon_{\text{s}_1\text{d}}^{\varphi_2,\text{C}_3}+\varepsilon_{\text{s}_1\text{s}_2}^{\varphi_1}\varepsilon_{\text{s}_1\text{s}_2}^{\varphi_2}\varepsilon_{\text{s}_1\text{d}}^{\varphi_2,\text{C}_3} \\ &= \varepsilon_{e,\text{s}_1\text{d}}^{\text{TL-HARQ}} \end{aligned} \tag{4.42}$$

where $\varepsilon_{\text{s}_1\text{s}_2}^{\varphi_2}$ is the bound to the error probability of the mother turbo code transmitted over the s_1-to-s_2 link (due to the retransmission requested by the partner node). It is given by

$$P_{e,\text{s}_1\text{s}_2}^{\varphi_2} \leq 1-e^{-c_0\gamma_{\text{s}_1\text{s}_2}^{-1}} = \varepsilon_{\text{s}_1\text{s}_2}^{\varphi_2}. \tag{4.43}$$

For simplicity, in the remainder of this chapter, a reciprocal inter-source channel is considered, i.e., $\gamma_{\text{s}_1\text{s}_2}=\gamma_{\text{s}_2\text{s}_1}=\gamma_{\text{ss}}$. For fair comparisons, all results depicted in figures given in the remainder of this chapter are given in terms of γ^b, where $\gamma^b=\gamma\bar{R}$, $\bar{R}$ being the average rate of the system. Note that the average rate of the system depends on the code rate and on the number of retransmission attempts. Using the bounds on the frame error probability, the average rate of the system can be approximated by

$$\bar{R}_{\text{CCoop}} = R \tag{4.44}$$

$$\bar{R}_{\text{DL-HARQ}} \approx (1-\varepsilon_{\text{s}_1\text{d}}^{\varphi_1})(1-\varepsilon_{\text{s}_2\text{d}}^{\varphi_1})\frac{R}{\alpha}+\left[1-(1-\varepsilon_{\text{s}_1\text{d}}^{\varphi_1})(1-\varepsilon_{\text{s}_2\text{d}}^{\varphi_1})\right]R \tag{4.45}$$

and

$$\begin{aligned} \bar{R}_{\text{TL-HARQ}} &\approx (1-\varepsilon_{\text{s}_1\text{d}}^{\varphi_1})(1-\varepsilon_{\text{s}_2\text{d}}^{\varphi_1})\frac{R}{\alpha} \\ &\quad+\left[1-(1-\varepsilon_{\text{s}_1\text{d}}^{\varphi_1})(1-\varepsilon_{\text{s}_2\text{d}}^{\varphi_1})\right]\left[(1-\varepsilon_{\text{s}_1\text{s}_2}^{\varphi_1})R+\varepsilon_{\text{s}_1\text{s}_2}^{\varphi_1}\frac{R}{2-\alpha}\right] \end{aligned} \tag{4.46}$$

for the turbo coded cooperation scheme, the DL-HARQ protocol, and the TL-HARQ protocol, respectively. For the TL-HARQ protocol, $\frac{2-\alpha}{\alpha}$ is the time duration of the

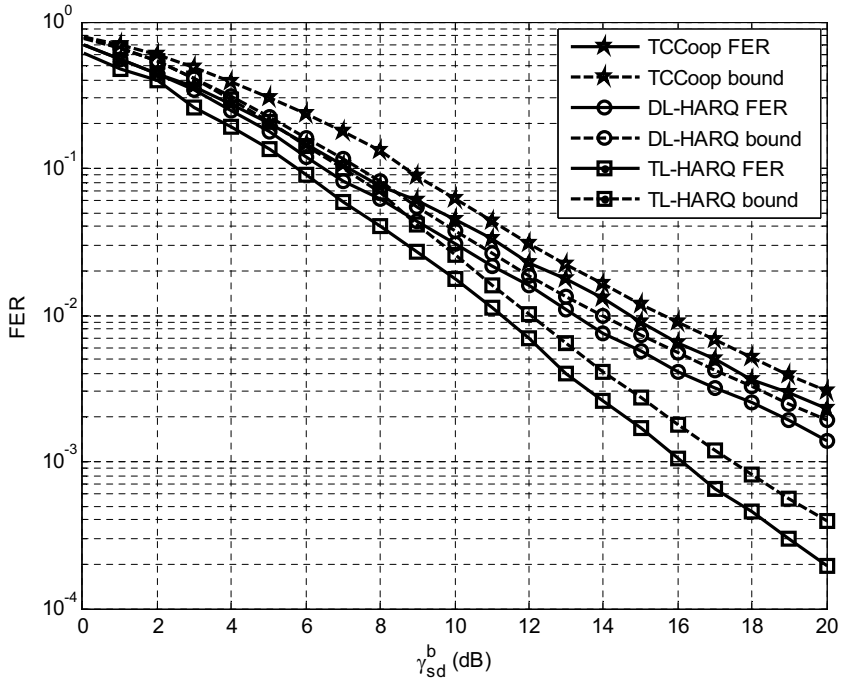

FIGURE 4.6: Bound on the frame error probability and FER simulation results for the symmetric case. $\gamma_{ss}^{b} = 6$ dB.

three phases: Direct phase (α), retransmission phase to the partner node ($1-\alpha$), and cooperation phase ($1-\alpha$).

In Figure 4.6, FER simulation results as well as the bounds on the frame error probability are given for $\gamma_{ss}^{b} = 6$ dB as a function of γ_{sd}^{b} (symmetric uplink case). We obtain the non-surprising result that the frame error probability bound curves are parallel to the simulated FER curves, with a certain offset, relatively to the considered system and in particular, the considered turbo code. The bounds on the frame error probability can therefore be adopted as a starting point for all analytical guidelines given in this study. The simulation results are given for the example given in Section 3.4.

4.5 Frame Error Probability Based Analysis

4.5.1 Frame Error Probability Retransmission Gain

In the following, we formalize the concept of the *frame error probability retransmission gain*, to quantify the performance improvement (in terms of probability of error) of DL-HARQ and TL-HARQ protocols over the original turbo coded cooperation where no HARQ is performed.

Definition 4.1. For a fixed distributed channel code, the frame error probability retransmission gain is defined as

$$G^{\mathrm{Rtx}}_{f,\text{DL-HARQ}} = \frac{\varepsilon^{\mathrm{CCoop}}_{e,\mathrm{s_1d}} + \varepsilon^{\mathrm{CCoop}}_{e,\mathrm{s_2d}}}{\varepsilon^{\text{DL-HARQ}}_{e,\mathrm{s_1d}} + \varepsilon^{\text{DL-HARQ}}_{e,\mathrm{s_2d}}} \tag{4.47}$$

and

$$G^{\mathrm{Rtx}}_{f,\text{TL-HARQ}} = \frac{\varepsilon^{\mathrm{CCoop}}_{e,\mathrm{s_1d}} + \varepsilon^{\mathrm{CCoop}}_{e,\mathrm{s_2d}}}{\varepsilon^{\text{TL-HARQ}}_{e,\mathrm{s_1d}} + \varepsilon^{\text{TL-HARQ}}_{e,\mathrm{s_2d}}} \tag{4.48}$$

for the DL-HARQ protocol and the TL-HARQ protocol, respectively.

A frame error probability retransmission gain larger than one means that the cooperative system of Figure 3.4 with HARQ outperforms (i.e., the probability of error is lower) the original turbo coded cooperation system.

Proposition 4.1. *$G^{Rtx}_{f,DL\text{-}HARQ}$ is always greater than or equal to 1. However, $G^{Rtx}_{f,TL\text{-}HARQ}$ can be in some cases smaller than 1.*

Proof. The DL-HARQ protocol is based on the conventional turbo coded cooperative system, where the cooperation phase is controlled by feedback messages from the destination. If both sources are successfully decoded, the cooperation phase is canceled and a certain gain related to a better system efficiency is noted. On the other hand, if only one source is decoded correctly, the cooperation phase is adjusted to help the other source, without degrading the system spectral efficiency (no extra information is transmitted for the source which has already been correctly decoded). Finally, if none of the sources are decoded successfully, the cooperation phase is identical to that performed in the conventional turbo coded cooperative system and consequently no gain is noted. Therefore, $G^{\mathrm{Rtx}}_{f,\text{DL-HARQ}} \geq 1$. For the TL-HARQ protocol, the additional retransmission phase requested by the partner node cannot always be beneficial. For instance, when decoding still fails for both sources at the destination after the retransmission and cooperation phases, a system throughput degradation is observed compared to original system, and consequently $G^{\mathrm{Rtx}}_{f,\text{TL-HARQ}} < 1$. □

Proposition 4.2. *Consider a symmetric cooperation between sources $\mathrm{s_1}$ and $\mathrm{s_2}$ ($\gamma_{\mathrm{s_1d}} = \gamma_{\mathrm{s_2d}} = \gamma_{\mathrm{sd}}$). $G^{Rtx}_{f,DL\text{-}HARQ}$ is an increasing function of γ_{ss} and has an optimum value for a certain uplink SNR γ^*_{sd}. $G^{Rtx}_{f,TL\text{-}HARQ}$ is an increasing function of γ_{sd} and has an optimum value for an inter-source SNR γ^*_{ss}.*

Proof. Recall that both $G^{\mathrm{Rtx}}_{f,\text{DL-HARQ}}$ and $G^{\mathrm{Rtx}}_{f,\text{TL-HARQ}}$ are functions of γ_{ss} and γ_{sd}. Since $\frac{\partial G^{\mathrm{Rtx}}_{f,\text{DL-HARQ}}}{\partial \gamma_{\mathrm{ss}}} > 0$ and $\frac{\partial G^{\mathrm{Rtx}}_{f,\text{TL-HARQ}}}{\partial \gamma_{\mathrm{sd}}} > 0$, then $G^{\mathrm{Rtx}}_{f,\text{DL-HARQ}}$ is an increasing function of γ_{ss}, and $G^{\mathrm{Rtx}}_{f,\text{TL-HARQ}}$ is an increasing function of γ_{sd}. Furthermore, it can be shown numerically

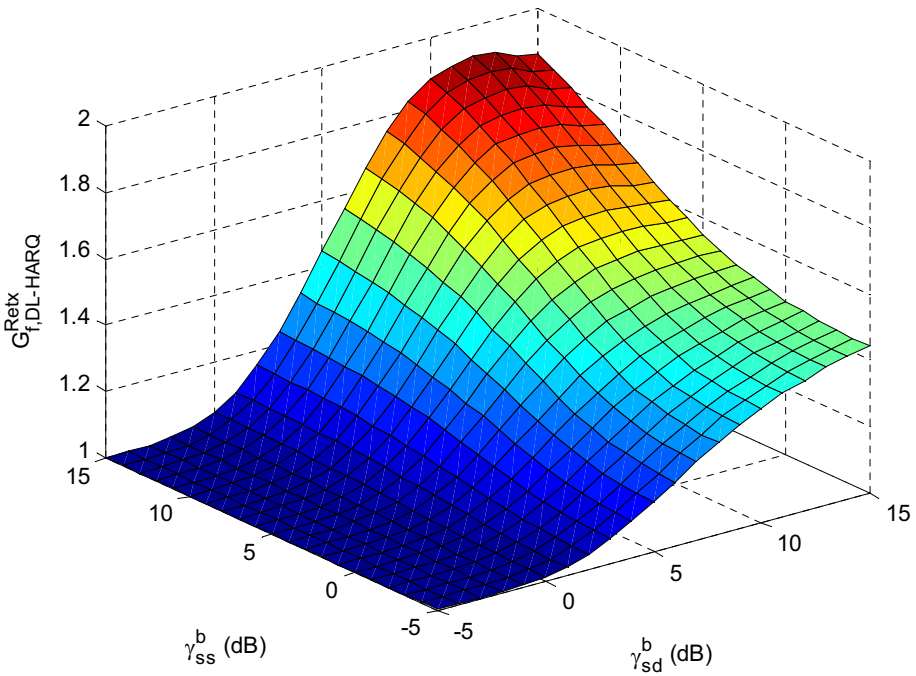

FIGURE 4.7: $G^{\text{Rtx}}_{f,\text{DL-HARQ}}$ for the symmetric case, as a function of γ^b_{ss} and γ^b_{sd}.

that there exist γ^*_{sd} and γ^*_{ss} such that $\left.\frac{\partial G^{\text{Rtx}}_{f,\text{DL-HARQ}}}{\partial \gamma_{\text{sd}}}\right|_{\gamma_{\text{sd}}=\gamma^*_{\text{sd}}} = 0$ and $\left.\frac{\partial G^{\text{Rtx}}_{f,\text{TL-HARQ}}}{\partial \gamma_{\text{ss}}}\right|_{\gamma_{\text{ss}}=\gamma^*_{\text{ss}}} = 0$. Therefore, $G^{\text{Rtx}}_{f,\text{DL-HARQ}}$ and $G^{\text{Rtx}}_{f,\text{TL-HARQ}}$ attain a maximum for γ^*_{sd} and γ^*_{ss}, respectively. □

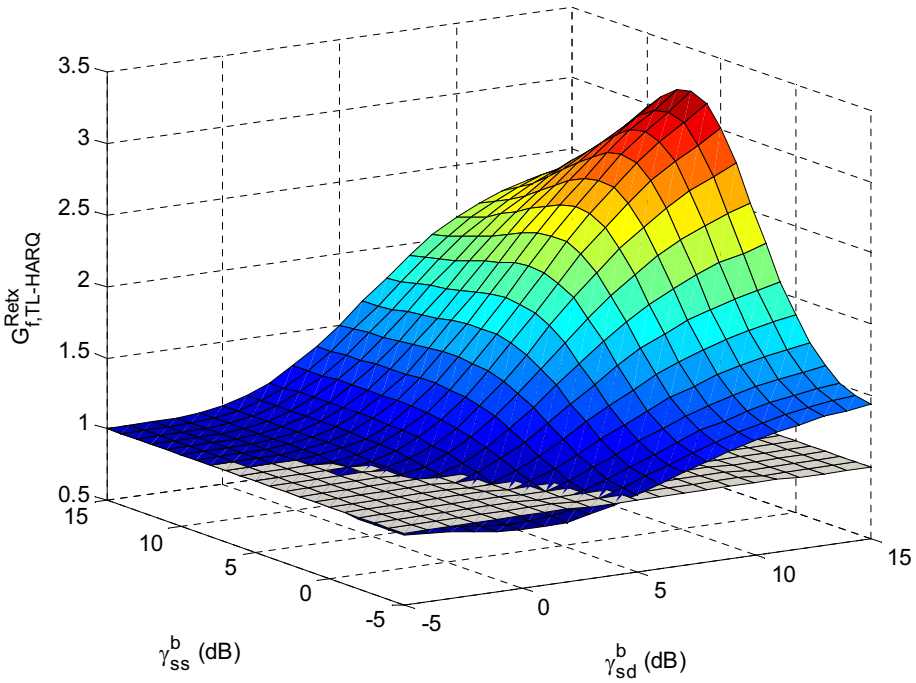

FIGURE 4.8: $G^{\text{Rtx}}_{f,\text{TL-HARQ}}$ for the symmetric case, as a function of γ^b_{ss} and γ^b_{sd}.

In Figure 4.7 and Figure 4.8, we plot the frame error probability retransmission gain of the DL-HARQ protocol and the TL-HARQ protocol, respectively, with respect to the original turbo coded cooperation system with no ARQ as a function of γ_{sd}^{b} and γ_{ss}^{b}. In Figure 4.7, we observe that for any fixed value of γ_{sd}^{b} and γ_{ss}^{b}, the DL-HARQ is always beneficial over a two-source turbo coded cooperative system. This matches with Proposition 4.1. In Figure 4.8, we observe that for a certain range of γ_{sd}^{b} and γ_{ss}^{b} values (poor uplink and inter-source links), the frame error probability retransmission gain is smaller than 1, as suggested in Proposition 4.1. Furthermore, for the DL-HARQ (Fig. 4.7), we can see that the best performance is achieved for a certain $\gamma_{\mathrm{sd}}^{b*}$ which depends on γ_{ss}^{b}. For the TL-HARQ (Figure 4.8), the best behavior is noted for a certain $\gamma_{\mathrm{ss}}^{b*}$. These results are in agreement with Proposition 4.2.

4.5.2 Frame Error Probability Cooperation Gain

We formalize the concept of the *frame error probability cooperation gain*, to quantify the performance improvement (in terms of probability of error) of DL-HARQ and TL-HARQ protocols over a conventional point-to-point IR-HARQ protocol.

Definition 4.2. For a fixed distributed channel code, the frame error probability cooperation gain is defined as

$$G_{f,\text{DL-HARQ}}^{\text{Coop}} = \frac{\varepsilon_{e,\mathrm{s_1d}}^{\text{IR-HARQ}} + \varepsilon_{e,\mathrm{s_2d}}^{\text{IR-HARQ}}}{\varepsilon_{e,\mathrm{s_1d}}^{\text{DL-HARQ}} + \varepsilon_{e,\mathrm{s_2d}}^{\text{DL-HARQ}}} \tag{4.49}$$

and

$$G_{f,\text{TL-HARQ}}^{\text{Coop}} = \frac{\varepsilon_{e,\mathrm{s_1d}}^{\text{IR-HARQ}} + \varepsilon_{e,\mathrm{s_2d}}^{\text{IR-HARQ}}}{\varepsilon_{e,\mathrm{s_1d}}^{\text{TL-HARQ}} + \varepsilon_{e,\mathrm{s_2d}}^{\text{TL-HARQ}}} \tag{4.50}$$

for the DL-HARQ protocol and the TL-HARQ protocol, respectively. $\varepsilon_{e,\mathrm{s}_i\mathrm{d}}^{\text{IR-HARQ}}$, $i = 1, 2$, denotes the bound on the frame error probability of the point-to-point IR-HARQ protocol.

Conjecture 4.1. *For the symmetric case, if γ_{ss} is sufficiently high, $G_{f,DL\text{-}HARQ}^{Coop} > 1$ for $\gamma_{\mathrm{sd}} > \gamma_{\mathrm{sd}}^{*1}$ and $G_{f,TL\text{-}HARQ}^{Coop} > 1$ for $\gamma_{\mathrm{sd}} > \gamma_{\mathrm{sd}}^{*2}$, where both uplink SNRs $\gamma_{\mathrm{sd}}^{*1}$ and $\gamma_{\mathrm{sd}}^{*2}$ depend on γ_{ss} and verify $\gamma_{\mathrm{sd}}^{*1} > \gamma_{\mathrm{sd}}^{*2}$.*

From Conjecture 4.1, it turns out that cooperation is not always useful. Moreover, TL-HARQ is more efficient compared to DL-HARQ since it gives higher gains, and for a larger range of uplink SNRs.

Proposition 4.3. *For the asymmetric case, where we assume that $\gamma_{\mathrm{s_1d}} = \gamma_{\mathrm{ss}}$ and the asymmetry degree between uplink SNRs is quantified by $\tau = \gamma_{\mathrm{s_2d}}/\gamma_{\mathrm{s_1d}}$, $G_{f,DL\text{-}HARQ}^{Coop}$ and $G_{f,TL\text{-}HARQ}^{Coop}$ are increasing functions of τ.*

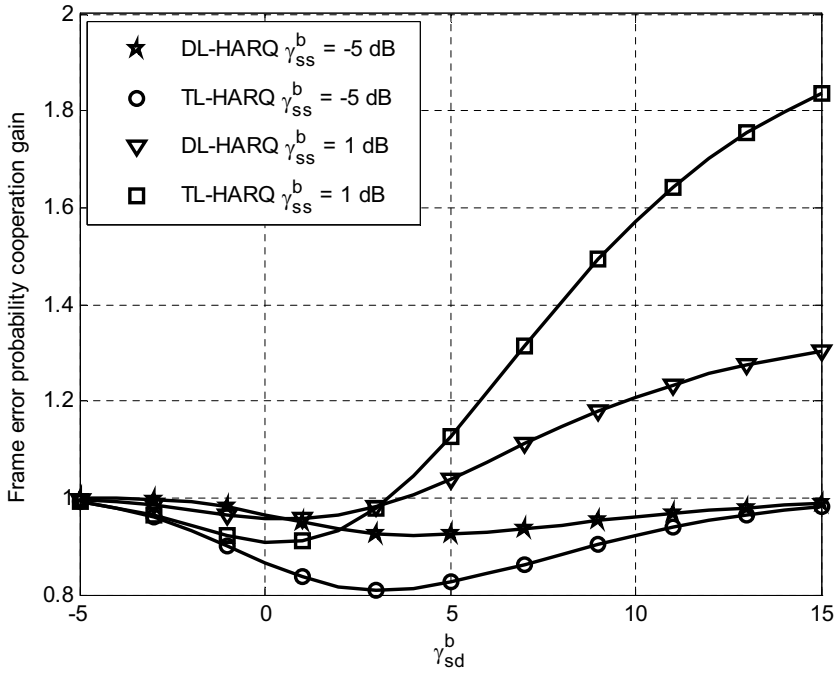

FIGURE 4.9: $G^{\text{Coop}}_{f,\text{DL-HARQ}}$ and $G^{\text{Coop}}_{f,\text{TL-HARQ}}$ for the symmetric case, as a function of γ^b_{sd}.

Proof. Recall that both $G^{\text{Rtx}}_{f,\text{DL-HARQ}}$ and $G^{\text{Rtx}}_{f,\text{TL-HARQ}}$ are functions of γ_{ss}, $\gamma_{\text{s}_1\text{d}}$ and $\gamma_{\text{s}_2\text{d}}$. When we fix both γ_{ss} and $\gamma_{\text{s}_1\text{d}}$, $G^{\text{Rtx}}_{f,\text{DL-HARQ}}$ and $G^{\text{Rtx}}_{f,\text{TL-HARQ}}$ are functions of τ. We have $\frac{\partial G^{\text{Rtx}}_{f,\text{DL-HARQ}}}{\partial \tau} > 0$ and $\frac{\partial G^{\text{Rtx}}_{f,\text{TL-HARQ}}}{\partial \tau} > 0$, consequently, $G^{\text{Coop}}_{f,\text{DL-HARQ}}$ and $G^{\text{Coop}}_{f,\text{TL-HARQ}}$ are increasing functions of τ. □

In order to illustrate Conjecture 4.1, we plot in Figure 4.9 the frame error probability cooperation gains for the DL-HARQ and the TL-HARQ protocols as a function of γ^b_{sd} (symmetric uplink case), for different values of γ^b_{ss}. For a poor inter-source channel ($\gamma^b_{\text{ss}} = -5$ dB), we see no gain over the point-to-point IR-HARQ. However, for sufficiently high γ^b_{ss}, a gain is observed for some range of γ^b_{sd}.

Figure 4.10 reports the frame error probability cooperation gains of the DL-HARQ and the TL-HARQ protocols as a function of τ (the asymmetry degree between uplink channels), for two different values of γ^b_{ss}. We note that $G^{\text{Coop}}_{f,\text{DL-HARQ}}$ and $G^{\text{Coop}}_{f,\text{TL-HARQ}}$ are increasing functions of τ, which is consistent with Proposition 4.3. Consequently, we conclude that a better link quality for one of the partner sources over the other guarantees cooperation benefits to the whole system for a sufficiently high inter-source quality.

4.6 Throughput Efficiency Based Analysis

In this section, we consider the throughput efficiency behavior of the DL-HARQ and TL-HARQ protocols. We first analyze the throughput efficiency performance of

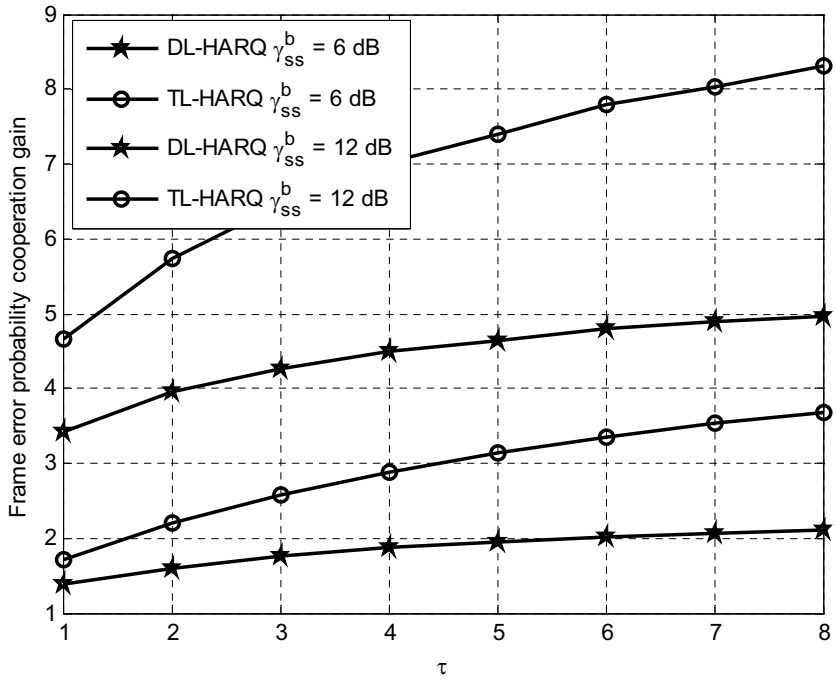

FIGURE 4.10: $G^{\text{Coop}}_{f,\text{DL-HARQ}}$ and $G^{\text{Coop}}_{f,\text{TL-HARQ}}$ for the asymmetric case, as a function of τ.

both protocols and then formalize the retransmission and cooperation gains from the throughput efficiency perspective.

We recall that from the renewal theorem [ZR96] and the renewal-reward theorem [CT01], the throughput efficiency is given by

$$\eta = \frac{E\left[\mathcal{R}\right]}{E\left[D\right]} \tag{4.51}$$

where $E\left[\mathcal{R}\right]$ is the average reward, used to define the average rate of the transmission, and $E\left[D\right]$ is the expected inter-renewal time, used to illustrate the average transmission delay. Both $E\left[\mathcal{R}\right]$ and $E\left[D\right]$ are functions of the frame error probability. However, since the exact frame error probability cannot be computed, we compute $E\left[\mathcal{R}\right]$ and $E\left[D\right]$ by approximating the frame error probability by its upper bound. Therefore, instead of using an exact η, we rely on an approximated efficiency, denoted by $\bar{\eta}$, in order to define the throughput efficiency retransmission gain and the throughput efficiency cooperation gain.

The average reward with respect to source s_1 using the bound on the frame error probability is given by

$$E\left[\mathcal{R}\right] = \frac{R}{\alpha}\left(1 - \varepsilon_{e,\text{s}_1\text{d}}^{\text{DL-HARQ}}\right) \tag{4.52}$$

and

$$E\left[\mathcal{R}\right] = \frac{R}{\alpha}\left(1 - \varepsilon_{e,\text{s}_1\text{d}}^{\text{TL-HARQ}}\right) \tag{4.53}$$

for the DL-HARQ protocol and the TL-HARQ protocol, respectively.

The inter-renewal time gives the average delay of the HARQ protocol. For all incremental redundancy techniques, since the receiver attempts decoding after every transmission phase, the transmission delay is variable. This is due to that the retransmission process is stopped upon successful decoding at the receiver. For the DL-HARQ protocol, the average inter-renewal delay is given by

$$E[D] = (1-\varepsilon_{\mathrm{s_1d}}^{\varphi_1})(1-\varepsilon_{\mathrm{s_2d}}^{\varphi_1}) + \frac{1}{\alpha}\left[1-(1-\varepsilon_{\mathrm{s_1d}}^{\varphi_1})(1-\varepsilon_{\mathrm{s_2d}}^{\varphi_1})\right] \tag{4.54}$$

This expression is obtained from the observation of the expected delay for all possible transmission cases: If decoding is successful for both sources after the first phase, no retransmission is performed (only the first phase takes place); if incorrect decoding happens for at least one of the sources, the cooperation phase is necessary and the time duration of the whole transmission is $\frac{1}{\alpha}$.

For the TL-HARQ protocol, the average inter-renewal delay is given by

$$\begin{aligned} E[D] = (1-\varepsilon_{\mathrm{s_1d}}^{\varphi_1})(1-\varepsilon_{\mathrm{s_2d}}^{\varphi_1}) + \left[1-(1-\varepsilon_{\mathrm{s_1d}}^{\varphi_1})(1-\varepsilon_{\mathrm{s_2d}}^{\varphi_1}\right] \\ \left[\frac{1}{\alpha}\left(1-\varepsilon_{\mathrm{s_1s_2}}^{\varphi_1}\right) + \frac{2-\alpha}{\alpha}\varepsilon_{\mathrm{s_1s_2}}^{\varphi_1}\right] \end{aligned} \tag{4.55}$$

4.6.1 Throughput Efficiency Retransmission Gain

We define the throughput efficiency retransmission gain as the gain (in terms of throughput efficiency) of the DL- HARQ and TL-HARQ protocols over the original turbo coded cooperation where no HARQ is performed.

Definition 4.3. For a fixed distributed channel code, the throughput efficiency retransmission gain is defined as

$$G_{t,\mathrm{DL\text{-}HARQ}}^{\mathrm{Rtx}} = \frac{\bar{\eta}_{\mathrm{s_1d}}^{\mathrm{DL\text{-}HARQ}} + \bar{\eta}_{\mathrm{s_2d}}^{\mathrm{DL\text{-}HARQ}}}{\bar{\eta}_{\mathrm{s_1d}}^{\mathrm{CCoop}} + \bar{\eta}_{\mathrm{s_2d}}^{\mathrm{CCoop}}} \tag{4.56}$$

and

$$G_{t,\mathrm{TL\text{-}HARQ}}^{\mathrm{Rtx}} = \frac{\bar{\eta}_{\mathrm{s_1d}}^{\mathrm{TL\text{-}HARQ}} + \bar{\eta}_{\mathrm{s_2d}}^{\mathrm{TL\text{-}HARQ}}}{\bar{\eta}_{\mathrm{s_1d}}^{\mathrm{CCoop}} + \bar{\eta}_{\mathrm{s_2d}}^{\mathrm{CCoop}}} \tag{4.57}$$

for the DL-HARQ protocol and the TL-HARQ protocol, respectively.

A throughput efficiency retransmission gain larger than one means that the cooperative system of Figure 3.4 with HARQ outperforms (in terms of throughput efficiency) the original turbo coded cooperation system.

Similar to Propositions 4.1 and 4.2, we obtain the following results for the system throughput efficiency.

Conjecture 4.2. $G_{t,DL\text{-}HARQ}^{Rtx} \geq 1$. $G_{t,TL\text{-}HARQ}^{Rtx} \geq 1$ *for sufficiently high* γ_{ss}.

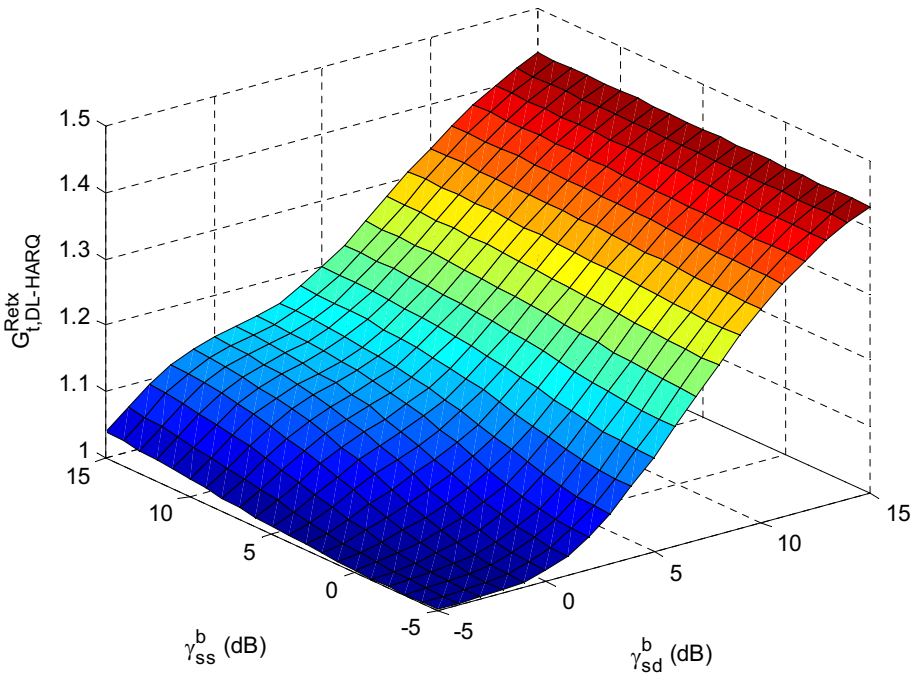

FIGURE 4.11: $G^{\text{Rtx}}_{t,\text{DL-HARQ}}$ for the symmetric case, as a function of γ^b_{ss} and γ^b_{sd}.

Proposition 4.4. *Consider a symmetric system ($\gamma_{\text{s}_1\text{d}} = \gamma_{\text{s}_2\text{d}} = \gamma_{\text{sd}}$). $G^{Rtx}_{t,DL\text{-}HARQ}$ is an increasing function of γ_{sd}. $G^{Rtx}_{t,TL\text{-}HARQ}$ has an optimum value for an uplink SNR γ^*_{sd}.*

Proof. Recall that both $G^{\text{Rtx}}_{t,\text{DL-HARQ}}$ and $G^{\text{Rtx}}_{t,\text{TL-HARQ}}$ are functions of γ_{ss} and γ_{sd}. We have $\frac{\partial G^{\text{Rtx}}_{t,\text{DL-HARQ}}}{\partial \gamma_{\text{sd}}} > 0$, therefore $G^{\text{Rtx}}_{t,\text{DL-HARQ}}$ is an increasing function of γ_{sd}. Furthermore, $\left.\frac{\partial G^{\text{Rtx}}_{t,\text{TL-HARQ}}}{\partial \gamma_{\text{sd}}}\right|_{\gamma_{\text{sd}}=\gamma^*_{\text{sd}}} = 0$, then $G^{\text{Rtx}}_{t,\text{TL-HARQ}}$ has a maximum for γ^*_{sd}. □

We plot in Figure 4.11 and Figure 4.12 the gain $G^{\text{Rtx}}_{t,\text{DL-HARQ}}$ and $G^{\text{Rtx}}_{f,\text{TL-HARQ}}$, respectively, for the symmetric case. We notice that the DL-HARQ protocol always improves the turbo coded cooperation system. However, a minimum inter-source channel quality is required to benefit from the TL-HARQ protocol, as suggested in Conjecture 4.2. Furthermore, we can note that the TL-HARQ attains a maximum for a certain γ^{b*}_{sd} (see Proposition 4.4).

4.6.2 Throughput Efficiency Cooperation Gain

We define the throughput efficiency cooperation gain as the gain (in terms of throughput efficiency) of the DL- HARQ and TL-HARQ protocols over a non cooperative system using point-to-point IR-HARQ.

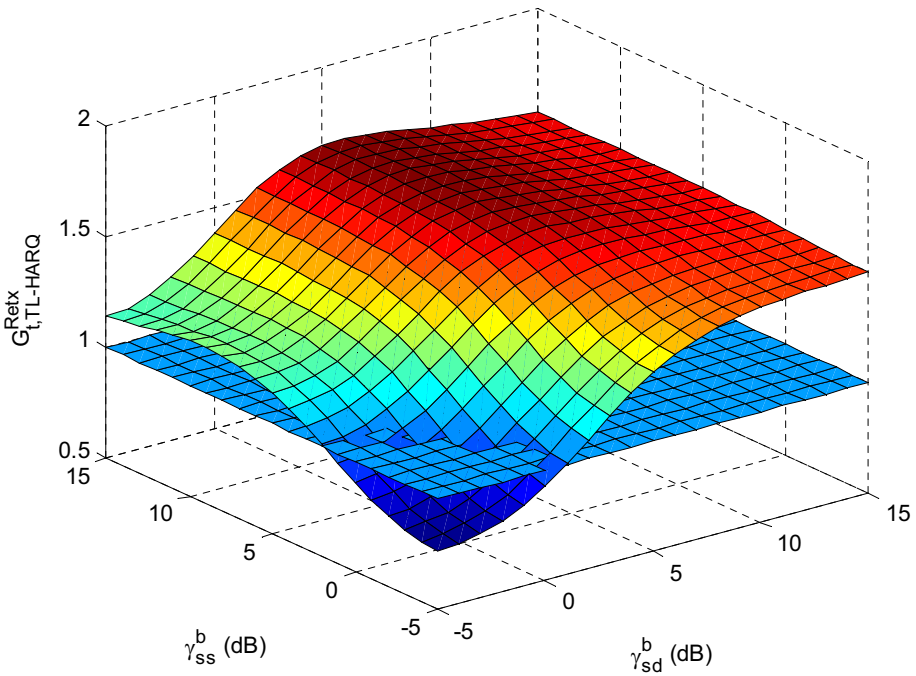

FIGURE 4.12: $G^{\text{Rtx}}_{t,\text{TL-HARQ}}$ for the symmetric case, as a function of γ^b_{ss} and γ^b_{sd}.

Definition 4.4. For a fixed distributed channel code, the throughput efficiency cooperation gain is defined as

$$G^{\text{Coop}}_{t,\text{DL-HARQ}} = \frac{\bar{\eta}^{\text{DL-HARQ}}_{\text{s}_1\text{d}} + \bar{\eta}^{\text{DL-HARQ}}_{\text{s}_2\text{d}}}{\bar{\eta}^{\text{IR-HARQ}}_{\text{s}_1\text{d}} + \bar{\eta}^{\text{IR-HARQ}}_{\text{s}_2\text{d}}} \tag{4.58}$$

and

$$G^{\text{Coop}}_{t,\text{TL-HARQ}} = \frac{\bar{\eta}^{\text{TL-HARQ}}_{\text{s}_1\text{d}} + \bar{\eta}^{\text{TL-HARQ}}_{\text{s}_2\text{d}}}{\bar{\eta}^{\text{IR-HARQ}}_{\text{s}_1\text{d}} + \bar{\eta}^{\text{IR-HARQ}}_{\text{s}_2\text{d}}} \tag{4.59}$$

for the DL-HARQ protocol and the TL-HARQ protocol, respectively.

Conjecture 4.3. *Consider a symmetric system.* $G^{Coop}_{t,DL\text{-}HARQ} \leq 1$. *However,* $G^{Coop}_{t,TL\text{-}HARQ} \geq 1$ *for sufficiently high* γ_{sd}.

We observed that for medium-to-high γ_{ss}, $G^{\text{Coop}}_{t,\text{DL-HARQ}}$ approaches 1, meaning that the throughput efficiency of DL-HARQ is very close to that of the non-cooperative system using point-to-point IR-HARQ. To assess the benefit of DL-HARQ, $G^{\text{Coop}}_{f,\text{DL-HARQ}}$ is therefore a more significative decision parameter.

4.7 Geometrical Analysis

In the following, we determine the geometric conditions under which using cooperative HARQ protocols is useful. A free space environment is assumed ($\beta = 2$) . The results are given for optimal time allocation α_{opt}, depicted in Figure 4.3, when the mother code

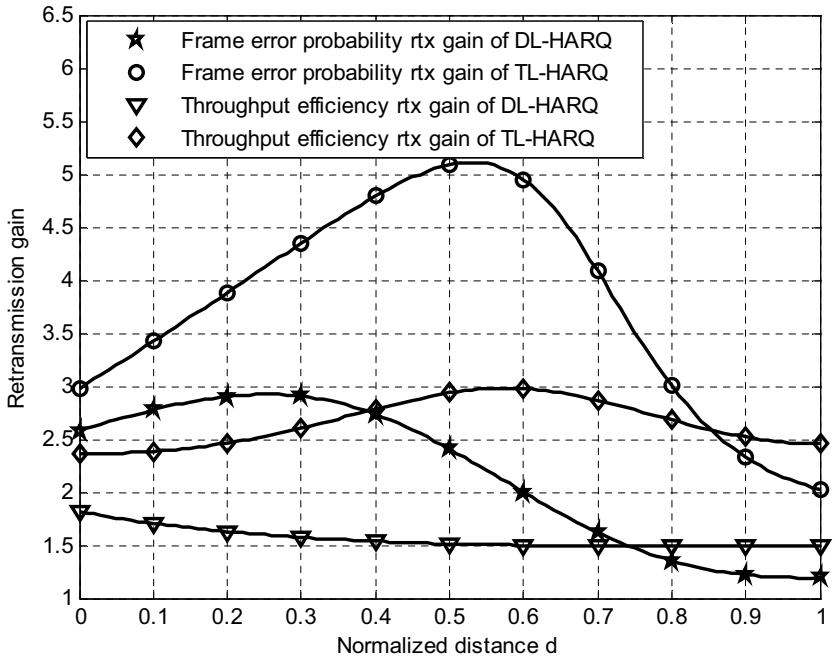

FIGURE 4.13: Retransmission gain for the linear scenario ($\gamma^b_{\mathrm{s_1d}} = 5$ dB).

rate is 1/3. α_{opt} is 2/3, 1/2, and 1/3, for the coded cooperation scheme, the DL-HARQ protocol, and the TL-HARQ protocol, respectively. Moreover, when comparisons with the point-to-point IR-HARQ protocol are addressed, the same permeability rate (α) is used. We adopt two different geometrical setups. First, we consider a three-node system where the source $\mathrm{s_1}$ is fixed and $\mathrm{s_2}$ is moving on the same line from $\mathrm{s_1}$ towards the destination. Taking into account the path loss effect, the received SNRs of the $\mathrm{s_1}$-to-d, $\mathrm{s_1}$-to-$\mathrm{s_2}$ and $\mathrm{s_2}$-to-d channels are given by (E_s/N_0), $(E_s/N_0)d^{-\beta}$ and $(E_s/N_0)(1-d)^{-\beta}$, respectively, where d is the normalized inter-source distance (normalized by $d_{\mathrm{s_1d}}$). In Figure 4.13, we examine the frame error probability retransmission gain as well as the throughput efficiency retransmission gain of DL-HARQ and TL-HARQ as a function of d, for a fixed $\gamma^b_{\mathrm{s_1d}} = 5$ dB.

Regardless the location of $\mathrm{s_2}$, the DL-HARQ and TL-HARQ protocols benefit to the whole cooperative system with respect to the turbo coded cooperation scheme, from both frame error probability and throughput efficiency perspectives. They yield to sizable retransmission gains (values greater than one). Notice that the TL-HARQ protocol gives the best results. The DL-HARQ protocol is more beneficial when $\mathrm{s_2}$ is located closer to $\mathrm{s_1}$ than to the destination, since it guarantees a certain inter-source channel quality. However, for the TL-HARQ protocol, the best FER behavior is obtained when $\mathrm{s_2}$ is closer to the destination. Since another retransmission phase to the partner node is possible, the inter-source link becomes less critical. From simulation results, we obtain

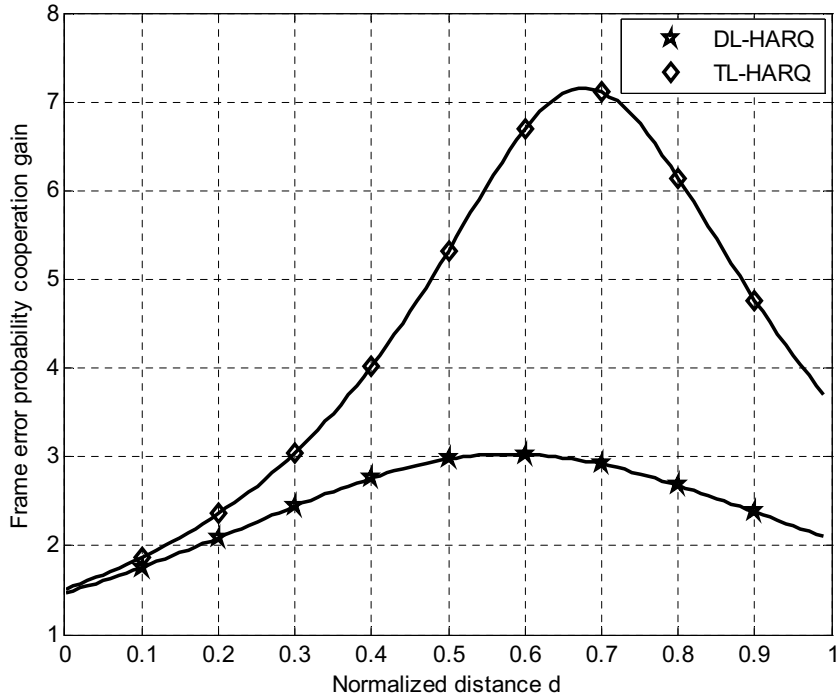

FIGURE 4.14: Frame error probability cooperation gain for the linear scenario ($\gamma^b_{\mathrm{s_1d}} = 1$ dB).

the distances $d^*_{\text{DL-HARQ}} = 0.26$ and $d^*_{\text{TL-HARQ}} = 0.58$ that maximize the frame error probability retransmission gain of the DL-HARQ and the TL-HARQ protocol, respectively. A good match between the simulation and the analytical results is observed. According to the throughput efficiency analysis, for the DL-HARQ protocol, the retransmission gain varies very little when the uplink SNR is fixed. On the other hand, for the TL-HARQ protocol the best performance according to the throughput efficiency analysis and to the frame error probability analysis are obtained for a similar normalized distance d.

In the following, we consider the frame error probability analysis to predict the best locations, as from Figure 4.13 it turns to be a better measure for DL-HARQ. In Figure 4.14, we plot the frame error probability cooperation gain of the considered cooperative HARQ protocols as a function of the normalized inter-source distance for a fixed $\gamma^b_{\mathrm{s_1d}} = 1$ dB. Compared to the point-to-point IR-HARQ protocol, both DL-HARQ and TL-HARQ bring sizable improvements if $\mathrm{s_2}$ is closer to the destination than to $\mathrm{s_1}$. This guarantees a good $\mathrm{s_2}$-to-d link. We obtain the optimal distances $d^*_{\text{DL-HARQ}} = 0.62$ and $d^*_{\text{TL-HARQ}} = 0.65$, which closely match those obtained analytically.

We consider now a two-dimensional scenario where the cooperating sources are located on a plane, and fix the location of the destination at the (0,0) point, the location of $\mathrm{s_1}$ at the (1,0) point, and $\gamma^b_{\mathrm{s_1d}} = 10$ dB. The distances are normalized with respect to $d_{\mathrm{s_1d}}$. In Figure 4.15, we plot the geometrical region boundaries where each cooperative HARQ protocol guarantees a minimum frame error probability retransmission gain. For

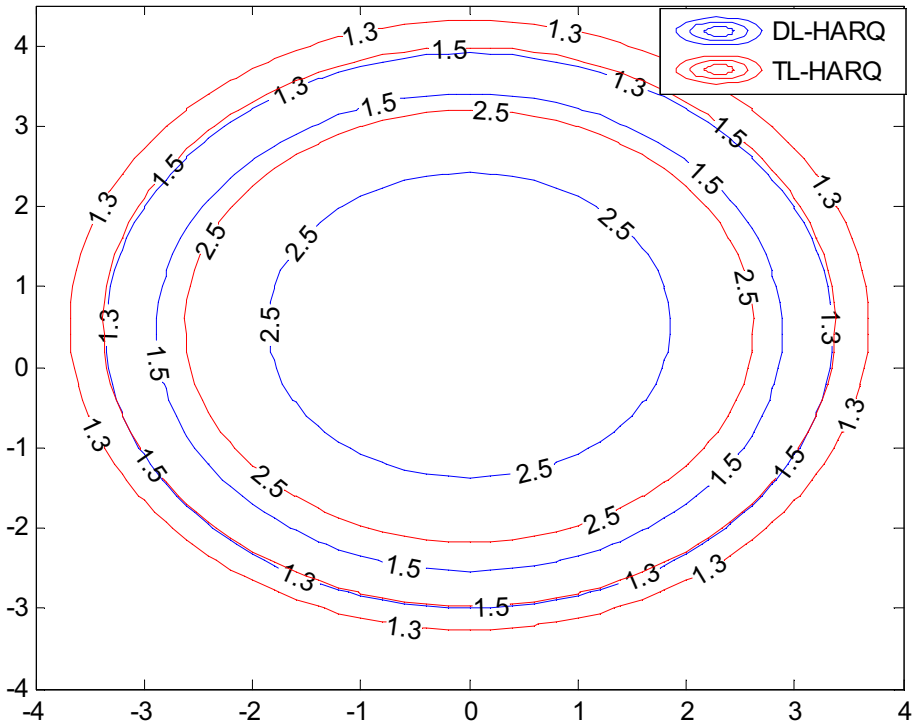

FIGURE 4.15: Frame error probability retransmission gain for the 2-dimensional scenario ($\gamma^b_{\mathrm{s_1 d}} = 10$ dB).

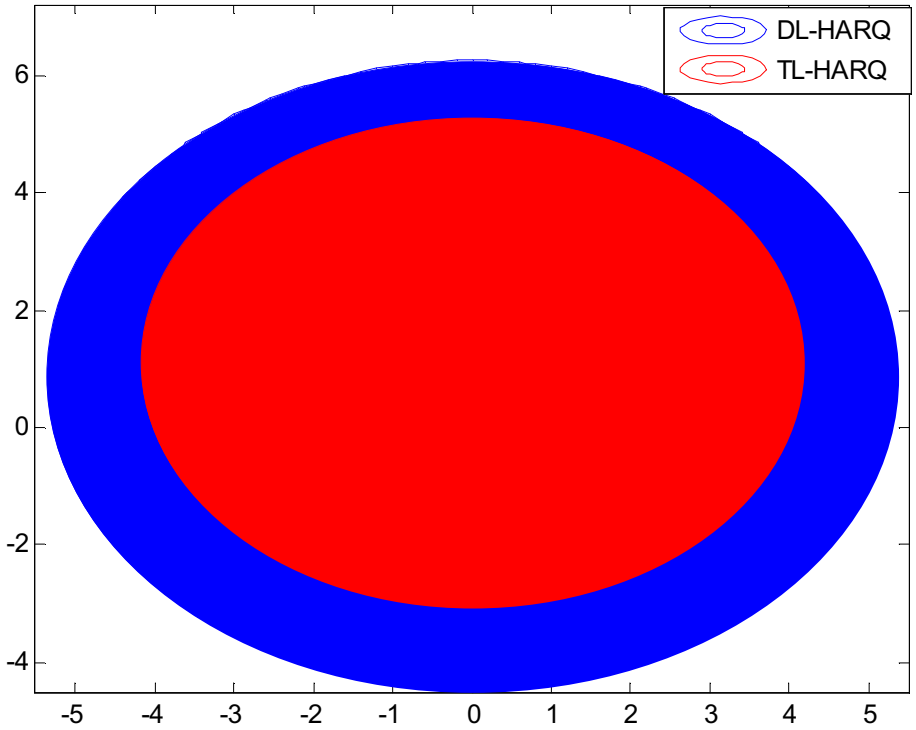

FIGURE 4.16: Regions where DL-HARQ and TL-HARQ perform the best in terms of frame error probability and with reference to a point-to-point IR-HARQ, in a 2-dimensional scenario ($\gamma^b_{\mathrm{s_1 d}} = 10$ dB).

instance, if source s_2 is located inside the contour marked by 1.5, the corresponding cooperative HARQ protocol yields a frame error probability retransmission gain greater than 1.5 (exactly 1.5 on the contour). It is shown that the TL-HARQ protocol yields a larger region satisfying a given frame error probability retransmission gain.

Finally, in Figure 4.16, we plot the geometrical regions where the cooperative HARQ protocols perform the best in terms of frame error probability cooperation gain. The TL-HARQ protocol is preferred to the DL-HARQ for a large region (the red region). However, when s_2 is far from s_1 (the blue region), DL-HARQ performs the best. In this case, no retransmission is allowed between sources, avoiding an unnecessary system throughput degradation. If s_2 is very far away from s_1, cooperative HARQ brings no gain.

4.8 Chapter Summary

In this chapter, we considered coded cooperation with hybrid ARQ. First, we analyzed the protocols proposed in Chapter 3 in terms of the outage probability. Reporting the outage behavior of the proposed HARQ protocols versus the transmission rate, we can conclude that for the low-rate regime, all HARQ protocols give a significant improvement with respect to coded cooperation and non-cooperation, with TL-HARQ giving the best performance. However, for high rates ($R > 1$), coded cooperation and RL-HARQ perform worse than non-cooperation.

As all the protocols have the same diversity order, to better distinguish between them, we performed a diversity-multiplexing tradeoff analysis. Interestingly, not all HARQ protocols provide some gain. The diversity gain for RL-HARQ is, for any rate and for some values of α, smaller than that offered by the coded cooperation scheme. This is an immediate consequence of decreasing the transmission rate when unnecessarily retransmissions can occur even if the packet is correctly decoded at the destination in the broadcast phase. It is then shown that DL-HARQ and TL-HARQ offer the best performance.

Thereafter, we defined the retransmission gain and the cooperation gain of DL-HARQ and TL-HARQ protocols (offering good results in terms of reliability as well as in terms of efficiency), to quantify their benefits over two reference systems: The turbo coded cooperation system, and the point-to-point IR-HARQ protocol, respectively. These gains were defined in terms of frame error probability and throughput efficiency.

Making use of the retransmission gain and the cooperation gain as decision parameters, and adopting the geometrical approach as in [LES06], we determine the geometric conditions under which using Dl-HARQ and TL-HARQ protocols is useful. The basis of this performance analysis is the so-called code threshold of a turbo code ensemble. Combined with the outage concept, a frame error probability bound as well as a throughput

efficiency bound can be derived, that predict well the simulation results. We showed that, while avoiding extensive computations, these analytical performance metrics can be adopted to optimally design our cooperative HARQ protocols from different perspectives.

Chapter 5

Decode-and-Forward Relaying with Correlated Sources

In this chapter, we consider a wireless communication system with two sources that transmit their data to one common destination with the help of a relay (see Figure 5.1). The data of the two sources is assumed to be *correlated*, an assumption that applies, for example, to wireless sensor networks (WSNs) [ASSC02], where nearby sensors measure statistically dependent data and transmit this data to a common processing node. We further restrict ourselves to uncoded transmission, which is practically relevant since power is a scarce resource in inexpensive sensor nodes and hence a coding/decoding stage may be infeasible.

The relay works in a half-duplex mode and uses the DF strategy. The relay makes a hard decision on the transmitted data and forwards it to the destination. Instead of relaying the information of the individual sources in an alternating way, network coding [ACLY00] is used at the relay to combine the data of the two sources, thereby increasing the transmission capacity. The relay network in Figure 5.1 was first considered in [HD06], where coding strategies were proposed. For the same relay network, performance bounds for convolutionally coded DF were derived in [iAL10]. These works assumed that the data transmitted by the two sources is statistically independent. Joint detection of correlated sources (for a non-cooperative system) has been recently addressed in [AFM11].

In this chapter, we derive analytical bounds on the error probability for the relay system shown in Figure 5.1. Our work extends the results in [iAL10] by introducing correlation between the sources. We consider two types of detectors at the destination: i) the optimal maximum a posteriori (MAP) decoding rule which explicitly takes into account that detection errors may occur at the relay; ii) a simplified MAP decoder that works on the assumption that the two-hop source-to-relay-to-destination channel can be approximated by a virtual single-hop memoryless channel between the sources and

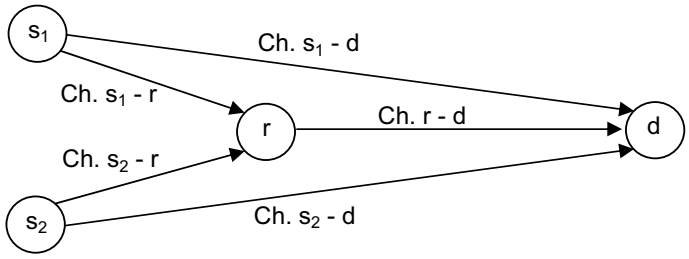

FIGURE 5.1: Relay network consisting of two correlated sources with a common destination and one relay.

the destination (this assumption has been previously used e.g. in [WCGL07]); the corresponding receiver will be termed the *virtual-channel MAP* (VC-MAP) decoder. We demonstrate the performance gain that can be obtained by exploiting the correlation between the sources and we compare our results to a correlation-aware system without relay. It turns out that the gain achievable with a relay decreases with increasing correlation, i.e., for scenarios with very high correlation the gain is limited. Furthermore, we show that by tuning a free parameter in the sub-optimal detector the performance of the optimal detector can be closely approached. Simulation results confirm the tightness of the bounds obtained. The remainder of this chapter is structured as follows.

In Section 5.1, we introduce the system model. Section 5.2 contains the derivation of the analytical expressions for the error probability bounds for Gaussian channels. These results are extended for Rayleigh channels in Section 5.3. A comparison between analytical and numerical results is given in Section 5.4. Finally, conclusions are drawn in Section 5.5.

5.1 System Model

We consider the wireless relay channel with two sources, one relay and one destination depicted in Figure 5.1. In practice, terminals cannot transmit and receive at the same time and over the same frequency band and hence we assume that all transmissions are over orthogonal channels. We restrict ourselves to uncoded binary transmission and BPSK modulation. Each source s_i, $i = 1, 2$, wants to transmit an information bit $x_{\mathrm{s}_i} \in \{0, 1\}$ to the destination (we assume $p(x_{\mathrm{s}_i} = 0) = p(x_{\mathrm{s}_i} = 1) = 0.5$). The statistical dependence of the two source bits can be represented by the relation [AFM11] $x_{\mathrm{s}_2} = x_{\mathrm{s}_1} \oplus a$, where $\oplus$ is the modulo-2 addition; here, $a \in \{0, 1\}$ is a random variable that is independent of x_{s_1} and x_{s_2} and determines the amount of correlation. We denote by p_a the probability that a equals 0 ($p_a = 0.5$ corresponds to the case where x_{s_1} and x_{s_2} are uncorrelated). Note that $p(x_{\mathrm{s}_1}, x_{\mathrm{s}_2}) = p_a/2$ for $x_{\mathrm{s}_1} = x_{\mathrm{s}_2}$ and $p(x_{\mathrm{s}_1}, x_{\mathrm{s}_2}) = (1-p_a)/2$ for $x_{\mathrm{s}_1} \neq x_{\mathrm{s}_2}$.

The sources modulate their information bits x_{s_i} to BPSK symbols $\tilde{x}_{\mathrm{s}_i} \in \{\pm 1\}$ using the mapping $0 \to +1$, $1 \to -1$ and broadcast these BPSK symbols to the relay and the destination, which receive the signals

$$y_{\mathrm{s}_i\mathrm{r}} = h_{\mathrm{s}_i\mathrm{r}}\tilde{x}_{\mathrm{s}_i} + w_{\mathrm{s}_i\mathrm{r}} \tag{5.1}$$

$$y_{\mathrm{s}_i\mathrm{d}} = h_{\mathrm{s}_i\mathrm{d}}\tilde{x}_{\mathrm{s}_i} + w_{\mathrm{s}_i\mathrm{d}}, \qquad i = 1, 2 \tag{5.2}$$

Here $w_{\mathrm{s}_i\mathrm{r}}$ and $w_{\mathrm{s}_i\mathrm{d}}$ are additive white Gaussian noise (AWGN) variables with zero-mean and respective variance $\sigma^2_{\mathrm{s}_i\mathrm{r}}$ and $\sigma_{\mathrm{s}_i\mathrm{d}}$, and $h_{\mathrm{s}_i\mathrm{r}}$ and $h_{\mathrm{s}_i\mathrm{d}}$ denote the source-to-relay and source-to-destination channel coefficients, respectively. Two different channel models are considered: binary-input AWGN ($h_{\mathrm{s}_i\mathrm{r}} = h_{\mathrm{s}_i\mathrm{d}} = 1$) and Rayleigh fading. In the fading case, each coefficient is a Rayleigh distributed, unit-variance random variable. The signal-to-noise ratio (SNR) for the source-to-relay and source-to-destination links are in both cases given by $\gamma_{\mathrm{s}_i\mathrm{r}} = 1/(2\sigma^2_{\mathrm{s}_i\mathrm{r}})$ and $\gamma_{\mathrm{s}_i\mathrm{d}} = 1/(2\sigma^2_{\mathrm{s}_i\mathrm{d}})$, respectively.

In order to exploit the correlation between the source symbols, the relay uses both $y_{\mathrm{s}_1\mathrm{r}}$ and $y_{\mathrm{s}_2\mathrm{r}}$ to jointly detect the source signals. The relay then forwards the modulo-2 sum $x_{\mathrm{r}} = \hat{x}_{\mathrm{s}_1\mathrm{r}} \oplus \hat{x}_{\mathrm{s}_2\mathrm{r}}$ of the two detected signals $\hat{x}_{\mathrm{s}_1\mathrm{r}}$ and $\hat{x}_{\mathrm{s}_2\mathrm{r}}$ to the destination, which receives

$$y_{\mathrm{rd}} = h_{\mathrm{rd}}\tilde{x}_{\mathrm{r}} + w_{\mathrm{rd}} \tag{5.3}$$

Here, w_{rd} is AWGN with variance σ^2_{rd} and h_{rd} is the relay-to-destination channel coefficient which in case of a pure AWGN channel equals 1 and in case of fading has Rayleigh distribution with variance 1. Correspondingly, the relay-destination SNR equals $\gamma_{\mathrm{rd}} = 1/(2\sigma^2_{\mathrm{rd}})$. Since detection errors may occur at the relay, x_{r} may be different from $x_{\mathrm{s}_1} \oplus x_{\mathrm{s}_2}$. Based on the noisy observations $y_{\mathrm{s}_1\mathrm{d}}$, $y_{\mathrm{s}_2\mathrm{d}}$, and y_{rd}, the destination attempts to detect x_{s_1} and x_{s_2}. The detected symbols are denoted by $\hat{x}_{\mathrm{s}_1}$ and $\hat{x}_{\mathrm{s}_2}$.

5.2 Error Bounds for Gaussian Channels in Single-Relay Case

The error event at the destination is defined by

$$e = \{\hat{x}_{\mathrm{s}_1} \neq x_{\mathrm{s}_1} \vee \hat{x}_{\mathrm{s}_2} \neq x_{\mathrm{s}_2}\} \tag{5.4}$$

For our analysis, we assume $x_{\mathrm{s}_1} = 0$. This implies no loss of generality since x_{s_1} has a symmetric distribution.

Defining the error events at the relay,

$$e_{\mathrm{r}_1} = \{\hat{x}_{\mathrm{s}_1\mathrm{r}} \neq x_{\mathrm{s}_1}\}, \quad e_{\mathrm{r}_2} = \{\hat{x}_{\mathrm{s}_2\mathrm{r}} \neq x_{\mathrm{s}_2}\} \tag{5.5}$$

and

$$e_{\mathrm{r}} = (e_{\mathrm{r}_1} \cup e_{\mathrm{r}_2}) \setminus (e_{\mathrm{r}_1} \cap e_{\mathrm{r}_2}), \tag{5.6}$$

the error probability at the destination can be written as

$$\begin{aligned} p(e) = {} & p(e|\bar{e}_{\mathrm{r}}, x_{\mathrm{s}_1} = x_{\mathrm{s}_2})\, p(\bar{e}_{\mathrm{r}}, x_{\mathrm{s}_1} = x_{\mathrm{s}_2}) \\ & + p(e|\bar{e}_{\mathrm{r}}, x_{\mathrm{s}_1} \neq x_{\mathrm{s}_2})\, p(\bar{e}_{\mathrm{r}}, x_{\mathrm{s}_1} \neq x_{\mathrm{s}_2}) \\ & + p(e|e_{\mathrm{r}}, x_{\mathrm{s}_1} = x_{\mathrm{s}_2})\, p(e_{\mathrm{r}}, x_{\mathrm{s}_1} = x_{\mathrm{s}_2}) \\ & + p(e|e_{\mathrm{r}}, x_{\mathrm{s}_1} \neq x_{\mathrm{s}_2})\, p(e_{\mathrm{r}}, x_{\mathrm{s}_1} \neq x_{\mathrm{s}_2}), \end{aligned} \tag{5.7}$$

where we distinguish between the four cases where the relay makes an error and where it does not, and where the source symbols are identical or not. We write $\bar{e}_{\mathrm{r}}$ for the complementary event of e_{r}. For example, in the event $\{\bar{e}_{\mathrm{r}}, x_{\mathrm{s}_1} = x_{\mathrm{s}_2}\}$, x_{r} is equal to 0.

For the detection at the relay we use a MAP detector that jointly detects x_{s_1} and x_{s_2} by taking into account the correlation between the sources according to

$$\begin{aligned} [\hat{x}_{\mathrm{s}_1\mathrm{r}}, \hat{x}_{\mathrm{s}_2\mathrm{r}}] &= \underset{[x'_{\mathrm{s}_1}, x'_{\mathrm{s}_2}]}{\operatorname{argmax}}\; p(x'_{\mathrm{s}_1}, x'_{\mathrm{s}_2} | y_{\mathrm{s}_1\mathrm{r}}, y_{\mathrm{s}_2\mathrm{r}}) \\ &= \underset{[x'_{\mathrm{s}_1}, x'_{\mathrm{s}_2}]}{\operatorname{argmax}}\; p(y_{\mathrm{s}_1\mathrm{r}} | x'_{\mathrm{s}_1}) p(y_{\mathrm{s}_2\mathrm{r}} | x'_{\mathrm{s}_2}) p(x'_{\mathrm{s}_1}, x'_{\mathrm{s}_2}) \end{aligned} \tag{5.8}$$

Alternatively, we can write the MAP detector using L-values (log-likelihood ratios) as

$$[\hat{x}_{\mathrm{s}_1\mathrm{r}}, \hat{x}_{\mathrm{s}_2\mathrm{r}}] = \underset{[x'_{\mathrm{s}_1}, x'_{\mathrm{s}_2}]}{\operatorname{argmax}}\; \bar{x}'_{\mathrm{s}_1} L_{\mathrm{s}_1\mathrm{r}} + \bar{x}'_{\mathrm{s}_2} L_{\mathrm{s}_2\mathrm{r}} + \ln p(x'_{\mathrm{s}_1}, x'_{\mathrm{s}_2}) \tag{5.9}$$

where $\bar{x} = x \oplus 1$ and the L-values are defined as

$$L_{\mathrm{s}_1\mathrm{r}} = \ln \frac{p(y_{\mathrm{s}_1\mathrm{r}} | x_{\mathrm{s}_1\mathrm{r}} = 0)}{p(y_{\mathrm{s}_1\mathrm{r}} | x_{\mathrm{s}_1\mathrm{r}} = 1)} = 4\gamma_{\mathrm{s}_1\mathrm{r}} y_{\mathrm{s}_1\mathrm{r}}, \quad L_{\mathrm{s}_2\mathrm{r}} = 4\gamma_{\mathrm{s}_2\mathrm{r}} y_{\mathrm{s}_2\mathrm{r}}. \tag{5.10}$$

The relay error probabilities in (5.7) can be developed as

$$\begin{aligned} p(\bar{e}_{\mathrm{r}}, x_{\mathrm{s}_1} = x_{\mathrm{s}_2}) &= p(\bar{e}_{\mathrm{r}_1}, \bar{e}_{\mathrm{r}_2}, x_{\mathrm{s}_1} = x_{\mathrm{s}_2}) + p(e_{\mathrm{r}_1}, e_{\mathrm{r}_2}, x_{\mathrm{s}_1} = x_{\mathrm{s}_2}) \\ p(\bar{e}_{\mathrm{r}}, x_{\mathrm{s}_1} \neq x_{\mathrm{s}_2}) &= p(\bar{e}_{\mathrm{r}_1}, \bar{e}_{\mathrm{r}_2}, x_{\mathrm{s}_1} \neq x_{\mathrm{s}_2}) + p(e_{\mathrm{r}_1}, e_{\mathrm{r}_2}, x_{\mathrm{s}_1} \neq x_{\mathrm{s}_2}) \\ p(e_{\mathrm{r}}, x_{\mathrm{s}_1} = x_{\mathrm{s}_2}) &= p(\bar{e}_{\mathrm{r}_1}, e_{\mathrm{r}_2}, x_{\mathrm{s}_1} = x_{\mathrm{s}_2}) + p(e_{\mathrm{r}_1}, \bar{e}_{\mathrm{r}_2}, x_{\mathrm{s}_1} = x_{\mathrm{s}_2}) \\ p(e_{\mathrm{r}}, x_{\mathrm{s}_1} \neq x_{\mathrm{s}_2}) &= p(\bar{e}_{\mathrm{r}_1}, e_{\mathrm{r}_2}, x_{\mathrm{s}_1} \neq x_{\mathrm{s}_2}) + p(e_{\mathrm{r}_1}, \bar{e}_{\mathrm{r}_2}, x_{\mathrm{s}_1} \neq x_{\mathrm{s}_2}) \end{aligned} \tag{5.11}$$

From (5.9), after some basic calculations, the error probabilities at the relay for the case $x_{\mathrm{s}_1} = x_{\mathrm{s}_2}$ and an AWGN channel are given by

$$\begin{aligned} p(\bar{e}_{\mathrm{r}_1}, e_{\mathrm{r}_2}, x_{\mathrm{s}_1} = x_{\mathrm{s}_2}) &\leq \frac{p_a}{2} \operatorname{erfc}\left(\frac{4\gamma_{\mathrm{s}_2\mathrm{r}} - L_a}{4\sqrt{\gamma_{\mathrm{s}_2\mathrm{r}}}}\right) \\ p(e_{\mathrm{r}_1}, \bar{e}_{\mathrm{r}_2}, x_{\mathrm{s}_1} = x_{\mathrm{s}_2}) &\leq \frac{p_a}{2} \operatorname{erfc}\left(\frac{4\gamma_{\mathrm{s}_1\mathrm{r}} - L_a}{4\sqrt{\gamma_{\mathrm{s}_1\mathrm{r}}}}\right) \\ p(e_{\mathrm{r}_1}, e_{\mathrm{r}_2}, x_{\mathrm{s}_1} = x_{\mathrm{s}_2}) &\leq \frac{p_a}{2} \operatorname{erfc}\left(\sqrt{\gamma_{\mathrm{s}_1\mathrm{r}} + \gamma_{\mathrm{s}_2\mathrm{r}}}\right) \\ p(\bar{e}_{\mathrm{r}_1}, \bar{e}_{\mathrm{r}_2}, x_{\mathrm{s}_1} = x_{\mathrm{s}_2}) &\leq p_a \end{aligned} \tag{5.12}$$

where

$$L_a = \ln \frac{p(x_{\mathrm{s}_2} \neq x_{\mathrm{s}_1})}{p(x_{\mathrm{s}_2} = x_{\mathrm{s}_1})} = \ln \frac{1 - p_a}{p_a}. \tag{5.13}$$

The bounds for the case $x_{\mathrm{s}_1} \neq x_{\mathrm{s}_2}$ are obtained by replacing p_a by $1 - p_a$ and L_a by $-L_a$ in (5.12).

Similar bounding expressions can be found for a Rayleigh fading channel. In this case, the SNRs in the expressions are random variables, and the bounds for the AWGN channel hold for a certain realization of these random variables. To obtain the average error probability for the fading channel, it is necessary to take the expection with respect to the joint distribution of the SNRs [Pro00].

5.2.1 Virtual Channel-Maximum a Priori Decoder

The VC-MAP decoder detects the symbols transmitted by the sources assuming that the observation y_{rd} is the output of a virtual memoryless channel with input $x_{\mathrm{s}_{12}} = x_{\mathrm{s}_1} \oplus x_{\mathrm{s}_2}$ and SNR $\gamma'_{\mathrm{rd}} \leq \gamma_{\mathrm{rd}}$. Therefore, the VC-MAP implicitly models the relay decoding errors via a degraded SNR. Note that the degraded SNR γ'_{rd} can be tuned to optimize the VC-MAP performance.

Based on this model, the VC-MAP detector reads

$$\begin{aligned} [\hat{x}_{s_1}, \hat{x}_{s_2}] &= \underset{[x'_{\mathrm{s}_1}, x'_{\mathrm{s}_2}]}{\operatorname{argmax}}\; p(x'_{\mathrm{s}_1}, x'_{\mathrm{s}_2}, x'_{\mathrm{s}_{12}} | y_{\mathrm{s}_1\mathrm{d}}, y_{\mathrm{s}_2\mathrm{d}}, y_{\mathrm{rd}}) \\ &= \underset{[x'_{\mathrm{s}_1}, x'_{\mathrm{s}_2}]}{\operatorname{argmax}}\; p(y_{\mathrm{s}_1\mathrm{d}}, y_{\mathrm{s}_2\mathrm{d}}, y_{\mathrm{rd}} | x'_{\mathrm{s}_1}, x'_{\mathrm{s}_2}, x'_{\mathrm{s}_{12}})\, p(x'_{\mathrm{s}_1}, x'_{\mathrm{s}_2}) \\ &= \underset{[x'_{\mathrm{s}_1}, x'_{\mathrm{s}_2}]}{\operatorname{argmax}}\; \bar{x}'_{\mathrm{s}_1} L_{\mathrm{s}_1} + \bar{x}'_{\mathrm{s}_2} L_{\mathrm{s}_2} + \bar{x}'_{\mathrm{s}_{12}} L_{\mathrm{r}} + \ln p(x'_{\mathrm{s}_1}, x'_{\mathrm{s}_2}) \end{aligned} \tag{5.14}$$

where $x'_{\mathrm{s}_{12}} = x'_{\mathrm{s}_1} \oplus x'_{\mathrm{s}_2}$, $L_{\mathrm{s}_i} = 4\gamma_{\mathrm{s}_i\mathrm{d}} y_{\mathrm{s}_i\mathrm{d}}$ and $L_{\mathrm{r}} = 4\gamma'_{\mathrm{rd}} y_{\mathrm{rd}}$. In the second equality we used the fact that $p(x_{\mathrm{s}_1}, x_{\mathrm{s}_2}, x_{\mathrm{s}_{12}}) = p(x_{\mathrm{s}_1}, x_{\mathrm{s}_2})$, since $x_{\mathrm{s}_{12}} = x_{\mathrm{s}_1} \oplus x_{\mathrm{s}_2}$. Given $\tilde{x}_{\mathrm{s}_i} = \pm 1$, L_{s_i} has mean $\pm 4\gamma_{\mathrm{s}_i\mathrm{d}}$ and variance $8\gamma_{\mathrm{s}_i\mathrm{d}}$; given $\tilde{x}_r = \pm 1$, L_{r} has mean $\pm 4\gamma'_{\mathrm{rd}}$ and variance $8\gamma'^2_{\mathrm{rd}}/\gamma_{\mathrm{rd}}$.

We next bound the four conditional error probabilities in (5.7).

Case 1 ($\bar{e}_{\mathrm{r}}$, $x_{\mathrm{s}_1}{=}x_{\mathrm{s}_2}$): This case is equivalent to the transmission of x_{s_1}, x_{s_2} and $x_{\mathrm{r}} = x_{\mathrm{s}_1} \oplus x_{\mathrm{s}_2}$ over three independent parallel channels with SNR $\gamma_{\mathrm{s}_1\mathrm{d}}$, $\gamma_{\mathrm{s}_2\mathrm{d}}$, and γ'_{rd}, respectively. Thus, the probability of error can be upper-bounded as (we define $\mathbf{x}'_s = [x'_{\mathrm{s}_1}, x'_{\mathrm{s}_2}]$)

$$\begin{aligned} p(e|\bar{e}_{\mathrm{r}}, x_{\mathrm{s}_1}{=}x_{\mathrm{s}_2}) &= p(e|x_{\mathrm{s}_1}=0, x_{\mathrm{s}_2}=0, x_{\mathrm{r}}=0) \\ &\leq \sum_{\mathbf{x}'_s \neq [0,0]} p\left(\bar{x}'_{\mathrm{s}_1} L_{\mathrm{s}_1} + \bar{x}'_{\mathrm{s}_2} L_{\mathrm{s}_2} + \bar{x}_{\mathrm{s}_{12}} L_{\mathrm{r}} < \ln \frac{p(\mathbf{x}'_s)}{p(0,0)}\right) \\ &= \frac{1}{2}\operatorname{erfc}\left(\frac{4(\gamma_{\mathrm{s}_2\mathrm{d}} + \gamma'_{\mathrm{rd}}) - L_a}{4\sqrt{\gamma_{\mathrm{s}_2\mathrm{d}} + \gamma'^2_{\mathrm{rd}}/\gamma_{\mathrm{rd}}}}\right) \\ &\quad + \frac{1}{2}\operatorname{erfc}\left(\frac{4(\gamma_{\mathrm{s}_1\mathrm{d}} + \gamma'_{\mathrm{rd}}) - L_a}{4\sqrt{\gamma_{\mathrm{s}_1\mathrm{d}} + \gamma'^2_{\mathrm{rd}}/\gamma_{\mathrm{rd}}}}\right) \\ &\quad + \frac{1}{2}\operatorname{erfc}\left(\sqrt{\gamma_{\mathrm{s}_1\mathrm{d}} + \gamma_{\mathrm{s}_2\mathrm{d}}}\right) \end{aligned} \tag{5.15}$$

The last expression is obtained by observing that $L_{\mathrm{s}_1}, L_{\mathrm{s}_2}$ and L_{r} have positive mean. Therefore, the random variable $\bar{x}'_{\mathrm{s}_1} L_{\mathrm{s}_1} + \bar{x}'_{\mathrm{s}_2} L_{\mathrm{s}_2} + \bar{x}_{\mathrm{s}_{12}} L_{\mathrm{r}}$ is Gaussian with mean $4(\bar{x}'_{\mathrm{s}_1}\gamma_{\mathrm{s}_1\mathrm{d}} + \bar{x}'_{\mathrm{s}_2}\gamma_{\mathrm{s}_2\mathrm{d}} + \bar{x}_{\mathrm{s}_{12}}\gamma'_{\mathrm{rd}})$ and variance $8(\bar{x}'_{\mathrm{s}_1}\gamma_{\mathrm{s}_1\mathrm{d}} + \bar{x}'_{\mathrm{s}_2}\gamma_{\mathrm{s}_2\mathrm{d}} + \bar{x}_{\mathrm{s}_{12}}\gamma'^2_{\mathrm{rd}}/\gamma_{\mathrm{rd}})$.

Case 2 ($\bar{e}_{\mathrm{r}}$, $x_{\mathrm{s}_1} \neq x_{\mathrm{s}_2}$): A bound for the probability $p(e|\bar{e}_{\mathrm{r}}, x_{\mathrm{s}_1} \neq x_{\mathrm{s}_2})$ is obtained by replacing L_a by $-L_a$ in (5.15).

Case 3 (e_{r}, $x_{\mathrm{s}_1}{=}x_{\mathrm{s}_2}$): In this case, the relay decodes one of the sources with error, i.e., $x_{\mathrm{r}} \neq x_{\mathrm{s}_1} \oplus x_{\mathrm{s}_2}$. The probability $p(e|e_{\mathrm{r}}, x_{\mathrm{s}_1}{=}x_{\mathrm{s}_2})$ can be upper-bounded as

$$\begin{aligned} p(e|e_{\mathrm{r}}, x_{\mathrm{s}_1}{=}x_{\mathrm{s}_2}) &= p(e|x_{\mathrm{s}_1}=0, x_{\mathrm{s}_2}=0, x_{\mathrm{r}}=1) \\ &\leq \frac{1}{2}\operatorname{erfc}\left(\frac{4(\gamma_{\mathrm{s}_2\mathrm{d}} - \gamma'_{\mathrm{rd}}) - L_a}{4\sqrt{\gamma_{\mathrm{s}_2\mathrm{d}} + \gamma'^2_{\mathrm{rd}}/\gamma_{\mathrm{rd}}}}\right) \\ &\quad + \frac{1}{2}\operatorname{erfc}\left(\frac{4(\gamma_{\mathrm{s}_1\mathrm{d}} - \gamma'_{\mathrm{rd}}) - L_a}{4\sqrt{\gamma_{\mathrm{s}_1\mathrm{d}} + \gamma'^2_{\mathrm{rd}}/\gamma_{\mathrm{rd}}}}\right) \\ &\quad + \frac{1}{2}\operatorname{erfc}\left(\sqrt{\gamma_{\mathrm{s}_1\mathrm{d}} + \gamma_{\mathrm{s}_2\mathrm{d}}}\right) \end{aligned} \tag{5.16}$$

The last expression is obtained by observing that L_{s_1} and L_{s_2} have positive mean while L_{r} has negative mean due to the error event at the relay. Therefore, $\bar{x}'_{\mathrm{s}_1} L_{\mathrm{s}_1} + \bar{x}'_{\mathrm{s}_2} L_{\mathrm{s}_2} + \bar{x}_{\mathrm{s}_{12}} L_{\mathrm{r}}$ is Gaussian with mean $4\left(\bar{x}'_{\mathrm{s}_1}\gamma_{\mathrm{s}_1\mathrm{d}} + \bar{x}'_{\mathrm{s}_2}\gamma_{\mathrm{s}_2\mathrm{d}} - \bar{x}_{\mathrm{s}_{12}}\gamma'_{\mathrm{rd}}\right)$ and variance $8(\bar{x}'_{\mathrm{s}_1}\gamma_{\mathrm{s}_1\mathrm{d}} + \bar{x}'_{\mathrm{s}_2}\gamma_{\mathrm{s}_2\mathrm{d}} + \bar{x}_{\mathrm{s}_{12}}\gamma'^2_{\mathrm{rd}}/\gamma_{\mathrm{rd}})$.

Case 4 (e_{r}, $x_{\mathrm{s}_1} \neq x_{\mathrm{s}_2}$): A bound for the probability $p(e|e_{\mathrm{r}}, x_{\mathrm{s}_1} \neq x_{\mathrm{s}_2})$ is obtained by replacing L_a (5.16) with $-L_a$.

Optimization of γ'_{rd}: As we have seen, modeling the source-relay-destination channel as Gaussian is optimal if the s-r channel is error-free. In general, however, γ'_{rd} should also be a function of γ_{sd}, and not only of γ_{sr} and γ_{rd}. Moreover, due to decoding at the relay, the noise on the virtual channel is not additive, not Gaussian, and not memoryless. Therefore the decoder is suboptimal, and the performance strongly depends on the value chosen for γ'_{rd}. Here, we propose to optimize γ'_{rd} as a function of the triplet $(\gamma_{\mathrm{sd}}, \gamma_{\mathrm{sr}}, \gamma_{\mathrm{rd}})$.

The virtual source-relay-destination channel is then only an approximation since it subsumes the channel quality on the source-to-relay and relay-to-destination links and the detection errors at the relay into an equivalent Gaussian model characterized by the degraded SNR γ'_{rd}. The SNR γ'_{rd} can be tuned such that the virtual channel approximation best matches the actual two-hop channel involving the source-to-relay and relay-to-destination links. Notice that in the decoding rule, the value of γ'_{rd} is used to trade-off the reliability of the source-to-destination channel to the reliability of the virtual source-relay-destination channel, depending on γ_{sd}, γ_{sr} and γ_{rd}, respectively. In particular, we use the lower bound on the probability of error derived above to perform this optimization. For each triplet $(\gamma_{\mathrm{sd}}, \gamma_{\mathrm{sr}}, \gamma_{\mathrm{rd}})$, we determine numerically the value of γ'_{rd} which minimizes the lower bound on the probability of error. We denote this optimum value by γ_{opt}. Such an optimization of the SNR of the equivalent channel has been proposed in [iAL10]. We will show via simulations in Section 5.4 that this optimization is feasible also for the case of correlated sources and that it allows the VC-MAP detector to closely approach the performance of the MAP detector. The optimal γ'_{rd} can be calculated off-line before deployment.

5.2.2 Maximum a Priori Decoder

In this section, we consider the MAP decoding rule, which is optimal for the scenario in Figure 5.1 and is given by

$$\begin{aligned}[\hat{x}_{s_1}, \hat{x}_{s_2}] &= \underset{[x'_{\mathrm{s}_1}, x'_{\mathrm{s}_2}]}{\operatorname{argmax}} p(x'_{\mathrm{s}_1}, x'_{\mathrm{s}_2} | y_{\mathrm{s}_1\mathrm{d}}, y_{\mathrm{s}_2\mathrm{d}}, y_{\mathrm{rd}}) \\ &= \sum_{x_{\mathrm{r}} \in \{0,1\}} p(x'_{\mathrm{s}_1}, x'_{\mathrm{s}_2}, x_{\mathrm{r}} | y_{\mathrm{s}_1\mathrm{d}}, y_{\mathrm{s}_2\mathrm{d}}, y_{\mathrm{rd}})\end{aligned} \tag{5.17}$$

Since the evaluation of (5.17) requires a marginalization with respect to x_{r}, we resort to a simplified approach that jointly estimates source and relay symbols. The corresponding

(joint) MAP decoding rule reads

$$\begin{aligned}[\hat{x}_{\mathrm{s}_1}, \hat{x}_{\mathrm{s}_2}, \hat{x}_{\mathrm{r}}] &= \underset{[x'_{\mathrm{s}_1}, x'_{\mathrm{s}_2}, x'_{\mathrm{r}}]}{\operatorname{argmax}} \; p(x'_{\mathrm{s}_1}, x'_{\mathrm{s}_2}, x'_{\mathrm{r}} | y_{\mathrm{s}_1\mathrm{d}}, y_{\mathrm{s}_2\mathrm{d}}, y_{\mathrm{rd}}) \\ &= \underset{[x'_{\mathrm{s}_1}, x'_{\mathrm{s}_2}, x'_{\mathrm{r}}]}{\operatorname{argmax}} \; p(y_{\mathrm{s}_1\mathrm{d}}, y_{\mathrm{s}_2\mathrm{d}}, y_{\mathrm{rd}} | x'_{\mathrm{s}_1}, x'_{\mathrm{s}_2}, x'_{\mathrm{r}})\, p(x'_{\mathrm{s}_1}, x'_{\mathrm{s}_2}, x'_{\mathrm{r}}) \\ &= \underset{[x'_{\mathrm{s}_1}, x'_{\mathrm{s}_2}, x'_{\mathrm{r}}]}{\operatorname{argmax}} \; \bar{x}'_{\mathrm{s}_1} L_{\mathrm{s}_1} + \bar{x}'_{\mathrm{s}_2} L_{\mathrm{s}_2} + \bar{x}'_{\mathrm{r}} L_{\mathrm{r}} \ln p(x'_{\mathrm{r}} | x'_{\mathrm{s}_1}, x'_{\mathrm{s}_2}) + \ln p(x'_{\mathrm{s}_1}, x'_{\mathrm{s}_2})\end{aligned} \tag{5.18}$$

Contrary to the VC-MAP rule, the fourth term in the last expression explicitly takes into account relay errors.

From this decision rule, bounds on the error probability of the (joint) MAP detector can again be derived based on the expansion (5.7) of the total error probability. We follow a similar procedure as with the VC-MAP decoder and as in [iALR11]. In our derivations below, we will use the following definitions:

$$\begin{aligned} L_s &= \ln \frac{p(x_{\mathrm{r}}=0|x_{\mathrm{s}_1}=x_{\mathrm{s}_2})}{p(x_{\mathrm{r}}=1|x_{\mathrm{s}_1}=x_{\mathrm{s}_2})}, \quad L_t = \ln \frac{p(x_{\mathrm{r}}=0|x_{\mathrm{s}_1}\neq x_{\mathrm{s}_2})}{p(x_{\mathrm{r}}=1|x_{\mathrm{s}_1}\neq x_{\mathrm{s}_2})}, \\ L_u &= \ln \frac{p(x_{\mathrm{r}}=0|x_{\mathrm{s}_1}=x_{\mathrm{s}_2})}{p(x_{\mathrm{r}}=0|x_{\mathrm{s}_1}\neq x_{\mathrm{s}_2})}, \quad L_v = \ln \frac{p(x_{\mathrm{r}}=1|x_{\mathrm{s}_1}=x_{\mathrm{s}_2})}{p(x_{\mathrm{r}}=1|x_{\mathrm{s}_1}\neq x_{\mathrm{s}_2})}, \\ L_w &= \ln \frac{p(x_{\mathrm{r}}=0|x_{\mathrm{s}_1}=x_{\mathrm{s}_2})}{p(x_{\mathrm{r}}=1|x_{\mathrm{s}_1}\neq x_{\mathrm{s}_2})}, \quad L_x = \ln \frac{p(x_{\mathrm{r}}=0|x_{\mathrm{s}_1}\neq x_{\mathrm{s}_2})}{p(x_{\mathrm{r}}=1|x_{\mathrm{s}_1}=x_{\mathrm{s}_2})} \end{aligned}$$

Case 1 ($\bar{e}_{\mathrm{r}}$, $x_{\mathrm{s}_1}=x_{\mathrm{s}_2}$): In this case, the probability of error can be upper-bounded as

$$\begin{aligned} p(e|\bar{e}_{\mathrm{r}}, x_{\mathrm{s}_1}=x_{\mathrm{s}_2}) \leq\; & \frac{1}{2}\operatorname{erfc}\left(\frac{4\gamma_{\mathrm{s}_1\mathrm{d}}+L_u-L_a}{4\sqrt{\gamma_{\mathrm{s}_1\mathrm{d}}}}\right) + \operatorname{erfc}\left(\frac{4\gamma_{\mathrm{s}_2\mathrm{d}}+L_u-L_a}{4\sqrt{\gamma_{\mathrm{s}_2\mathrm{d}}}}\right) \\ & + \frac{1}{2}\operatorname{erfc}\left(\frac{4(\gamma_{\mathrm{s}_1\mathrm{d}}+\gamma_{\mathrm{rd}})+L_w-L_a}{4\sqrt{\gamma_{\mathrm{s}_1\mathrm{d}}+\gamma_{\mathrm{rd}}}}\right) \\ & + \frac{1}{2}\operatorname{erfc}\left(\frac{4(\gamma_{\mathrm{s}_2\mathrm{d}}+\gamma_{\mathrm{rd}})+L_w-L_a}{4\sqrt{\gamma_{\mathrm{s}_2\mathrm{d}}+\gamma_{\mathrm{rd}}}}\right) \\ & + \frac{1}{2}\operatorname{erfc}\left(\sqrt{\gamma_{\mathrm{s}_1\mathrm{d}}+\gamma_{\mathrm{s}_2\mathrm{d}}}\right) \\ & + \frac{1}{2}\operatorname{erfc}\left(\frac{4(\gamma_{\mathrm{s}_1\mathrm{d}}+\gamma_{\mathrm{s}_2\mathrm{d}}+\gamma_{\mathrm{rd}})+L_s}{4\sqrt{\gamma_{\mathrm{s}_1\mathrm{d}}+\gamma_{\mathrm{s}_2\mathrm{d}}+\gamma_{\mathrm{rd}}}}\right) \end{aligned} \tag{5.19}$$

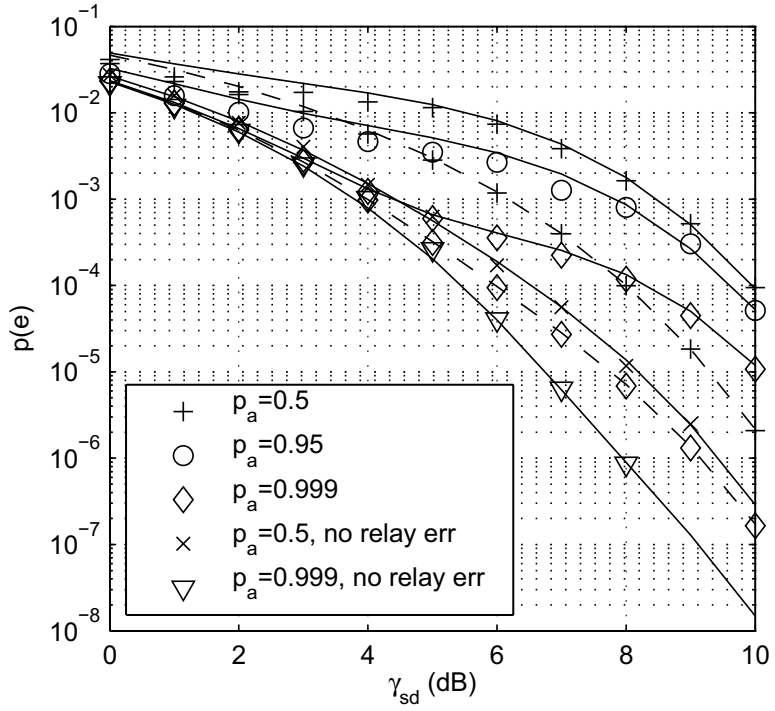

FIGURE 5.2: Error probability bounds (lines) and simulations (markers) of a relay system with two correlated sources for a VC-MAP decoder with AWGN channels for the cases $\gamma'_{\mathrm{rd}} = \gamma_{\mathrm{rd}}$ (solid lines) and $\gamma'_{\mathrm{rd}} = \gamma_{\mathrm{opt}}$ (dashed lines); here, $\gamma_{\mathrm{sr}} = \gamma_{\mathrm{rd}} = 5\,\mathrm{dB}$.

Case 2 ($\bar{e}_{\mathrm{r}}$, $x_{\mathrm{s}_1} \neq x_{\mathrm{s}_2}$): The bound here is obtained by replacing L_u, L_w, L_s, and $-L_a$ in (5.19) with $-L_w$, $-L_v$, $-L_t$, and L_a, respectively.

Case 3 (e_{r}, $x_{\mathrm{s}_1} = x_{\mathrm{s}_2}$): We have

$$\begin{aligned} p(e|e_{\mathrm{r}}, x_{\mathrm{s}_1} = x_{\mathrm{s}_2}) \leq{}& \frac{1}{2}\,\mathrm{erfc}\left(\frac{4\gamma_{\mathrm{s}_1\mathrm{d}}+L_v-L_a}{4\sqrt{\gamma_{\mathrm{s}_1\mathrm{d}}}}\right) + \mathrm{erfc}\left(\frac{4\gamma_{\mathrm{s}_2\mathrm{d}}+L_v-L_a}{4\sqrt{\gamma_{\mathrm{s}_2\mathrm{d}}}}\right) \\ &+ \frac{1}{2}\,\mathrm{erfc}\left(\frac{4(\gamma_{\mathrm{s}_1\mathrm{d}}+\gamma_{\mathrm{rd}}) - L_x - L_a}{4\sqrt{\gamma_{\mathrm{s}_1\mathrm{d}}+\gamma_{\mathrm{rd}}}}\right) \\ &+ \frac{1}{2}\,\mathrm{erfc}\left(\frac{4(\gamma_{\mathrm{s}_2\mathrm{d}}+\gamma_{\mathrm{rd}}) - L_x - L_a}{4\sqrt{\gamma_{\mathrm{s}_2\mathrm{d}}+\gamma_{\mathrm{rd}}}}\right) \\ &+ \frac{1}{2}\,\mathrm{erfc}\left(\sqrt{\gamma_{\mathrm{s}_1\mathrm{d}}+\gamma_{\mathrm{s}_2\mathrm{d}}}\right) \\ &+ \frac{1}{2}\,\mathrm{erfc}\left(\frac{4(\gamma_{\mathrm{s}_1\mathrm{d}}+\gamma_{\mathrm{s}_2\mathrm{d}}+\gamma_{\mathrm{rd}}) - L_s}{4\sqrt{\gamma_{\mathrm{s}_1\mathrm{d}}+\gamma_{\mathrm{s}_2\mathrm{d}}+\gamma_{\mathrm{rd}}}}\right) \end{aligned} \tag{5.20}$$

Case 4 (e_{r}, $x_{\mathrm{s}_1} \neq x_{\mathrm{s}_2}$): The error bound here is obtained by replacing L_v, L_x, $-L_s$, and $-L_a$ in (5.20) with $-L_u$, L_v, L_t, and L_a, respectively.

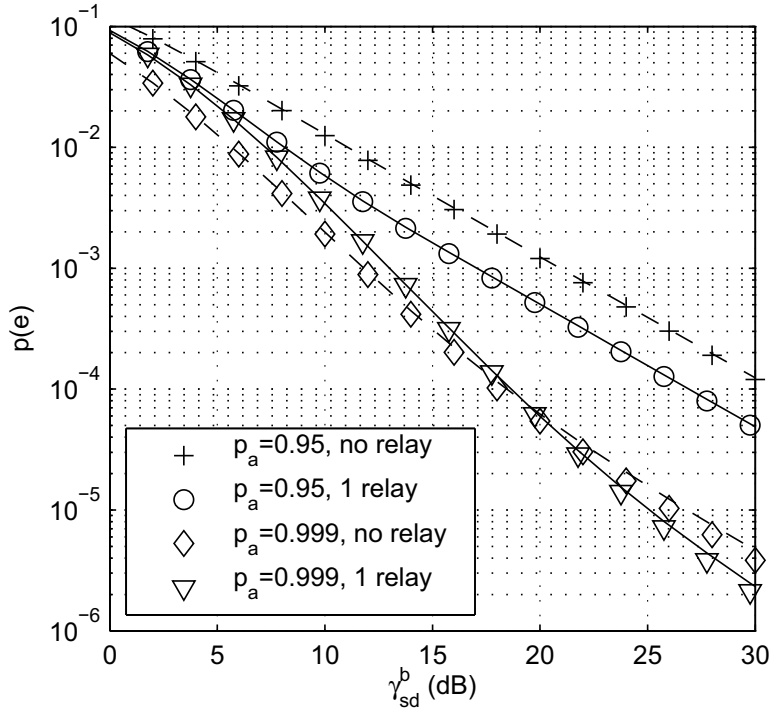

FIGURE 5.3: Error probability bounds (lines) and simulations (markers) of a relay system with two correlated sources for a VC-MAP decoder in Rayleigh fading for two cases: non-cooperative system (dashed lines) and single relay cooperative system (solid lines); here, $\gamma_{\mathrm{sr}} = \gamma_{\mathrm{rd}} = 15\,\mathrm{dB}$.

5.3 Error Bounds for Rayleigh Channels for the Single-Relay Case

We discussed the error probabilities for BPSK modulation of two correlated sources over an AWGN channel. These error probabilities can be easily modified to hold for the case of Rayleigh channel. We recall that for the AWGN channel, the probability of error of each case (1 to 4) is given for certain energy to noise ratio (γ) corresponding to the participating links. However in the presence of a channel gain h, the effective bit energy to noise ratio is

$$\bar{\gamma} = |h|^2 \gamma \tag{5.21}$$

So, for each case, the error probability for a given value of h is

$$p_{|h}(e) = p_{\bar{\gamma}}^{\mathrm{AWGN}}(e) \tag{5.22}$$

To find the error probability over all random values of $|h|^2$, we must evaluate the conditional probability density function $p_{|h}(e)$ over the probability density function of

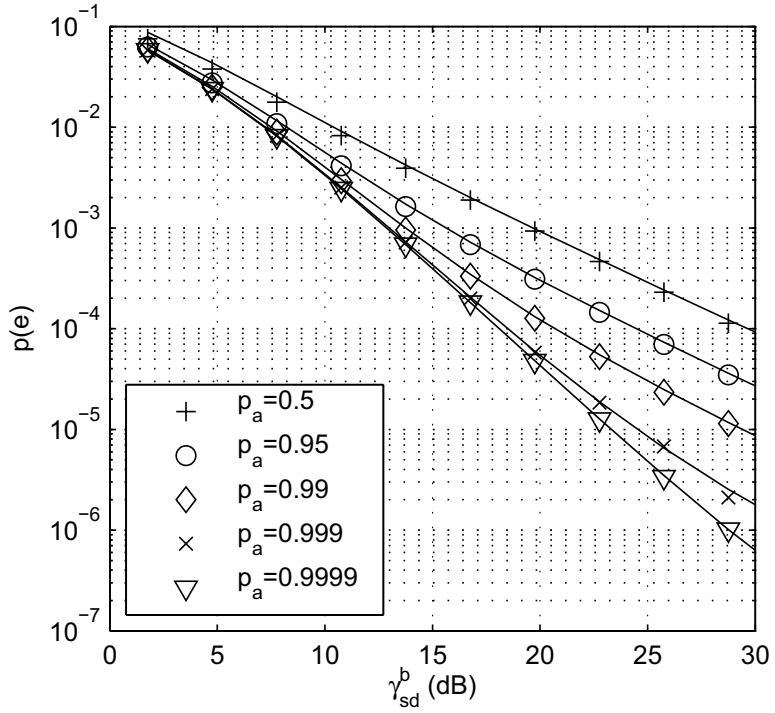

FIGURE 5.4: Error probability bounds (lines) and simulations (markers) of a relay system with two correlated sources for a MAP decoder in Rayleigh fading for different correlation factors p_a; here, $\gamma_{\mathrm{sr}} = \gamma_{\mathrm{rd}} = 15\,\mathrm{dB}$.

$\bar{\gamma}$, given by

$$p_{\bar{\gamma}}(x) = \frac{1}{\gamma} e^{-\frac{x}{\gamma}}, \quad x \geq 0 \tag{5.23}$$

Consequently, the error probability of each case is the integral of the conditional probability density function over the pdf of the participating links effective bit energy to noise ratios.

5.4 Numerical Results

In this section, we illustrate the tightness of the error probability bounds by comparing them to simulation results. We also compare the performance of the VC-MAP decoder and the MAP decoder. For simplicity, we assume that the SNRs are symmetric, i.e., $\gamma_{\mathrm{s_1d}} = \gamma_{\mathrm{s_2d}} = \gamma_{\mathrm{sd}}$ and $\gamma_{\mathrm{s_1r}} = \gamma_{\mathrm{s_2r}} = \gamma_{\mathrm{sr}}$. We also consider fixed γ_{sr} and γ_{rd}.

In Figure 5.2, we plot the bounds on the error probability for the VC-MAP decoder for $\gamma'_{\mathrm{rd}} = \gamma_{\mathrm{rd}}$ (solid lines) and for $\gamma'_{\mathrm{rd}} = \gamma_{\mathrm{opt}}$ (dashed lines) together with the simulation results (markers), as a function of γ_{sd} (in dB), for several degrees of correlation between the two sources, $\gamma_{\mathrm{sr}} = \gamma_{\mathrm{rd}} = 5$ dB, and AWGN channels. A good match between the simulations and the bounds is observed. We note that $\gamma'_{\mathrm{rd}} = \gamma_{\mathrm{rd}}$ yields a significant deviation from the case where the source-to-relay channels are error-free. However, for

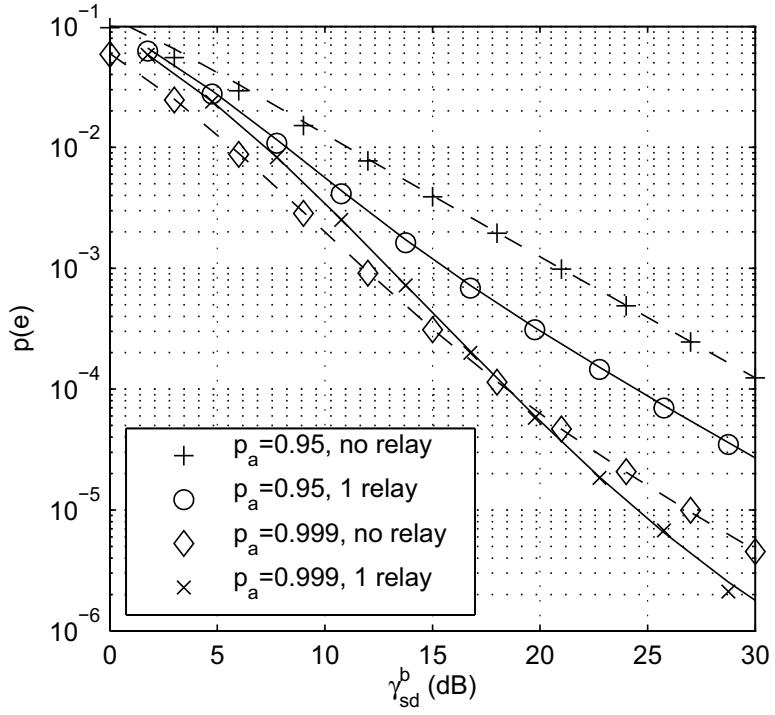

FIGURE 5.5: Error probability bounds (lines) and simulations (markers) of a relay system with two correlated sources for a MAP decoder in Rayleigh fading for two cases: non-cooperative system (dashed lines) and single relay cooperative system (solid lines); here, $\gamma_{\mathrm{sr}} = \gamma_{\mathrm{rd}} = 15\,\mathrm{dB}$.

optimized γ'_{rd} ($\gamma'_{\mathrm{rd}} = \gamma_{\mathrm{opt}}$), the bounds are much closer to the case of error-free source-to-relay channels.

Figure 5.3 shows the bounds on the error probability (lines), together with the corresponding simulation results (markers) as a function of γ_{sd}^b, where $\gamma_{\mathrm{sd}}^b = \gamma_{\mathrm{sd}}/R$, for the VC-MAP decoder over a Rayleigh channel for both a non-cooperative system and a single relay cooperative system. The system rate equals $R = 1$ and $R = 2/3$, respectively, for the case of no relay (dashed lines) and one relay (solid lines). In the figure, $\gamma'_{\mathrm{rd}} = \gamma_{\mathrm{opt}}$ and $\gamma_{\mathrm{sr}} = \gamma_{\mathrm{rd}} = 15\,\mathrm{dB}$. While performance is generally better for more strongly correlated sources, the relay is less useful in this situation.

Figure 5.4 shows the bounds on the error probability (solid lines) of the (joint) MAP detector, as well as the corresponding simulation results (markers) as a function of γ_{sd}^b for Rayleigh fading. Sizable gains with increasing level of correlation (increasing p_a) are observed over the uncorrelated case ($p_a = 0.5$). The latter case corresponds to the scenario where there is no source correlation or where a demodulator oblivious of existing correlation is used. For example, the gain for $p_a = 0.95$ is over 5 dB at an error probability of 10^{-4}.

Figure 5.5 shows the performance improvement that is achieved by the use of relaying and (joint) MAP detection over a scenario without cooperation (again for Rayleigh

fading). With $p_a = 0.95$, we observe a gain of about 6 dB at a $p(e)$ of 10^{-4}. However, the gain vanishes for very high correlation ($p_a = 0.999$). Finally, comparing Figure 5.3 with Figure 5.5, we observe that the (lower complexity) VC-MAP detector with optimized γ'_{rd} approaches the performance of the (optimal) MAP detector very closely.

5.5 Chapter Summary

In this chapter, we analyzed the performance of multiple access schemes where two correlated sources communicate to unique destination, in the absence and in the presence of cooperation (when one relay is used to assist sources transmission). Using an information-theoretic approach, we first derived analytical bounds on the error probability of a decode-and-forward relaying system consisting of two correlated sources, one relay, and one destination. We showed that by taking into account the source correlation via joint channel detection at the relay and at the destination, noticeable performance gains can be achieved. For a Rayleigh fading channel example, exploiting a very high level of correlation ($p_a = 0.95$) leads to a gain of more than 5 dB at an error probability of 10^{-4}. This is given for a symmetric uplink channels and sufficiently good source-to-relay and relay-to-destination links ($\gamma_{\mathrm{sr}} = \gamma_{\mathrm{rd}} = 15$ dB). We also showed that the use of a relay results in a performance improvement over a system without relay, specifically at medium correlation levels (p_a up to 0.95).

Chapter 6

Conclusions

Future wireless systems are expected to extensively rely on cooperation between terminals. In this thesis, we studied practical implementations of cooperative transmission over two different networks: the wireless cellular network and the wireless sensor network.

The main contribution of the thesis concerns cooperative retransmission protocols over a two-source cooperative system based on a turbo coded cooperation scheme, which implement cooperative ideas in practice for the wireless cellular network. We developed three different extensions of the turbo coded cooperation scheme: three cooperative HARQ protocols differing on where decision of retransmission is performed. The main motivation of combining HARQ protocols with the turbo coded cooperation scheme is to benefit not only from cooperative/retransmission diversity, but also from coding and turbo processing gain. This stems from the capacity-approaching nature of turbo coding, since it ensures a very efficient process of channel decoding.

In view of throughput preservation, a first HARQ protocol, DL-HARQ, was proposed to avoid unnecessary transmission through controlling the cooperation phase, a mandatory phase of the original turbo coded cooperation scheme. A second HARQ protocol, RL-HARQ, was then designed to improve inter-source channel quality, thus increasing the distributed diversity of the system. However, RL-HARQ brings a significant degradation in throughput. Finally, a third protocol, TL-HARQ, combining the benefits of DL-HARQ (higher throughput) and RL-HARQ (higher reliability) was proposed. The TL-HARQ protocol is an adaptive scheme, controlling retransmissions from different locations (partner side and destination side), in order to make the turbo coded cooperation framework more flexible. The simulation results showed that the TL-HARQ protocol achieved the best performance both in terms of error rate and throughput efficiency. Significant improvements were observed for the TL-HARQ protocol with respect to the non-ARQ scheme and the DL-HARQ and RL-HARQ protocols. Moreover, sizable gains

in terms of throughput efficiency were noted when we assumed non-orthogonal channels during cooperation phase and half-duplex mode operation. Using the IDMA technique, for superposed signal separation, we achieved asymptotically up to 20 % of throughput efficiency gain for DL-HARQ and TL-HARQ protocols.

However, not only designing an appropriate cooperation system can optimize the performance of cooperative networks. Actually, adjusting the cooperation partner, the employed channel code, or the cooperation level may be beneficial. In this line, we further analyzed the outage behavior of the previously proposed protocols. This constitute the second main contribution of the thesis. Making use of their corresponding outage probabilities, it was shown that all the protocols have the same diversity order. Therefore, to better distinguish between them, we performed a diversity-multiplexing tradeoff analysis. The key point resulting from this analysis is that DL-HARQ and TL-HARQ offer the best performance.

Thereafter, we presented the strategy we opted for to optimize the performance in terms of frame error probability and throughput efficiency according to terminal locations. We defined the retransmission gain and the cooperation gain of the DL-HARQ and TL-HARQ protocols to quantify their benefits over two reference systems: The turbo coded cooperation system, and the point-to-point IR-HARQ protocol, respectively. Geometric conditions, under which DL-HARQ and TL-HARQ are useful, were determined by adopting these gains as decision parameters. From the geometrical approach, the frame error probability gain can be materialized by a better system coverage compared to the reference system.

For wireless cellular networks, we studied cooperative schemes (cooperative HARQ protocols) when side information is available at the transmitting nodes, thanks to a feedback low-rate link. Likewise, different type of side information can be made available depending on the context. For instance, for wireless sensor networks, nodes transmit information that is statistically dependent. This source correlation can be exploited at the receiver as side information in order to improve performance. Thus, in the Chapter 5, we discussed two types of detectors at the destination in an uncoded decode-and-forward cooperative system with two correlated information sources and one relay. As a third contribution of the thesis, we derived analytical bounds on the error probability for the relay system according to both detectors: the optimal MAP detector taking into account errors detected at the relay and a simplified MAP detector approximating the two-hop source-to-relay-to-destination channel by a virtual single-hop memoryless channel. Numerical results showed that taking into account the source correlation, as side information at the relay and at the destination, leads to noticeable performance gains. For a Rayleigh fading channel example, exploiting a very high level of correlation

($p_a = 0.95$) leads to a gain of more than 5 dB at an error probability of 10^{-4}. This is given for a symmetric uplink channels and sufficiently good source-to-relay and relay-to-destination links ($\gamma_{\text{sr}} = \gamma_{\text{rd}} = 15$ dB). Comparison with the performance of a correlation-aware system without relay has been made, showing that the use of a relay results in a performance improvement over a system without relay, specifically at medium correlation levels.

At the end, we can highlight several interesting perspectives on how our work can be extended.

First of all, considering that all results and theoretical analysis made for the proposed HARQ protocols are based on the assumption of perfect feedback channel, it is now really important to investigate the case of erroneous feedback channel in order to take into account reality of practical implementation constraints.

Second, it is known that the achievable capacity of wireless communications increases when multiple transmitter and receiver antennas are used. Therefore, it would be interesting to study the proposed cooperative schemes when explicit space diversity is made available using multiple-antenna systems in the operating nodes. This study is insightful in order to check if MIMO techniques still bring further gains besides the distributed space diversity offered by the cooperative process.

The third perspective consists in the extension of the work performed in Chapter 5 where we considered a particular cooperation scheme for correlated sources under an uncoded case. For instance, multiple-source configuration has to be considered and performance results have to be interpreted. For the same context, we propose now to consider and to investigate a distributed joint source-channel coding techniques in order to benefit from signal correlation, compression efficiency as well as from cooperative diversity.

The last idea we can set up here is more general and will consist in applying some of our results to the Intelligent Transport Systems domain. Applications for collision avoidance, route planning, automatic tolling and traffic control, are considered crucial and require frequent information exchange between vehicles and infrastructure. Consequently, vehicle and infrastructures will be equipped soon with several communicating nodes and cooperative systems in transportation domain can bring new intelligence for vehicles, road systems, operators and individuals by creating a communication platform allowing vehicles and infrastructure to share information. The intelligent interaction between vehicle and infrastructures is then a key objective of ITS to improve traffic safety, efficiency and traveling comfort. This can be also immediately extended to public transport (buses, tramways, metros and trains). Therefore, there is an urgent need to adapt

the protocols proposed in this thesis to such kind of applications and in particular to vehicular environments. For example, as the majority of previous research work related to this issue aims in searching optimal partners under fixed conditions and a quite frozen network topology, the partner selection problem, in the context of ITS domain, has to be revised. In practice and for this particular environment, the rapidly changing inter-node channels, terminal asynchronicity, user mobility and users entering and leaving cells randomly impose more critical constraints for partner selection strategies. Therefore, the issue of partner node selection has to be examined differently by exploring novel partner selection strategies or by defining more appropriate selection criterion.

Vehicular environments and specifically mobile-to-mobile (M2M) channels are strongly dependent on the communication system topology. The characteristics of the links between the network nodes can be really different from classical Rayleigh channels. Therefore, as we have primarily highlighted the benefits of combining both retransmission protocols and coded cooperation in order to improve both the reliability and the efficiency of the system, for classical Rayleigh fading, we believe that it would also be interesting to extend our results and examine the performance of the proposed protocols considering various channels characterized with other fading distributions, such as Rician distributions varying the Rice factor to mimic different masking effects and Nakagami fading. Despite an increase in computation time, it could be also really interesting to take into account possible dynamic aspects in the vehicular channel environment considering frequency selective channels and associated Doppler spectrums.

Appendix A

Proof of the Tradeoff Curve of the Coded Cooperation Scheme

We compute $d_i(r,\alpha)$ in (4.18), for $i = 1$. To do so, we have to consider different cases, according to different rate ranges and values of α:

1. Case $\alpha \leq 1/2$: It follows $\alpha \leq 1-\alpha$

   - If $r \leq \alpha$, it follows $\alpha\,(1-\mu_{\mathrm{s_1d}})^+ + (1-\alpha)\,(1-\mu_{\mathrm{s_2d}})^+ \leq \alpha$ if $\mu_{\mathrm{s_2d}} \geq 1$ (i.e $(\mu_{\mathrm{s_2d}})_{\min} = 1$) and $\mu_{\mathrm{s_1d}} \leq 1$. Using $(\mu_{\mathrm{s_2d}})_{min}$, we have $\mu_{\mathrm{s_1d}} \geq 1 - \frac{r}{\alpha}$. Therefore, $\forall \alpha \leq 1/2, \forall r \leq \alpha$, $(\mu_{\mathrm{s_1d}} + \mu_{\mathrm{s_2d}}) \geq 2 - \frac{r}{\alpha}$ holds.
   - If $r > \alpha$, the main constraint of the outage region can be written as $1 - \alpha\mu_{\mathrm{s_1d}} - (1-\alpha)\mu_{\mathrm{s_2d}} < r$. Since $\alpha \leq 1-\alpha$, we have $1-(1-\alpha)(\mu_{\mathrm{s_1d}}+\mu_{\mathrm{s_2d}}) < r$. Therefore, $\forall \alpha \leq 1/2, \forall r > \alpha$, $(\mu_{\mathrm{s_1d}} + \mu_{\mathrm{s_2d}}) \geq \frac{1-r}{1-\alpha}$ holds.

2. Case $\alpha > 1/2$: It follows $\alpha > 1-\alpha$

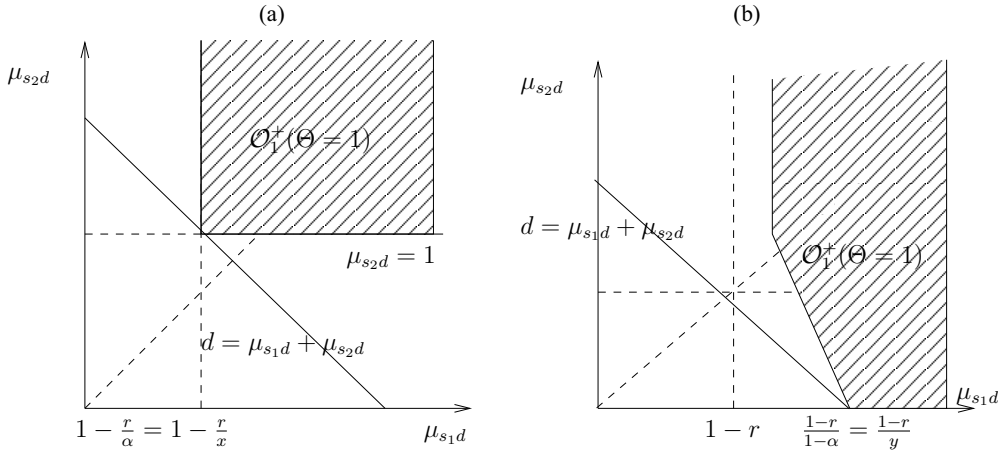

FIGURE A.1: The region $\mathcal{O}_1^+(\Theta=1)$ for (a) $\alpha \leq 1/2$ and $r \leq \alpha$, and (b) $\alpha \leq 1/2$ and $r > \alpha$.

- If $r \leq \alpha$, it follows $\alpha\left(1-\mu_{\mathrm{s_1d}}\right)^{+}+(1-\alpha)\left(1-\mu_{\mathrm{s_2d}}\right)^{+} \leq 1-\alpha$ if $\mu_{\mathrm{s_1d}} \geq 1$ (i.e., $\left(\mu_{1,d}\right)_{\min}=1$) and $\mu_{\mathrm{s_2d}} \leq 1$. Using $\left(\mu_{\mathrm{s_1d}}\right)_{min}$, we have $\mu_{\mathrm{s_2d}} \geq 1-\frac{r}{1-\alpha}$. Therefore, $\forall \alpha>1/2, \forall r \leq 1-\alpha$, $\left(\mu_{\mathrm{s_1d}}+\mu_{\mathrm{s_2d}}\right) \geq 2-\frac{r}{1-\alpha}$ holds.
- If $r>1-\alpha$, the main constraint of the outage region can be written as $1-\alpha\mu_{\mathrm{s_1d}}-(1-\alpha)\mu_{\mathrm{s_2d}}<r$. Since $\alpha>1-\alpha$, we have $1-\alpha(\mu_{\mathrm{s_1d}}+\mu_{\mathrm{s_2d}})<r$. Therefore, $\forall \alpha>1/2, \forall r>1-\alpha$, $\left(\mu_{\mathrm{s_1d}}+\mu_{\mathrm{s_2d}}\right) \geq \frac{1-r}{\alpha}$ holds.

Using Cases 1 and 2, $d_1(r,\alpha)$ can be written as

$$d_1(r,\alpha)=\begin{cases}2-\frac{r}{\min(\alpha,1-\alpha)} & r\in[0,\min(\alpha,1-\alpha)]\\ \frac{1-r}{\max(\alpha,1-\alpha)} & r\in[\min(\alpha,1-\alpha),1]\end{cases} \tag{A.1}$$

Figure A.1 illustrates the outage region for $\alpha \leq 1/2$. Similar figures are obtained for the case $\alpha>1/2$, by considering ranges $r \leq 1-\alpha$ and $r>1-\alpha$, and exchanging x and y values.

Appendix B

Proof of the Tradeoff Curve

We compute the solution of

$$d(r,\alpha) = \inf_{(\mu_{\mathrm{s_1d}},\mu_{\mathrm{s_2d}})\in\mathcal{O}_1^+} (\mu_{\mathrm{s_1d}} + \mu_{\mathrm{s_2d}}) \tag{B.1}$$

where $\mathcal{O}_1^+ \equiv \left\{(\mu_{\mathrm{s_1d}},\mu_{\mathrm{s_2d}}) \in \mathbb{R}_+^2 : \alpha(1-\mu_{\mathrm{s_1d}})^+ + k(1-\min(\mu_{\mathrm{s_1d}},\mu_{\mathrm{s_2d}}))^+ < lr\right\}$, for several values of k and l.

B.1 Computation of $d_{\mathbf{A}}(r,\alpha)$ ($d(r,\alpha)$ for $k = 1-\alpha$ and $l = \alpha$)

We distinguish between two different cases:

1. Case $\alpha \leq 1/2$: It follows $\alpha \leq 1-\alpha$

   - If $\mu_{\mathrm{s_1d}} \leq \mu_{\mathrm{s_2d}}$, $(\mu_{\mathrm{s_1d}})_{\min} = (\mu_{\mathrm{s_2d}})_{\min} = 1-\alpha r$. Therefore, $\forall \alpha \leq 1/2$ and $\mu_{\mathrm{s_1d}} \leq \mu_{\mathrm{s_2d}}$, $(\mu_{\mathrm{s_1d}} + \mu_{\mathrm{s_2d}}) \geq 2 - 2\alpha r$ holds.
   - If $\mu_{\mathrm{s_1d}} > \mu_{\mathrm{s_2d}}$, since $r \leq 1$, we have $\alpha\,(1-\mu_{\mathrm{s_1d}})^+ + (1-\alpha)\,(1-\mu_{\mathrm{s_2d}})^+ \leq \alpha$, which implies that $\mu_{\mathrm{s_2d}} \geq 1$ and $\mu_{\mathrm{s_1d}} \leq 1$. Taking into account that $\mu_{\mathrm{s_1d}} > \mu_{\mathrm{s_2d}}$, we obtain $\mu_{\mathrm{s_1d}} = \mu_{\mathrm{s_2d}}$. Therefore, $\forall \alpha \leq 1/2$ and $\mu_{\mathrm{s_1d}} > \mu_{\mathrm{s_2d}}$, $(\mu_{\mathrm{s_1d}} + \mu_{\mathrm{s_2d}}) \geq 2 - 2\alpha r$.

2. Case $\alpha > 1/2$: It follows $\alpha > 1-\alpha$

   - If $\mu_{\mathrm{s_1d}} \leq \mu_{\mathrm{s_2d}}$, $(\mu_{\mathrm{s_1d}} + \mu_{\mathrm{s_2d}}) \geq 2 - 2\alpha r$.
   - If $\mu_{\mathrm{s_1d}} > \mu_{\mathrm{s_2d}}$, we distinguish between two cases:
     - For $\alpha r \leq 1-\alpha$ (i.e., $r \leq \frac{1-\alpha}{\alpha}$), we have $\alpha\,(1-\mu_{\mathrm{s_1d}})^+ + (1-\alpha)\,(1-\mu_{\mathrm{s_2d}})^+ \leq 1-\alpha$ if $\mu_{\mathrm{s_1d}} \geq 1$ (i.e., $(\mu_{\mathrm{s_1d}})_{\min} = 1$) and $\mu_{\mathrm{s_2d}} \leq 1$. Using $(\mu_{\mathrm{s_1d}})_{\min}$, we have $\mu_{\mathrm{s_2d}} \geq 1 - \frac{\alpha r}{1-\alpha}$. Finally, we obtain $(\mu_{\mathrm{s_1d}} + \mu_{\mathrm{s_2d}}) \geq 2 - \frac{\alpha r}{1-\alpha}$.
     - For $r > \frac{1-\alpha}{\alpha}$, we use the fact that $\alpha > 1-\alpha$ to get $(\mu_{\mathrm{s_1d}} + \mu_{\mathrm{s_2d}}) \geq \frac{1-\alpha r}{\alpha}$.

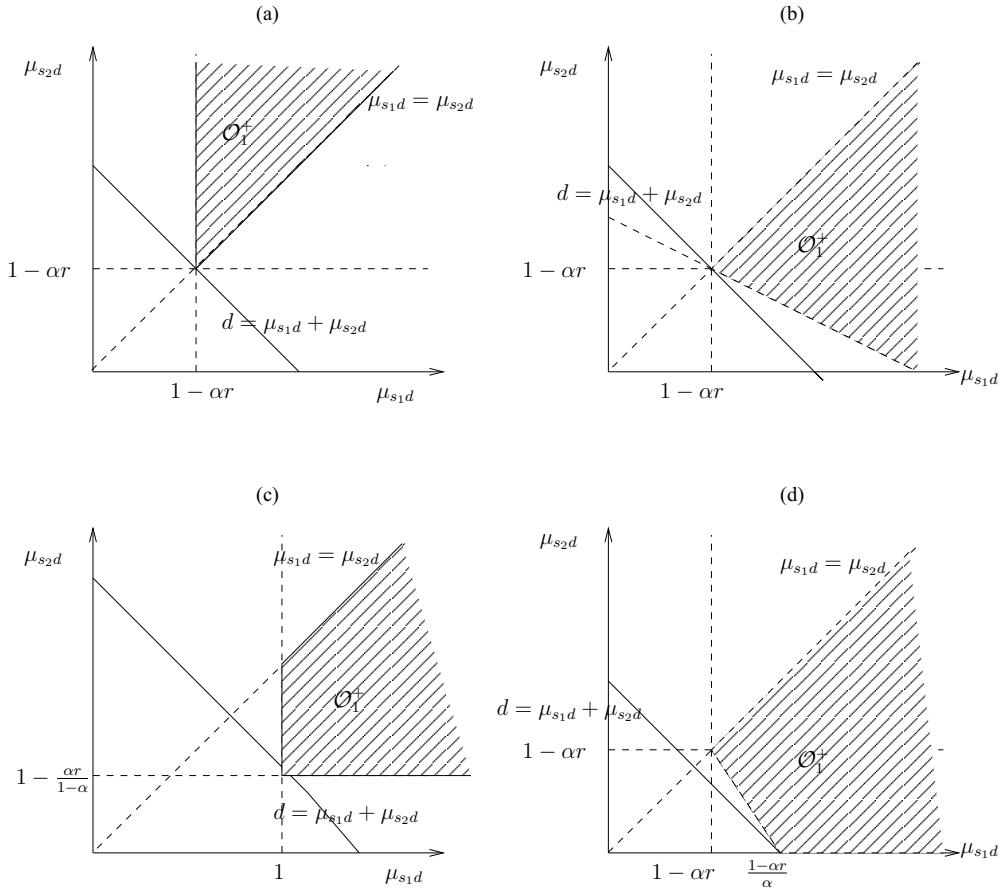

FIGURE B.1: The region $\mathcal{O}_1^+$ for (a) $\mu_{\mathrm{s_1d}} \leq \mu_{\mathrm{s_2d}}$, (b) $\mu_{\mathrm{s_1d}} > \mu_{\mathrm{s_2d}}$ and $\alpha \leq 1/2$, (c) $\mu_{\mathrm{s_1d}} > \mu_{\mathrm{s_2d}}$, $\alpha > 1/2$ and $r \leq \frac{1-\alpha}{\alpha}$, and (d) $\mu_{\mathrm{s_1d}} > \mu_{\mathrm{s_2d}}$, $\alpha \leq 1/2$ and $r > \frac{1-\alpha}{\alpha}$.

To complete the calculation, using Case 1 we compare $\left\{2 - 2\alpha r, 2 - \frac{\alpha r}{1-\alpha}\right\}$ for the rate range $\left[0, \frac{1-\alpha}{\alpha}\right]$, whereas using Case 2 we compare $\left\{2 - 2\alpha r, \frac{1-\alpha r}{\alpha}\right\}$ for the rate range $\left[\frac{1-\alpha}{\alpha}, 1\right]$. Finally, $d_{\mathrm{A}}(r, \alpha)$ can be written as

$$\begin{aligned} d_{\mathrm{A}}(r,\alpha) &= 2 - 2\alpha r && \text{for } \alpha \leq \tfrac{1}{2}, \\ d_{\mathrm{A}}(r,\alpha) &= \begin{cases} 2 - \frac{\alpha}{1-\alpha} r & r \in [0, \frac{1-\alpha}{\alpha}] \\ \frac{1-\alpha r}{\alpha} & r \in (\frac{1-\alpha}{\alpha}, 1] \end{cases} && \text{otherwise.} \end{aligned} \tag{B.2}$$

All cases are illustrated in Figure B.1.

B.2 Computation of $d_{\mathrm{B}}(r, \alpha)$ ($d(r, \alpha)$ for $k = \frac{1-\alpha}{2}$ and $l = 1$)

We distinguish between two different cases:

1. Case $\alpha \leq 1/3$: it follows $\alpha \leq \frac{1-\alpha}{2}$

   - If $\mu_{\mathrm{s_1d}} \leq \mu_{\mathrm{s_2d}}$, $(\mu_{\mathrm{s_1d}})_{\min} = (\mu_{\mathrm{s_2d}})_{\min} = 1 - \frac{2r}{1+\alpha}$. Therefore, $\forall \alpha \leq 1/2$ and $\mu_{\mathrm{s_1d}} \leq \mu_{\mathrm{s_2d}}$, $(\mu_{\mathrm{s_1d}} + \mu_{\mathrm{s_2d}}) \geq 2 - \frac{4r}{1+\alpha}$.

- If $\mu_{\mathrm{s_1d}} > \mu_{\mathrm{s_2d}}$, we have $(\mu_{\mathrm{s_1d}} + \mu_{\mathrm{s_2d}}) > \frac{1+\alpha}{1-\alpha} - \frac{2r}{1-\alpha}$. This is obtained by considering the fact that $\alpha \leq \frac{1-\alpha}{2}$.

2. Case $\alpha > 1/3$: It follows $\alpha > \frac{1-\alpha}{2}$

   - If $\mu_{\mathrm{s_1d}} \leq \mu_{\mathrm{s_2d}}$, $(\mu_{\mathrm{s_1d}} + \mu_{\mathrm{s_2d}}) \geq 1 - \frac{2r}{1+\alpha}$.
   - If $\mu_{\mathrm{s_1d}} > \mu_{\mathrm{s_2d}}$, we distinguish between two cases:
     - For $r \leq \frac{1-\alpha}{2}$, we have $\alpha\left(1-\mu_{\mathrm{s_1d}}\right)^+ + \frac{1-\alpha}{2}\left(1-\mu_{\mathrm{s_2d}}\right)^+ \leq \frac{1-\alpha}{2}$ if $\mu_{\mathrm{s_1d}} \geq 1$ (i.e., $(\mu_{\mathrm{s_1d}})_{\min} = 1$) and $\mu_{\mathrm{s_2d}} \leq 1$. Using $(\mu_{\mathrm{s_1d}})_{\min}$, we have $\mu_{\mathrm{s_2d}} \geq 1 - \frac{2r}{1-\alpha}$. Finally, we obtain $(\mu_{\mathrm{s_1d}} + \mu_{\mathrm{s_2d}}) \geq 2 - \frac{2r}{1-\alpha}$.
     - For $r > \frac{1-\alpha}{\alpha}$, using the fact that $\alpha > \frac{1-\alpha}{2}$, we get $(\mu_{\mathrm{s_1d}} + \mu_{\mathrm{s_2d}}) \geq \frac{1+\alpha-2r}{2\alpha}$.

Finally, $d_{\mathrm{B}}(r,\alpha)$ can be written as

$$
\begin{aligned}
d_{\mathrm{B}}(r,\alpha) &= \left[\tfrac{(1+\alpha)-2r}{1-\alpha}\right]^+ && \text{for } \alpha \leq \tfrac{1}{3}, \\
d_{\mathrm{B}}(r,\alpha) &= \begin{cases} 2 - \frac{2}{1-\alpha} r & r \in [0, \frac{1-\alpha}{2}] \\ \left[\frac{(1+\alpha)-2r}{2\alpha}\right]^+ & r > \frac{1-\alpha}{2} \end{cases} && \text{otherwise.}
\end{aligned} \tag{B.3}
$$

B.3 Computation of $d_{\mathrm{C}}(r,\alpha)$ ($d(r,\alpha)$ for $k = \frac{1-\alpha}{2}$ and $l = \alpha$)

We distinguish between two different cases:

1. Case $\alpha \leq 1/3$: It follows $\alpha \leq \frac{1-\alpha}{2}$

   - If $\mu_{\mathrm{s_1d}} \leq \mu_{\mathrm{s_2d}}$, $(\mu_{\mathrm{s_1d}})_{\min} = (\mu_{\mathrm{s_2d}})_{\min} = 1 - \frac{2\alpha r}{1+\alpha}$. Therefore, $\forall \alpha \leq 1/2$ and $\mu_{\mathrm{s_1d}} \leq \mu_{\mathrm{s_2d}}$, $(\mu_{\mathrm{s_1d}} + \mu_{\mathrm{s_2d}}) \geq 2 - \frac{4\alpha r}{1+\alpha}$.
   - If $\mu_{\mathrm{s_1d}} > \mu_{\mathrm{s_2d}}$, the solution corresponds to $\mu_{\mathrm{s_1d}} = \mu_{\mathrm{s_2d}}$. Therefore, the solution remains the same as in the previous subcase.

2. Case $\alpha > 1/3$: It follows $\alpha > \frac{1-\alpha}{2}$

   - If $\mu_{\mathrm{s_1d}} \leq \mu_{\mathrm{s_2d}}$, $(\mu_{\mathrm{s_1d}} + \mu_{\mathrm{s_2d}}) \geq 1 - \frac{2\alpha}{1+\alpha} r$.
   - If $\mu_{\mathrm{s_1d}} > \mu_{\mathrm{s_2d}}$, we distinguish between two cases:
     - For $\alpha r \leq \frac{1-\alpha}{2}$ (i.e., $r \leq \frac{1-\alpha}{2\alpha}$), we have $\mu_{\mathrm{s_1d}} \geq 1$ and $\mu_{\mathrm{s_2d}} \leq 1 - \frac{2\alpha}{1-\alpha} r$.
     - For $r > \frac{1-\alpha}{2\alpha}$, using the fact that $\alpha > \frac{1-\alpha}{2}$, we get $(\mu_{\mathrm{s_1d}} + \mu_{\mathrm{s_2d}}) \geq \frac{1+\alpha-2\alpha r}{2\alpha}$.

Finally, $d_{\mathrm{C}}(r,\alpha)$ can be written as

$$
\begin{aligned}
d_{\mathrm{C}}(r,\alpha) &= 2 - \tfrac{4\alpha}{1+\alpha} r \quad r \in [0,1] && \text{for } \alpha \leq \tfrac{1}{3}, \\
d_{\mathrm{C}}(r,\alpha) &= \begin{cases} 2 - \frac{2\alpha}{1-\alpha} r & r \in [0, \frac{1-\alpha}{2\alpha}] \\ \frac{1+\alpha}{2\alpha} - r & r \in (\frac{1-\alpha}{2\alpha}, 1] \end{cases} && \text{otherwise.}
\end{aligned} \tag{B.4}
$$

List of Publications

1. H. Farès, A. Graell i Amat, C. Langlais and M. Berbineau. Two-Level HARQ for turbo coded cooperation: system retransmission gain and optimal time allocation. *Proc. IEEE Wireless Commun. & Networking Conference (WCNC)*, April 2012 (*document in press*).

2. S. Schwandter, H. Farès, A. Graell i Amat and G. Metz. Error probability bounds for decode-and-forward relaying with two correlated sources. *Proc. IEEE Global Telecommun. Conf. (GLOBECOM)*, December 2011.

3. H. Farès, S. Ould Mohamed, C. Langlais, A. Graell i Amat and M. Berbineau. MIMO systems for turbo coded cooperation over orthogonal and non-orthogonal channels. *Proc. IEEE Int. Conf. ITS Telecommun. (ITST)*, pages 453-457, August 2011.

4. H. Farès, C. Langlais, A. Graell i Amat and M. Berbineau. Two-level HARQ for turbo coded cooperation. *Proc. IEEE Vehicular Technology Conference (VTC)*, pages 1-5, May 2010.

Bibliography

[ABS08] H. Adam, C. Bettstetter, and S. M. Senouci. Adaptive relay selection in cooperative wireless networks. In *Proc. IEEE Int. Sym. on Personal, Indoor and Mobile Radio Commun. (PIMRC)*, pages 1–5, September 2008.

[ACLY00] R. Ahlswede, N. Cai, S. Li, and R. Yeung. Network information flow. *IEEE Trans. Inf. Theory*, 46(4):1204–1216, July 2000.

[AFH08] F. Alazem, J.F. Frigon, and D. Haccon. Adaptive coded cooperation in wireless networks. In *International Wireless Commun. and Mobile Computing Conf.*, pages 899–904, August 2008.

[AFM11] A. Abrardo, G. Ferrari, and M. Martalò. On non-cooperative block-faded orthogonal multiple access schemes with correlated sources. *Accepted for publication in IEEE Trans. Commun.*, 2011.

[AGS05] K. Azarian, H. El Gamal, and P. Schniter. On the achievable diversity-multiplexing tradeoff in half duplex cooperative channels. *IEEE Trans. Inf. Theory*, 50(12):3062–3080, December 2005.

[AGS08] K. Azarian, H. El Gamal, and P. Schniter. On the optimality of the ARQ-DDF protocol. *IEEE Trans. Inf. Theory*, 54(4):1718–1724, April 2008.

[AH83] R. Ahlswede and T. Han. On source coding with side information via a multiple access channel and related problems in information theory. *IEEE Trans. Inf. Theory*, 29(3):396–411, May 1983.

[AKC08] F. Abi Abdallah, R. Knopp, and G. Caire. Transmission of correlated sources over gaussian multiple access channel with phase shifts. In *Proc. Allerton Conf. on Commun., Control, and Computing*, pages 873–878, September 2008.

[ASSC02] I. F. Akyildiz, W. Su, Y. Sankarasubramaniam, and E. Cayirci. Wireless sensor networks: a survey. *Computer Networks*, 38(4):393–422, 2002.

[Bab02] F. Babich. Performance of Hybrid ARQ schemes for the fading channel. *IEEE Trans. Commun.*, 50(12):1882–1885, December 2002.

[BCJR74] L. Bahl, J. Cocke, F. Jelinek, and J. Raviv. Optimal decoding of linear codes for minimizing symbol error rate. *IEEE Trans. Inf. Theory*, 20(2):284–287, March 1974.

[Ber00] H. Bertoni. *Radio propagation for modern wireless system*. NJ:Prentice-Hall, 2000.

[BGT93] C. Berrou, A. Glavieux, and P. Thitimajshima. Near Shannon limit error correcting coding and decoding: turbo-codes. In *Proc. IEEE Int. Conf. Commun. (ICC)*, pages 1064–1070, May 1993.

[BSTS10] R. Blasco-Serrano, R. Thobaben, and M. Skoglund. Compress-and-forward relaying based on symbol-wise joint source-channel coding. In *Proc. IEEE Int. Conf. Commun. (ICC)*, 2010.

[CCG79] J. B. Cain, G. C. Clark, and J . M. Geist. Punctured convolutional codes of rate (n-l)/n and simplified maximum likelihood decoding. *IEEE Trans. Inf. Theory*, 25(1):97–100, January 1979.

[CG79] T. Cover and A. El Gamal. Capacity theorems for the relay channel. *IEEE Trans. Inf. Theory*, 25(5):572–584, September 1979.

[CGS80] T.M. Cover, A. El Gamal, and M. Salehi. Multiple access channels with arbitrarily correlated sources. *IEEE Trans. Inf. Theory*, 26(6):648–657, November 1980.

[CT91] T.M. Cover and J.A. Thomas. *Elements of Information Theory*. Wiley Series in Telecommunications and Signal Processing, 1991.

[CT01] G. Caire and D. Tuninetti. The throughput of Hybrid ARQ protocols for the Gaussian collision channel. *IEEE Trans. Inf. Theory*, 47(5):1971–1988, July 2001.

[Div99] D. Divsalar. A simple tight bound on error probability of block codes with application to turbo codes. In *Tech. Rep. TMO 42-139, Jet Propulsion Lab, CIT, CA*, pages 42–139, November 1999.

[DP95] D. Divsalar and F. Pollora. Turbo codes for PCS applications. In *Proc. IEEE Int. Conf. Commun. (ICC)*, pages 54–59, June 1995.

[Due91] G. Dueck. A note on the multiple access channel with correlated sources. *IEEE Trans. Inf. Theory*, 27(2):232–235, March 1991.

[For66] G. D. Forney. *Concatenated codes*. M.I.T. Press., 1966.

[FU98] G. D. Jr. Forney and G. Ungerboeck. Modulation and coding for linear Gaussian channels. *IEEE Trans. Inf. Theory*, 44(6):2384–2415, October 1998.

[GCD06] H. El Gamal, G. Caire, and M. O. Damen. The MIMO ARQ channel: diversity-multiplexing–delay tradeoff. *IEEE Trans. Inf. Theory*, 52(8):3601–3621, August 2006.

[GF01] J. Garcia-Frias. Joint source-channel decoding of correlated sources over noisy channels. In *Data Compression Conference*, pages 283–292, March 2001.

[GV97] A. J. Goldsmith and P. P. Varaiya. Capacity of fading channels with channel side information. *IEEE Trans. Inf. Theory*, 43(6):1986–1992, November 1997.

[Hag88] J. Hagenauer. Rate-compatible punctured convolutional codes (RCPC codes) and their applications. *IEEE Trans. Commun.*, 36(4):389–400, April 1988.

[HD06] C. Hausl and P. Dupraz. Joint network-channel coding for the multiple-access relay channel. In *Proc. IEEE Commun. Society on Sensor and Ad Hoc Commun. and Networks (SECON)*, pages 817–822, September 2006.

[HH89] J. Hagenauer and P. Hoeher. A viterbi algorithm with soft-decision outputs and its applications. In *Proc. IEEE Global Telecommun. Conf. (GLOBECOM)*, pages 1680–1686, November 1989.

[HN06] T. Hunter and A. Nosratinia. Diversity through coded cooperation. *IEEE Trans. Commun.*, 5(2):283–289, February 2006.

[HSN06] T. Hunter, S. Sanayei, and A. Nosratinia. Outage analysis of coded cooperation. *IEEE Trans. Inf. Theory*, 52(2):375–391, February 2006.

[iAL10] A. Graell i Amat and I. Land. Bounds of the probability of error for decode-and-forward relaying with two sources. In *Proc. IEEE Symp. on Turbo Codes & Iterative Information Processing*, pages 196–200, September 2010.

[iALR11] A. Graell i Amat, I. Land, and L. K. Rasmussen. Error bounds for relaying with decode-and-forward. *Submitted to IEEE Trans. Inf. Theory*, 2011.

[JHHN04] M. Janani, A. Hedayat, T. E. Hunter, and A. Nosratinia. Coded cooperation in wireless communications: space-time transmission and iterative decoding. *IEEE Trans. Signal Processing*, 52(2):362–371, February 2004.

[JJ02] H. Jin and J.McEliece. Coding theorems for turbo code ensembles. *IEEE Trans. Inf. Theory*, 48(6):1451–1461, June 2002.

[KGG05] G. Kramer, M. Gastpar, and P. Gupta. Cooperative strategies and capacity theorems for relay networks. *IEEE Trans. Inf. Theory*, 51(9):3036–3063, September 2005.

[KH00] R. Knopp and P. A. Humblet. On coding for block fading channels. *IEEE Trans. Inf. Theory*, 46(1):189–205, January 2000.

[LC83] S. Lin and D. Costello. *Error control coding: fundamental and applications*. Upper Saddle River, NJ:Prentice-Hall, 1983.

[LES06] Z. Lin, E. Erkip, and A. Stefanov. Cooperative regions and partner choice in coded cooperative systems. *IEEE Trans. Commun.*, 54(7):1323–1334, July 2006.

[LI97] J. Li and H. Imai. Performance of Hybrid-ARQ with rate compatible turbo codes. In *Proc. IEEE Symp. on Turbo Codes & Iterative Information Processing*, pages 188–191, September 1997.

[LL08] D. Lin and K. Letaief. Throughput maximization of ad-hoc wireless networks using adaptive cooperative diversity and truncated ARQ. *IEEE Trans. Commun.*, 56(11):1907–1918, April 2008.

[LSBM10] S. Lee, W. Su, S. Batalama, and J. D. Matyjas. Cooperative decode-and-forward ARQ relaying: performance analysis and power optimization. *IEEE Trans. Wireless Commun.*, 9(8):2632–2642, August 2010.

[LSS03] R. Liu, P. Spasojevic, and E. Soljanin. Punctured turbo code ensembles. In *Inf. Theory Workshop*, pages 249–252, March 2003.

[LSS06] R. Liu, P. Spasojevic, and E. Soljanin. Reliable channel regions for good binary codes transmitted over parallel channels. *IEEE Trans. Inf. Theory*, 52:1405–1424, April 2006.

[LTW04] J. N. Laneman, D. N. C. Tse, and G. W. Wornell. Cooperative diversity in wireless networks: Efficient protocols and outage behavior. *IEEE Trans. Inf. Theory*, 50(12):3062–3080, December 2004.

[LU06] N. Liu and S. Ulukus. Capacity region and optimum power control stategies for fading gaussian multiple access channels with common data. *IEEE Trans. Commun.*, 54(10):1815–1826, October 2006.

[LW00] J. N. Laneman and G. W. Wornell. Energy-efficient antenna sharing and relaying for wireless networks. In *Proc. IEEE Wireless Commun. & Networking Conference (WCNC)*, pages 7–12, September 2000.

[LZG02] A.D. Liveris, X. Zixiang, and C.N. Georghiades. Joint source-channel coding of binary sources with side information at the decoder using ira codes. In *IEEE Workshop on Multimedia Signal Processing*, pages 53–56, July 2002.

[ML99] E. Malkamki and H. Leib. Evaluating the performance of convolutional codes over block fading channels. *IEEE Trans. Inf. Theory*, 45(5):1643–1646, July 1999.

[NAGS05] Y. Nam, K. Azarian, H. El Gamal, and P. Schniter. Cooperation through ARQ. In *IEEE Proc. on Signal Processing Advances in Wireless Communications (SPAWC)*, pages 1023–1027, June 2005.

[Nar08] R. Narasimhan. Throughput-delay performance of half-duplex HARQ relay channels. In *Proc. IEEE Int. Conf. Commun. (ICC)*, pages 986–990, May 2008.

[NHH04] A. Nosratinia, T. Hunter, and A. Hedayat. Cooperative communication in wireless networks. *IEEE Commun. Mag.*, 42(10):68–73, October 2004.

[NS97] K.R. Narayanan and G.L. Stüber. A novel ARQ technique using the turbo coding principle. *IEEE Commun. Lett.*, 1(2):49–51, March 1997.

[OSW94] L. H. Ozarow, S. Shamai, and A. D. Wyner. Information theoretic considerations for cellular mobile radio. *IEEE Trans. Inf. Theory*, 43(2):359–378, May 1994.

[PLWL03] Li Ping, L. Liu, K. Y. Wu, and W. K. Leung. Interleave Division Multiple Access (IDMA) communications. In *Proc. IEEE Symp. on Turbo Codes & Related Topics*, pages 173–180, September 2003.

[PLWL04] Li Ping, L. Liu, K. Y. Wu, and W. K. Leung. Approaching the capacity of multiple access channels using interleaved low-rate codes. *IEEE Trans. Inf. Theory*, 8(1):4–6, January 2004.

[PLWL06] Li Ping, L. Liu, K. Y. Wu, and W. K. Leung. Interleave-division multiple-access. *IEEE Trans. Wireless Commun.*, 5(4):938–947, April 2006.

[Pro00] John Proakis. *Digital Communications*. McGraw-Hill Science/Engineering/Math, 4 edition, August 2000.

[RM00] D. N. Rowitch and L. B. Milstein. On the performance of Hybrid FEC/ARQ systems using rate compatible punctured turbo (RCPT) codes. *IEEE Trans. Commun.*, 48(6):948–959, June 2000.

[RVS08] R. Rajesh, V. K. Varsheneya, and V. Sharma. Distributed joint source channel coding on a multiple access channel with side information. In *Proc. IEEE Int. Symp. Inf. Theory (ISIT)*, pages 2707–2711, July 2008.

[Sau06] M. Sauter. *Communications systems for the mobile information society.* John Wiley, 2006.

[Sha48] C. E. Shannon. A mathematical theory of communication. *Bell Syst. Tech. Journal*, 27(1):79–423, July 1948.

[SLS03] P. Spasojevic, R. Liu, and E. Soljanin. On the role of the puncturing in Hybrid ARQ schemes. In *Proc. IEEE Int. Symp. Inf. Theory (ISIT)*, page 449, June 2003.

[SLS04] E. Soljanin, R. Liu, and P. Spasojevic. Hybrid ARQ with random transmission assignments. In *Proc. DIMACS Workshop on Network Inf. Theory*, pages 321–334, March 2004.

[SLW09] Y. Sun, Y. Li, and X. Wang. Cooperative HARQ protocol with network coding. In *Proc. Wireless Commun. and Networking Symp.*, August 2009.

[SSBN06] I. Stanojev, O. Simeone, and Y. Bar-Ness. Performance analysis of collaborative HARQ incremental redundancy protocols over fading channels. In *IEEE Proc. on Signal Processing Advances in Wireless Communications (SPAWC)*, May 2006.

[SSBNC06] I. Stanojev, O. Simeone, Y. Bar-Ness, and C.You. Performance of multi-relay collaborative HARQ protocols over fading channels. *IEEE Commun. Lett.*, 10(7):522–524, July 2006.

[SSCL01] Ming-Der Shieh, Ming-Hwa Sheu, Chung-Ho Chen, and Hsin-FU Lo. A systematic approach for parallel CRC computations. *Journal of information science and engineering*, 17(1):445–461, September 2001.

[SSS08] H. A. Suraweera, P. J. Smith, and N. A. Surobhi. Exact outage probability of cooperative diversity with opportunistic spectrum access. In *Proc. IEEE Int. Conf. Commun. (ICC)*, pages 79–84, May 2008.

[SW04] D. Slepian and J K. Wolf. Noiseless coding of correlated information sources. *IEEE Trans. Inf. Theory*, 19(4):471–780, July 2004.

[TDK07] T. Tabet, S. Dusad, and R. Knopp. Diversity-multiplexing-delay tradeoff in half-duplex ARQ relay channels. *IEEE Trans. Inf. Theory*, 53(10):3797–3805, October 2007.

[vdM71] E. C. van der Meulen. Three-terminal communication channels. *Adv. Appl. Prob.*, 3(1):120–154, 1971.

[VS06] V. K. Varsheneya and V. Sharma. Distributed coding for multiple access communication with side information. In *Proc. IEEE Wireless Commun. & Networking Conference (WCNC)*, pages 1–5, April 2006.

[VZ03] M.C. Valenti and B. Zhao. Distributed turbo coded diversity for the relay channel. *Electron. Lett.*, 39(10):786–787, May 2003.

[WCGL07] T. Wang, A. Cano, G. B. Giannakis, and J. N. Laneman. High-performance cooperative demodulation with decode-and-forward relays. *IEEE Trans. Commun.*, 55(7):1427–1438, July 2007.

[Wic95] S. B. Wicker. *Error Control Systems for Digital Communications and Storage*. Englewood Cliffs, XJ: Prentice Hall, 1995.

[Win87] J. H. Winters. On the capacity of radio communication systems with diversity in a rayleigh fading environment. *IEEE J. Sel. Areas in Commun.*, 5(5):871–878, June 1987.

[WP99] X. Wang and H. V. Poor. Iterative (turbo) soft interference cancellation and decoding for coded CDMA. *IEEE Trans. Commun.*, 47(7):1046–1061, July 1999.

[WSG94] J.H. Winters, J. Salz, and R.D. Gitlin. The impact of antenna diversity on the capacity of wireless communication systems. *IEEE Trans. Commun.*, 42(2):1740–1751, April 1994.

[YZQ06] G. Yu, Z. Zhang, and P. Qiu. Cooperative ARQ in wireless networks: protocols description and performance analysis. In *Proc. IEEE Int. Conf. Commun. (ICC)*, pages 3608–3614, June 2006.

[YZQ07] G. Yu, Z. Zhang, and P. Qiu. Efficient ARQ protocols for exploiting cooperative relaying in wireless sensor networks. *Elsevier Journal of Computer Communications*, 30:2765–2773, June 2007.

[ZHF04] E. Zimmermann, P. Herhold, and G. Fettweis. The impact of cooperation on diversity–exploiting protocols. In *Proc. IEEE Vehicular Technology Conference (VTC)*, pages 410–414, May 2004.

[ZR96] M. Zorzi and R. Rao. On the use of renewal theory in the analysis of ARQ protocols. *IEEE Trans. Commun.*, 44(9):1077–1081, September 1996.

[ZT03] L. Zheng and D. Tse. Diversity and multiplexing: a fundamental tradeoff in multiple antenna channels. *IEEE Trans. Inf. Theory*, 49(5):1073–1096, May 2003.

[ZV05] B. Zho and M. C. Valenti. Practical relay networks: A generalization of HARQ. *IEEE J. Sel. Areas in Commun.*, 23(1):7–18, January 2005.

[ZWW09] C. Zhang, W. Wang, and G. Wei. Design of ARQ protocols for two-user cooperative diversity systems in wireless networks. *Elsevier Journal of Computer Communications*, 32(1):1111–1117, April 2009.